

P1274
4164



C10036
65104

BIBLIOTHEEK TU Delft
P 1274 4164



C

366510

THEORY OF X-RAY DIFFRACTION IN UNSTRAINED AND LIGHTLY STRAINED PERFECT CRYSTALS

PROEFSCHRIFT

TER VERKRIJGING VAN DE GRAAD VAN DOCTOR
IN DE TECHNISCHE WETENSCHAPPEN AAN DE
TECHNISCHE HOGESCHOOL TE DELFT
OP GEZAG VAN DE RECTOR MAGNIFICUS
IR. H. J. DE WIJS, HOOGLERAAR IN DE AFDELING
DER MIJNBOUWKUNDE, VOOR EEN COMMISSIE
UIT DE SENAAT TE VERDEDIGEN OP WOENSDAG
16 FEBRUARI 1966 DES NAMIDDAGS OM 4 UUR

DOOR

PAUL PENNING

NATUURKUNDIG INGENIEUR

GEBOREN TE EINDHOVEN



1274 4164

DIT PROEFSCHRIFT IS GOEDGEKEURD DOOR DE PROMOTOR
PROF. DRS. D. POLDER



*Thou art worthy, O Lord, to receive
glory and honour and power: for
thou hast created all things, and for
thy pleasure they are and were created.*

Revelation 4:11

*In dankbare herinnering aan
mijn Vader, Dr. F. M. Penning*

De directie van het Natuurkundig Laboratorium der N.V. Philips' Gloeilampenfabrieken ben ik bijzonder erkentelijk voor de mij gegeven mogelijkheid deze studie in de benodigde rust te volbrengen.

Zonder de bijdrage van Dr Ir B. Okkerse zou dit werk niet gereedgekomen zijn. Hij heeft met het tonen van veel belangstelling en het doen van duidelijke experimenten de uitwerking van de theorie zeer gestimuleerd.

Mr A. E. Jenkinson, B.Sc., ben ik dankbaar dat hij het manuscript zo zorgvuldig gelezen heeft. Door zijn commentaar is het Engels duidelijk verbeterd.

De heer A. H. Goemans heeft bijgedragen door het maken van numerieke berekeningen en het maken van enkele tekeningen.

CONTENTS

1. INTRODUCTION

1.1. Historical introduction	1
1.2. Survey of this study	2

2. DEFINITIONS

2.1. Introduction	4
2.2. Perfect crystals	4
2.3. Scattering mechanism	5
2.4. Atomic scattering factor and structure factor	6
2.5. Susceptibility	8
2.6. Absorption	9

3. GEOMETRICAL THEORY

3.1. Von Laue's treatment	10
3.2. Bragg's equation	10
3.3. Discussion and further definitions	11

4. KINEMATICAL THEORY

4.1. Von Laue's treatment	12
4.2. Darwin's treatment	13
4.3. Discussion	14

5. DYNAMICAL THEORY

5.1. Darwin's approach	16
5.1.1. Scattering by one layer of atoms	16
5.1.2. Wave fields inside the crystal	17
5.1.3. Wave vector characterizing the wave field inside the crystal	19
5.2. Von Laue's treatment	22
5.3. Basic equations of the dynamical theory	23

6. MODES OF PROPAGATION, GROUP VELOCITY AND ω -SURFACE

6.1. Introduction	24
6.2. Modes of propagation	24
6.3. Power flow, group velocity and velocity of energy transport	25
6.4. The ω -surface	26
6.5. Wave fields consisting of two modes	29

7. MATCHING AT THE BOUNDARIES	
7.1. Definitions	31
7.2. Matching of \mathbf{k} -vectors	32
7.3. Matching of amplitudes	33
7.4. Total reflexion	34
8. ABSORPTION AND EXTINCTION	
8.1. Introduction	36
8.2. Mathematical treatment	38
8.3. The " ω -surface"	41
8.4. Absorption coefficient	44
9. X-RAY BEAMS	
9.1. Introduction	47
9.2. Gaussian wave packet in the linear approximation	48
9.2.1. Definition	48
9.2.2. Upward-travelling wave field	49
9.2.3. Downward-travelling wave field	53
9.2.4. Power flow	54
9.3. Well-behaved beams in plane-parallel crystal slabs	56
10. DYNAMICAL THEORY FOR LIGHTLY DEFORMED CRYSTALS	
10.1. Introduction	63
10.2. Outline of the ray theory	65
10.3. Reciprocal-lattice vector and structure factor in deformed crystals	65
10.4. Effects of deformation on the ω -surface	67
10.5. Wave-field matching along the path	68
10.6. Discussion	70
10.7. Examples of beam transmission through deformed crystals	70
10.7.1. Deformations that do not influence the beam behaviour	70
10.7.2. Reflecting planes curved, but parallel and equidistant	72
10.7.3. Reflecting planes flat and parallel, but not equidistant	75
10.8. Comparison with electron-band theory	78
11. DIFFRACTION IN CRYSTALS WHERE THE STRAIN IS A LINEAR FUNCTION OF ONE SPACE COORDINATE	
11.1. Introduction	79

11.2. Derivation of differential equations	80
11.3. Results and discussion	81
11.4. Derivation of results	85
11.4.1. General solution	85
11.4.2. Reflecting planes curved, but parallel and equidistant	88
11.4.3. Reflecting planes flat and parallel, but not equidistant	90
11.4.4. Kinematical approach	92

12. COMPARISON WITH OTHER THEORIES

12.1. Classification	95
12.2. Taupin's theory	95
12.2.1. Results in general terms	95
12.2.2. Application to perfect crystals	96
12.2.3. Deformation a function of one space coordinate . . .	98
12.2.4. General deformation	99
12.3. Bonse's theory	100
12.3.1. Summary of results	100
12.3.2. Discussion	101

APPENDIX	103
--------------------	-----

LIST OF FREQUENTLY USED SYMBOLS	106
---	-----

REFERENCES	109
----------------------	-----

Summary	110
-------------------	-----

Samenvatting	111
------------------------	-----

1. INTRODUCTION

1.1. Historical introduction

In 1912 Von Laue suggested an investigation on the interaction between X-rays and crystals. At that time neither the nature of X-rays nor the atomic structure of crystals had been firmly established, although it had been mentioned that X-rays might be electromagnetic waves with a wavelength much shorter than that of visible light, and that crystals had a periodic structure. For an excellent survey of the relevant knowledge at that time, see the book "Fifty years of X-ray diffraction" edited by P. P. Ewald ¹⁾. Von Laue, being trained in optics, combined these two possibilities and concluded that if both were true, the crystal might act as a three-dimensional grating for the X-rays. Friedrich and Knipping performed the experiment and very soon found that a parallel incident beam is diffracted by the crystal into many beams. The directions of the diffracted beams turned out to be closely connected with the orientation of the crystal with respect to the incident beam. In 1912 ²⁾ Von Laue and his collaborators published a theory explaining these results as a diffraction phenomenon. This theory was mainly concerned with the *geometrical* aspects of diffraction: the orientation relationship between the incident and diffracted beams relative to the orientation of the crystal. A diffracted beam in his view was the result of constructive interference between the wavelets emitted by the individual scattering centres.

In the following year Sir W. L. Bragg ³⁾ published an alternative formulation of Von Laue's results, in a form simpler to visualize. In his view diffraction was the result of mirror reflexion against densely packed atom planes, with the restriction that the waves reflected by successive parallel planes have to be in phase. The mathematical formulation is the well-known Bragg equation.

Both forms of geometrical theory lend themselves to quantitative treatment and expressions for the intensities of the diffracted beams can be obtained. The result of such a treatment is the *kinematical theory* of X-ray diffraction. It fits remarkably well the experimental data on nearly all crystals.

Von Laue's interest in the possibility of X-ray diffraction arose from a discussion with Ewald in the beginning of 1912. Ewald was preparing his doctor's thesis under Sommerfeld on the double refraction in crystals. He could show that for an orthorhombic array of dipoles it was not necessary to assume an anisotropic scattering by the dipoles to explain double refraction. For some unsolved questions he wanted the advice of Von Laue, who was fully trained in optics. The discussion did not help Ewald very much since Von Laue was obviously preoccupied with one question in this matter: "What is the distance between the dipoles in actual crystals?" Ewald could give only the unsatis-

factory answer that it must be much smaller than the wavelength of visible light. In spite of the lack in advice Ewald finished his thesis in February 1912. It is clear that Ewald's work has some bearing on the diffraction of X-rays. In 1916 Ewald⁴⁾ extended his theory to the case of X-rays, having a wavelength comparable with the distance between neighbouring scattering centres. This extension is the basis of the *dynamical theory* of X-ray diffraction. The results agree with the geometrical theory, but are contradictory to the kinematical theory in many important aspects. It was therefore regarded as an impractical theory since it did not fit the experimental data. However, in 1941, Borrmann⁵⁾ observed diffraction phenomena in quartz crystals, which could be explained by Von Laue via the dynamical theory.

The first papers on the dynamical theory, however, were published in 1914 by Darwin⁶⁾. His theory, based on Bragg's way of approach, is easier to visualize and comprises less mathematics. The results are identical with those obtained by Ewald later, although Darwin restricts his treatment unnecessarily to the special situation of the symmetrical Bragg case.

In 1931, when the stormy evolutions of the initial period had calmed down, Von Laue⁷⁾ gave a third approach to the dynamical theory, by solving Maxwell's equations for a medium with a periodic dielectric constant. It is remarkable that Von Laue does not refer to the famous paper by Bloch⁸⁾, published 3 years earlier in 1928, dealing with the propagation of electron waves in periodic media, in spite of the fact that the problems treated are very similar. It may be mentioned further that Darwin's approach, published in 1914, is comparable to the Kronig-Penney model⁹⁾ published in 1931. Although there is a close relationship between the dynamical theory of X-ray diffraction and the electron-band theory, the line of thought is different in the two, and different concepts are used. In this thesis we shall have several opportunities to demonstrate the analogy in results in detail.

1.2. Survey of this study

From the moment that perfect crystals became available much experimental work has been done to verify the dynamical theory. The agreement between theory and experiment is excellent. At the same time data were obtained on perfect crystals deformed lightly by means of a temperature gradient or external forces. To explain the data on a theoretical basis, the dynamical theory has to be extended to deformed crystals. A first approach to this problem was given in 1961 by Penning and Polder. It is based on a number of assumptions not all of which were derived from first principles. It is the aim of this thesis to give a more extensive discussion of the different ideas underlying the theory and to determine its limitations.

The dynamical theory differs in a fundamental way from the kinematical

theory, widely used in the interpretation of X-ray data. Therefore, in this thesis, much attention is paid to the way X-ray diffraction is approached in the two disciplines. In chapter 2 the definitions are considered and in chapter 3 the geometrical theory. The specific kinematical way of approach is briefly discussed in chapter 4. Since we want to deal with almost perfect crystals the dynamical theory for perfect crystals is considered next. Special attention is given to the definition of the wave vector (chapter 5), the relation between the possible wave vectors for given wavelength and the modes of propagation by which the X-ray energy is transported through the crystal (chapter 6). The boundary conditions for matching the wave fields inside and outside the crystal are given in chapter 7. In actual crystals the amplitude of a mode of propagation decreases when the mode travels deeper into the crystal. The cause may be either absorption of X-ray energy by the crystal or extinction, an interference phenomenon that exists also in non-absorbing crystals. The consequences of introducing extinction and absorption on the behaviour of the modes of propagation and on the allowed wave vectors for given wavelength are discussed in chapter 8. An important question is whether an absorption coefficient in its normal meaning is an adequate description of the damping in amplitude.

The theory for diffraction in lightly deformed crystals (chapter 10) is based on the idea that an incident pencil beam gives a well-behaved beam inside the crystal. In chapter 9 it is shown that in undeformed crystals normal beams result only if the extinction does not contribute substantially to the damping in amplitude. The basic assumption of the theory is that in deformed crystals well-defined beams are present also. To find the path of the beam a matching procedure is proposed, analogous to the matching of light waves in inhomogeneous media. The resulting paths in general are not straight. In principle the theory may be applied to any type of deformation provided the strain is not too inhomogeneous, leading to expressions for the path and the overall absorption along the path. The simple examples discussed in chapter 10, lend themselves also to an exact treatment that does not require the basic assumptions of the ray theory (chapter 11). From this exact treatment it follows that for sufficiently slowly varying strain the ray theory gives correct results. The limit of validity is in good agreement with that derived in chapter 10 on intuitive arguments. For rapidly varying strains the kinematic approach gives the right answer.

Finally we shall give in chapter 12 a comparison with other theories.

2. DEFINITIONS

2.1. Introduction

In the theories of X-ray diffraction a number of special concepts are used. It is the aim of this chapter to clarify the definitions and the use of those concepts that are needed later. It is not the intention to give exact definitions. They are to be found in several textbooks^{10,11,12}). This chapter is also necessary to introduce the symbols that will be used later. Unfortunately the different authors use different symbols for the same parameter and the same symbol for different parameters. The symbols used here are again different.

2.2. Perfect crystals

A perfect crystal is defined¹³) as a body composed of atoms arranged in such a way that there exist 3 translation vectors \mathbf{a}_1 , \mathbf{a}_2 and \mathbf{a}_3 , with the property that the atomic arrangement looks the same in every respect when viewed from any point \mathbf{r} as when viewed from the point

$$\mathbf{r}' = \mathbf{r} + n_1\mathbf{a}_1 + n_2\mathbf{a}_2 + n_3\mathbf{a}_3, \quad (2.2.1)$$

where n_1 , n_2 and n_3 are integers. If we specify that n_1 , n_2 and n_3 are integers for *all* points that have the property given above, the 3 vectors are referred to as primitive translation vectors. The parallelepiped on these 3 vectors is called the (primitive) unit cell. The atomic arrangement within the unit cell, together with the 3 primitive translation vectors provide all the information necessary to describe the positions of all atoms within the crystal. The geometrical theory is based on the translation symmetry only. The intensity of the diffracted beams is determined by the atomic arrangement within the unit cell, via the structure factor.

In dealing with the propagation of waves in such periodic media it is convenient to introduce the reciprocal lattice. We define the primitive translation vectors $2\mathbf{b}_1$, $2\mathbf{b}_2$ and $2\mathbf{b}_3$ in the following way:

$$\begin{aligned} 2\mathbf{b}_i \cdot \mathbf{a}_i &= 2\pi, \\ \mathbf{b}_i \cdot \mathbf{a}_j &= 0; \quad i \neq j. \end{aligned} \quad (2.2.2)$$

The reciprocal lattice is given by the points

$$2\mathbf{h}b_{hkl} = 2h\mathbf{b}_1 + 2k\mathbf{b}_2 + 2l\mathbf{b}_3. \quad (2.2.3)$$

The factor 2 is included to obtain simpler formulae later in the text. The vector \mathbf{b}_{hkl} is perpendicular to the crystal-lattice plane (hkl) and its magnitude is π divided by the distance between two neighbouring planes (hkl), d_{hkl} :

$$|\mathbf{b}_{hkl}| = \pi/d_{hkl}. \quad (2.2.4)$$

The interaction between the crystal and the X-rays takes place via the electrons. The electron density ^{*)} ρ in a periodic crystal may be written as a Fourier sum:

$$\rho(\mathbf{r}) = \sum_{hkl} \rho_{hkl} \exp(2j\mathbf{b}_{hkl} \cdot \mathbf{r}), \quad (2.2.5)$$

with

$$\rho_{hkl} = (1/V_c) \int_{V_c} \rho(\mathbf{r}) \exp(-2j\mathbf{b}_{hkl} \cdot \mathbf{r}) dV, \quad (2.2.6)$$

where V_c is the volume of the unit cell.

Actual crystals can never be perfect, because of the motion of the atoms. As a matter of fact it was generally thought in 1912, that Von Laue's idea would bear no fruit because of the thermal motion. Since diffraction was observed, we consider in detail the case that all atoms are located at their average position. The effects of thermal motion are discussed in sec. 10.1.

2.3. Scattering mechanism

The alternating electric field of the X-ray sets the electrons inside the crystal into forced vibrations. The vibrating dipoles emit radiation (scattered wavelets) that is coherent with the exciting field in polarization, frequency, phase and amplitude.

The polarization relationship is shown in fig. 2.1. With reference to the

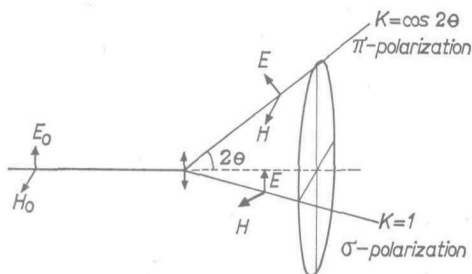


Fig. 2.1. The two main directions of polarization.

direction in which the wavelet is emitted, distinction can be made between two main directions of polarization: the σ -polarization if the wavelet is emitted in a direction perpendicular to the electric-field strength of the exciting field and the π -polarization if emission takes place in a direction perpendicular to the magnetic-field strength of the exciting field. If the wavelet is emitted in an arbitrary direction, the exciting field may be decomposed into two parts, each corresponding with one of the main polarization directions given above. In the mathematical treatment, it is sufficient to introduce a parameter K to account for the polarization effects:

^{*)} See also sec. 2.4 for what is meant by electron density.

$$\begin{aligned} K &= 1 && \sigma\text{-polarization,} \\ K &= \cos 2\theta && \pi\text{-polarization,} \end{aligned} \tag{2.3.1}$$

with 2θ the scattering angle.

The relation between the amplitude and phase of the exciting field strength E_0 and the emitted wave is conveniently described by introducing as a unit of scattering, the scattering by one free electron. The amplitude of the forced vibration is so small, that the vibrating free electron may be considered as a Hertzian dipole. In the "distant zone" (distance from dipole $r \gg \lambda$) the amplitude of the scattered wave is equal to

$$E = (-r_e K/r) E_0 \exp(-j\omega r/c), \tag{2.3.2}$$

where r_e is the classical electron radius:

$$r_e = e^2/4\pi\epsilon_0 mc^2 = 2.818 \cdot 10^{-15} \text{ (m)}. \tag{2.3.3}$$

The other parameters have their usual meaning. In using this standard two important points have to be kept in mind. Firstly, the electrons are not free. This point will be dealt with in the next section. Secondly, the field strength in the distant zone is used. The argument for this is different in the kinematical and dynamical theory. In the *kinematical theory* only small crystals are considered and the point of observation of the diffracted beams lies well outside the crystal. Hence eq. (2.3.2) is valid and the r^{-1} dependence of the amplitude may be neglected. In the summing of the contributions from all atoms the r dependence of the phase factor plays an important part. Further it is assumed in the kinematical theory that the crystal is so small that the total amplitude of the diffracted waves is always negligible compared with the incident wave. Accordingly the amplitude of the exciting wave is constant and equal to the amplitude of the incident wave. In the *dynamical theory* the crystals may have infinite size and the point of observation may lie within the crystal. Furthermore the situation may be such that the diffracted waves have amplitudes comparable with the amplitude of the incident wave. To obtain such large amplitudes a large number of electrons must contribute because one electron is only a poor scatterer. The majority of this large number lies in the "distant zone" for which eq. (2.3.2) is valid. Since the diffracted waves may have appreciable amplitudes in the dynamical theory the exciting field strength E_0 in eq. (2.3.2) must be the total amplitude of the incident and diffracted wave. In this respect the dynamical and kinematical theory differ fundamentally.

2.4. Atomic scattering factor and structure factor

The *atomic scattering factor* is defined as the ratio in amplitudes of the wave scattered by one atom and the wave scattered by a free electron. Quantum-

mechanical treatment shows that one may define a local electron density ρ (charge density ρe) that vibrates under the influence of an electromagnetic field as if it were completely free. This value of ρ is equal to the real electron density if the frequency of the electromagnetic field is large compared with the resonance frequency of any electron in the atom. For lower frequencies a dispersion correction has to be applied to determine ρ (Hönl correction¹⁴).

The mathematical expression for the atomic scattering factor f , follows from eq. (2.3.2):

$$f = \int \rho(\mathbf{r}) \exp \{-j(\mathbf{k}_0 - \mathbf{k}_0') \cdot \mathbf{r}\} dV, \quad (2.4.1)$$

where \mathbf{k}_0 and \mathbf{k}_0' represent vectors of length $2\pi/\lambda$ in the direction of the phase velocity of the incident and diffracted waves, resp. In most cases ρ may be considered as spherically symmetric. Choosing the origin at the nucleus gives a real value of f , which is a function of $\sin(\theta)/\lambda$, with θ half the angle between \mathbf{k}_0 and \mathbf{k}_0' . In fig. 2.2 an example is given.

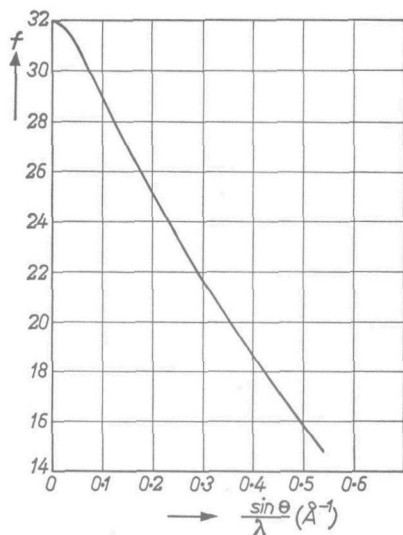


Fig. 2.2. The atomic scattering factor for germanium calculated by Berghuis et al.²⁴.

It will be discussed later (sec. 2.6) that it is possible to account for absorption by adding to ρ a small imaginary part that usually shows spherical symmetry also. With the origin again in the centre of symmetry the value of f is now necessarily complex.

The *structure factor*, F , is defined as the amplitude of the wave scattered by all atoms in one unit cell in comparison with the amplitude of the wave scattered by one classical free electron located somewhere within the unit cell.

$$F = \sum_i f_i \exp \{-j(\mathbf{k}_0 - \mathbf{k}_0') \cdot \mathbf{r}_i\}, \quad (2.4.2)$$

where \mathbf{r}_i is the distance between the nucleus of the i -th atom and the location of the reference electron. The summation has to be carried out over all atoms in the unit cell. Combining eqs (2.4.1) and (2.4.2) gives

$$F = \int_{V_c} \rho \exp \{-j(\mathbf{k}_0 - \mathbf{k}_0') \cdot \mathbf{r}\} dV. \quad (2.4.3)$$

The value of F is dependent on the choice of the location of the reference electron. In non-absorbing crystals (ρ real) it is always possible to choose the origin in such a way that F is real. The value of F is then insensitive to the sign of $\mathbf{k}_0 - \mathbf{k}_0'$. In absorbing crystals (ρ complex) the value of F is in general complex and sensitive to a reversal in sign of $\mathbf{k}_0 - \mathbf{k}_0'$. In the following we shall treat only the case that the crystal structure shows inversion symmetry. Locating the origin in the inversion centre leads to complex values of F but the real and imaginary parts are independent of the sign of $\mathbf{k}_0 - \mathbf{k}_0'$.

We shall see later (sec. 4.1) that the diffracted wave has an appreciable amplitude if the vectors \mathbf{k}_0 and \mathbf{k}_0' satisfy or almost satisfy the relation (see eq. 3.2.1)

$$\mathbf{k}_0 - \mathbf{k}_0' = 2\mathbf{b}_{hkl}.$$

Hence one may write also

$$F_{hkl} = \int_{V_c} \rho \exp \{-j2\mathbf{b}_{hkl} \cdot \mathbf{r}\} dV, \quad (2.4.4)$$

and by using eq. (2.2.6),

$$F_{hkl} = V_c \rho_{hkl}. \quad (2.4.5)$$

2.5. Susceptibility

To solve Maxwell's equations for the propagation of X-rays in crystalline solids one has to attribute to the medium a value of ϵ on a sub-atomic scale ($\mu = \mu_0$). Von Laue ⁷⁾ argues as follows: the heavy positive nucleus is not set into motion by the electromagnetic field. Hence the distribution of the positive charge over the medium is irrelevant and may be chosen in any convenient way, provided it is treated as stationary. By distributing it in such a way that the crystal is electrically neutral on a sub-atomic scale, a medium is obtained for which ϵ may be calculated in the usual way:

$$\epsilon = \epsilon_0 - \rho e^2 / m\omega^2. \quad (2.5.1)$$

In this equation ρ is the density of electrons that are free to move and accordingly equal to the electron density introduced in the previous section. In absorbing crystals it is complex.

The susceptibility ψ ,

$$\psi = (\epsilon - \epsilon_0) / \epsilon_0 = -\rho e^2 / \epsilon_0 m\omega^2, \quad (2.5.2)$$

is periodic in a perfect crystal and may be analysed in a triple Fourier series as discussed in sec. 2.2:

$$\psi_{hkl} = -\frac{e^2}{\epsilon_0 m \omega^2 V_c} \int_{V_c} \rho \exp(-2j \mathbf{b}_{hkl} \cdot \mathbf{r}) dV, \quad (2.5.3)$$

or by using eq. (2.4.4) for F_{hkl} :

$$\psi_{hkl} = -e^2 F_{hkl} / \epsilon_0 m \omega^2 V_c. \quad (2.5.4)$$

Later we shall frequently use the parameter V_{hkl} :

$$V_{hkl} = (\omega^2 / c^2) K \psi_{hkl} = -4\pi r_e K F_{hkl} / V_c. \quad (2.5.5)$$

The order of magnitude of ψ is the same for all crystals. It may be estimated by calculating ψ_{000} for Ge and CuK α radiation ($\lambda = 1.54 \text{ \AA}$). In Ge crystals there are 8 atoms with each 32 electrons in a cube with edges of 5.35 \AA :

$$\psi_{000} = -3.10^{-5}.$$

The susceptibility is hence much smaller than unity. So small indeed, that ψ^2 and often ψ itself may be neglected in comparison with unity.

2.6. Absorption

Up till now the interaction between the X-rays and electrons was assumed to be "elastic". The electron acts as a "transmitter" of energy from the incident to the diffracted wave. However, there are other possibilities, where the energy absorbed by the electrons is emitted in a way not coherent with the exciting wave. Examples of such processes are the photo-electric effect and the Compton effect.

To account for these inelastic scattering mechanisms we shall follow Prins¹⁵), unquestioned, in his suggestion to add a small imaginary part to the electron density ρ . According to eq. (2.5.2) this is identical with adding a small imaginary part to the susceptibility. Since not all the electrons of an atom will suffer inelastic scattering to the same extent, the argument of ρ need not be the same everywhere. We shall be mainly interested in the case of X-rays not very close in wavelength to an absorption edge on the short-wavelength side where the absorption is very strong. The imaginary part in ρ is then small compared with the real part.

3. GEOMETRICAL THEORY

3.1. Von Laue's treatment

According to Von Laue²⁾ the diffraction phenomenon must be interpreted as a result of constructive interference between the wavelets emitted by all atoms. The necessary and sufficient condition is that the difference in path lengths from source to observer via the reference point in the different unit cells is an integral number of wavelengths. For sufficiently large distances from source and observer to the crystal the condition, in mathematical terms, is

$$\begin{aligned}(\mathbf{k}_0 - \mathbf{k}_0') \cdot \mathbf{a}_1 &= 2\pi h, \\(\mathbf{k}_0 - \mathbf{k}_0') \cdot \mathbf{a}_2 &= 2\pi k, \\(\mathbf{k}_0 - \mathbf{k}_0') \cdot \mathbf{a}_3 &= 2\pi l,\end{aligned}\tag{3.1.1}$$

where h , k and l are integers and \mathbf{k}_0 and \mathbf{k}_0' vectors of length $2\pi/\lambda$, in the direction of the incident and diffracted waves, respectively. The structure factor does not enter, since we are dealing with the geometrical aspects only. In their original paper²⁾ Von Laue, Friedrich and Knipping could interpret the X-ray photograph by assigning a set of integers, hkl , to each spot.

3.2. Bragg's equation

The equation (3.1.1) may be written in a simpler form by using reciprocal-lattice vectors. It is easily shown that they are equivalent to the vector equation

$$\mathbf{k}_0 - \mathbf{k}_0' = 2hb_1 + 2kb_2 + 2lb_3 = 2\mathbf{b}_{hkl}.\tag{3.2.1}$$

In fig. 3.1 an example is given. Since the vector \mathbf{b}_{hkl} is perpendicular to the

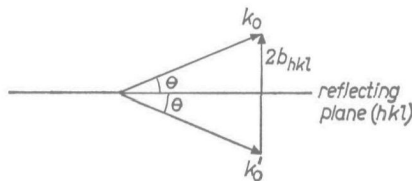


Fig. 3.1. The relation between the wave vector \mathbf{k}_0 of the incident wave and \mathbf{k}_0' of the diffracted wave for maximum diffracted intensity, according to the geometrical theory.

plane (hkl) and the vectors \mathbf{k}_0 and \mathbf{k}_0' have equal length, they must make equal angles θ with the plane (hkl). Bragg³⁾ pays special attention to this result and concludes that diffraction may be interpreted also as a mirror reflexion against planes. This view is generally accepted. The plane (hkl) is referred to as the reflecting plane (see next section, point (3)) and the wave travelling parallel to \mathbf{k}_0' as the reflected wave.

Remembering that $|\mathbf{b}_{hkl}| = \pi/d_{hkl}$ (eq. (2.2.4), eq. (3.2.1) may be trans-

formed into the well-known Bragg equation in a slightly modified formulation (see next section, point (3)):

$$\lambda = 2 d_{hkl} \sin \theta. \quad (3.2.2)$$

The major advantage of Bragg's view is that the diffraction phenomenon is reduced from the 3-dimensional Von Laue's treatment to a 1-dimensional one. For a given reflected wave the distribution of atoms over the reflecting plane is immaterial as far as the geometrical condition for constructive interference is concerned. Of the entire crystal lattice only the distance d_{hkl} plays a part. In a quantitative theory, however, this is not true in general, but in the X-ray case it holds in most situations because of the weak interaction between wave field and electron clouds. The only exception is a direction of \mathbf{k}_0 such that the Bragg condition is satisfied for more than one set of reflecting planes (multiple diffraction). Such situations will be excluded in this thesis.

3.3. Discussion and further definitions

Regarding the results obtained above, the following remarks have to be made:

- (1) The index of refraction of the medium was set equal to unity, since we used as wavelength its value in vacuum. We shall deal with this point in sec. 5.1.
- (2) Of the 4 parameters defining \mathbf{k}_0 and \mathbf{k}_0' , only 3 can be determined from eqs (3.1.1) or (3.2.1). One remains free to choose, corresponding to a rotation of \mathbf{k}_0 and \mathbf{k}_0' around the vector \mathbf{b}_{hkl} . This ambiguity is avoided by understanding in the following that the plane through \mathbf{k}_0 , \mathbf{k}_0' and \mathbf{b}_{hkl} is given: the *plane of incidence*.
- (3) Usually Bragg's equation is given in the form

$$n\lambda = 2d \sin \theta. \quad (3.3.1)$$

It is then implicitly understood that the crystal may be considered as a regular stacking of layers that contain all atoms. The distance between the layers is d . The parameter n is then the order of reflexion. Darwin for example uses such a model for the derivation of a kinematical and dynamical theory. It must be remarked, however, that such a model is useful only for crystal structures with a small number of atoms per primitive unit cell. In general the planes through the atoms are not equidistant (see for example the planes (111) in the diamond lattice). Therefore we prefer in the general case the description with (hkl) as the indices of the reflecting plane, even when h , k and l have a common multiple.

- (4) The geometrical theory gives only the direction of \mathbf{k}_0 in the plane of incidence for which the diffracted wave has maximum amplitude. It is the aim of the kinematical and dynamical theories to calculate the diffracted intensity as a function of the direction of \mathbf{k}_0 .

4. KINEMATICAL THEORY

4.1. Von Laue's treatment

To calculate the intensity of a diffracted wave, Von Laue considers a crystal, irradiated by a plane-parallel wave in such a way that the diffracted wave hkl is generated. He assumes the crystal to be so small that the amplitude of the diffracted wave is very small in comparison with the amplitude of the incident wave. It is this assumption that makes his treatment a kinematical one. All unit cells are hence subject to the same exciting field. The amplitude of the diffracted wave is calculated by summing the wavelets scattered by all unit cells to a point at a large distance R from the crystal. If the crystal is a parallelepiped with sides along the primitive translation vectors \mathbf{a}_i of length $N_i\mathbf{a}_i$, the intensity of the diffracted beam, I_R , is related to the intensity I_0 , incident on the crystal:

$$I_R = I_0 (r_e^2 K^2 / R^2) |F_{hkl}|^2 g_1^2 g_2^2 g_3^2. \quad (4.1.1)$$

The factors g_i depend on the orientation of the wave vectors \mathbf{k}_v and \mathbf{k}_r of the incident and diffracted wave, resp.:

$$g_i = \sin \{N_i(\mathbf{k}_r - \mathbf{k}_v) \cdot \mathbf{a}_i\} / \sin \{(\mathbf{k}_r - \mathbf{k}_v) \cdot \mathbf{a}_i\}. \quad (4.1.2)$$

The value of I_R is only appreciable if $\mathbf{k}_r - \mathbf{k}_v$ is almost equal to $2\mathbf{b}_{hkl}$. In fig. 4.1 the areas are shown in which the vectors \mathbf{k}_v and \mathbf{k}_r have to be located for an appreciable diffracted intensity if the crystal is a cube with sides of 10^{-4} cm.

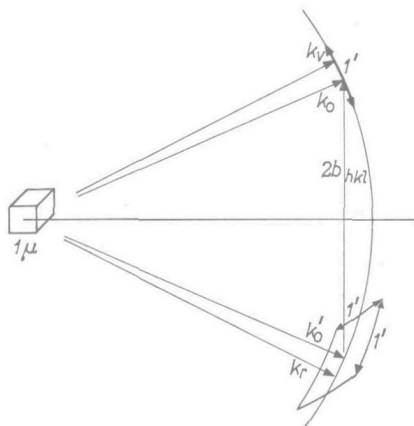


Fig. 4.1. A reasonable amplitude of the wave diffracted by a small crystal is expected if the wave vectors of the incident wave \mathbf{k}_v in a given plane of incidence, and the wave vector of the diffracted wave \mathbf{k}_r fall within the regions indicated.

In this diagram the vector \mathbf{k}_v is kept in the plane of incidence, see remark (2) in sec. 3.3. For given \mathbf{k}_v the angular divergence in \mathbf{k}_r is of the order of 1 minute of arc. For a smaller crystal the divergence is correspondingly larger.

The diffracted intensity is a maximum if $\mathbf{k}_v - \mathbf{k}_r$ is exactly equal to $2\mathbf{b}_{hkl}$ in agreement with the geometrical theory, and hence $g_i = N_i$:

$$I_{R,\max} = I_0 (r_e^2 K^2 / R^2) |F_{hkl}|^2 (N_1 N_2 N_3)^2. \quad (4.1.3)$$

To obtain results that allow for an experimental check, the diffracted intensity has to be integrated over the divergence in \mathbf{k}_r in two directions and over the divergence in \mathbf{k}_v in one direction. The resulting integrated diffracted intensity is directly proportional to $N_1 N_2 N_3$, the total number of unit cells in the crystal and proportional to $|F_{hkl}|^2$. Both results are typical for the kinematical theory and in contradiction with the results of the dynamical theory.

4.2. Darwin's treatment

Darwin⁶⁾ is thinking along the lines given by Bragg. One infinite single sheet of unit cells acts as a (poor) reflector for an incident plane-parallel wave*). The vectors \mathbf{k}_v and \mathbf{k}_r are rigidly coupled. The vector \mathbf{k}_r lies in the plane of incidence through \mathbf{k}_v and \mathbf{b}_{hkl} and makes the same angle with the reflecting plane (fig. 4.2). This is in sharp contrast with Von Laue's result where \mathbf{k}_r shows

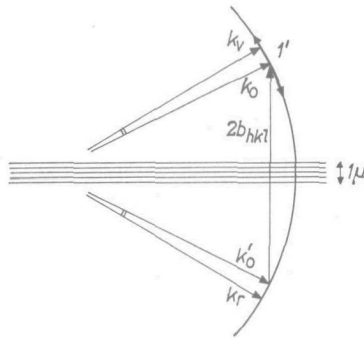


Fig. 4.2. In Darwin's model of the crystal the wave vectors \mathbf{k}_v (incident wave) and \mathbf{k}_r (reflected wave) are coupled because of mirror reflexion. In a given plane of incidence the range of \mathbf{k}_v -values that give a reasonable diffracted intensity is indicated.

an angular divergence. The explanation is that Darwin's sheet is unbounded. The ratio in amplitude of the reflected and the incident wave $j q$, can be calculated (see sec. 11.4.4):

$$j q = j \lambda F_{hkl} r_e K d / V_c \sin \theta = -j \lambda d V_{hkl} / 4 \pi \sin \theta, \quad (4.2.1)$$

where d/V_c is the number of unit cells per unit area in the sheet. The factor $+j$ indicates that there is a jump in phase of $\pi/2$ during reflexion.

The intensity per unit area of the reflected wave may now be calculated by summing the contribution of all n_s sheets that constitute the crystal. In the

*) See for a more detailed discussion sub-section 5.1.1.

situation that the Bragg condition is satisfied exactly all the sheets contribute in phase and the reflected intensity is a maximum. It follows immediately that the maximum in reflected intensity is proportional to $|F_{hkl}|^2$ and n_s^2 .

The integrated reflected intensity R , obtained by integrating over variations in \mathbf{k}_v while keeping it in the plane of incidence, is proportional to $|F_{hkl}|^2$ and n_s , in agreement with the results obtained by Von Laue.

4.3. Discussion

The kinematical theory, although in agreement with the greater part of experimental evidence, cannot be correct from a theoretical point of view. According to Von Laue's treatment the reflected intensity is proportional to the volume of the crystal and may exceed the incident intensity for a sufficiently large crystal. This result is partly trivial, since the increase in I_R is partly caused by an increase in I_0 which was defined as the intensity incident on the crystal. But in Darwin's treatment with a crystal of infinite size in two directions the reflected intensity per unit area of the slab still rises with increasing thickness. This unsatisfactory result is simply due to the assumption that all sheets are subject to the same exciting field, the constant amplitude $|E_i|$ of the incident wave. Apparently the kinematical theory gives correct results only as long as the amplitude of the reflected wave $|E_r|$ remains small compared with $|E_i|$.

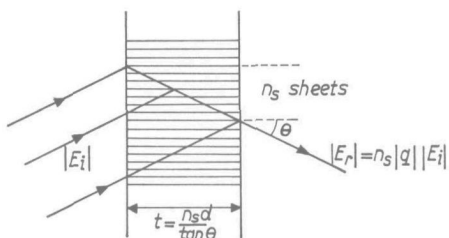


Fig. 4.3. Schematic drawing to demonstrate how the maximum in diffracted intensity is calculated in the kinematical theory.

According to the example given in fig. 4.3, this condition amounts to

$$|q|n_s < 1,$$

which may be transformed into a requirement for the thickness:

$$t < 2 \cos(\theta) \omega / c |V_{hkl}|. \quad (4.3.1)$$

Substituting orders of magnitude for ω/c ($4 \cdot 10^8 \text{ cm}^{-1}$) and $|V_{hkl}|$ ($2 \cdot 10^{12} \text{ cm}^{-3}$) one finds an upper limit for t of a few microns. In practice the crystals are usually thicker. That the kinematical theory still applies to these crystals was explained by Darwin by introducing the concept "mosaic crystal" (see sec. 10.1).

The length $\cos(\theta)\omega/c |V_{hkl}|$ appearing in eq. (4.3.1) plays an important part in the dynamical theory, the "Pendellösung"-length L (eq. (6.5.1)).

The loss in intensity of the incident wave because of the generation of the reflected wave is called primary extinction. For strong reflexions it is much larger than the loss due to absorption. Even for an absorption coefficient of 1000 cm^{-1} the incident wave would lose only 10% in intensity over a distance of 1μ .

To improve the kinematical theory in this respect, one could suggest introducing an "absorption" coefficient to account for the loss in intensity to the reflected wave. However, this would not lead to correct results, since in the situation where such a correction is necessary the atoms are subject to both the incident and the reflected wave. The best solution in this line of thought is to introduce an incident and a reflected wave right from the start and to investigate the scattering due to the sum of both waves. Such a procedure was followed by Darwin in his dynamical theory.

5. DYNAMICAL THEORY *)

5.1. Darwin's approach

5.1.1. Scattering by one layer of atoms

In sec. 4.2 it was pointed out that Darwin regards the crystal as a regular stacking of layers (distance d) and these contained all the atoms. Although the atoms have finite dimensions, they are considered to be so small that in between the layers there is a region where the medium is essentially vacuum.

When a plane-parallel wave with wave vector \mathbf{k}_i strikes a layer the influence is twofold. The vibrating electrons give a scattering in the forward direction and in the reflected direction. Far from the layer both scattered waves are plane and travel parallel to \mathbf{k}_i and \mathbf{k}_i' , respectively. The vectors \mathbf{k}_i and \mathbf{k}_i' make exactly the same angle θ with the layer (mirror reflexion). These results were used in sec. 4.2 in deriving the kinematical expression for the reflected intensity. In the dynamical theory the observer is inside the infinitely large crystal and one has to know the disturbance very close to the layer. Darwin follows the simplest course by assuming that in the vacuum both scattered waves are plane parallel even at distances $d/2$ or less from the central plane of the layer. This assumption is identical with spreading out the electrons evenly in directions parallel to the layer, so that the electron density is only a function of the coordinate, z , perpendicular to the layer. The situation is now very similar to that in the Kronig-Penney model. In the latter case the electron density is a specified function of z , whereas in Darwin's treatment it may be any function. Such a fictitious crystal is characterized by one primitive translation vector \mathbf{a}_D and one primitive reciprocal-lattice vector $2\mathbf{b}_D$, where

$$|\mathbf{b}_D| = \pi/|\mathbf{a}_D| = \pi/d. \quad (5.1.1)$$

Darwin shows that the amplitude of the forward-scattered wave is jq_0 times the amplitude of the undisturbed wave at the same place. The value of q_0 , following from eq. (4.2.1) by substituting $\theta = 0$ in $F_{hkl} (\rightarrow F_{000})$, is very small compared to unity. Apparently the layer gives an extra phase shift q_0 to the incident wave while passing through the layer. The amplitude of the reflected wave is jq times the amplitude of the incident wave, with jq given in eq. (4.2.1). The argument of jq depends on the location of the place where the two waves are compared via the structure factor F . We shall take the point of reference in the plane of symmetry inside the layer. In non-absorbing crystals q is then real.

It is important to keep in mind that in this way the influence of the layer as the unit is given. The behaviour inside the layer is not considered. It may be included by making a Kronig-Penney model of the crystal, by transforming the

*) Reviews of the dynamical theory are found in refs 16 and 17.

constant electron density inside the layer into a dielectric constant deviating from unity, by using eq. (2.5.1).

In general the two waves will be present on both sides of the layer. With the assumptions made above it is possible to relate the amplitudes of the waves above and below the layer. The amplitude of the wave parallel to \mathbf{k}_i is denoted by T , the amplitude of the wave parallel to \mathbf{k}_i' by S . Let us compare the amplitudes T_2 and S_2 in point B, a distance $a_D/2$ above the centre of the layer with the amplitudes T_1 and S_1 in A, a distance a_D below B (fig. 5.1). The vector \mathbf{a}_D

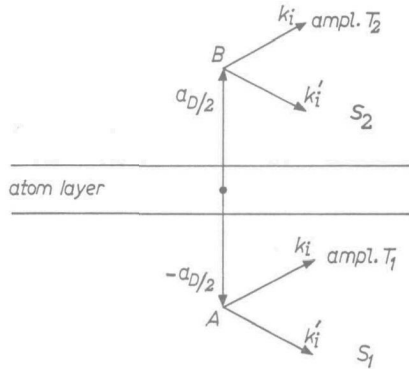


Fig. 5.1. Explanation of the symbols used in the text to determine the influence of one layer of atoms on the amplitudes of the incident and reflected waves (eqs (5.1.2)).

is perpendicular to the layer and so large that both A and B lie in vacuum. The amplitude T_2 consists of two parts: one arising from the transmitted wave and one arising from the reflected wave. The same is true for S_1 . Note that here an improvement is obtained over the kinematical theory where the influence of S on T and of T on S is neglected. It is easily verified that

$$T_2 = T_1 (1 + jq_0) \exp(-j\mathbf{k}_i \cdot \mathbf{a}_D) + jqS_2 \exp\{\frac{1}{2}j(\mathbf{k}_i' - \mathbf{k}_i) \cdot \mathbf{a}_D\}$$

and (5.1.2)

$$S_1 = S_2 (1 + jq_0) \exp(-j\mathbf{k}_i \cdot \mathbf{a}_D) + jqT_1 \exp\{\frac{1}{2}j(\mathbf{k}_i' - \mathbf{k}_i) \cdot \mathbf{a}_D\}.$$

Use is made of the relation $\mathbf{k}_i' \cdot \mathbf{a}_D = -\mathbf{k}_i \cdot \mathbf{a}_D$ that exists because of the mirror reflexion of the wave. In the plane through A or B the amplitudes vary with the phase factor

$$\exp\{-\frac{1}{2}j(\mathbf{k}_i + \mathbf{k}_i') \cdot \mathbf{r}\}.$$

5.1.2. Wave fields inside the crystal

By setting the period in the crystal lattice equal to a_D ($|a_D| = d$) the change in T and S over one period is given in eq. (5.1.2). The translation behaviour over an arbitrary number of distances \mathbf{a}_D follows from a multiple application

of eq. (5.1.2). Such a procedure is lengthy and tedious. It results in general in amplitudes that change in magnitude and phase for each step. Following Darwin we shall proceed in a different way, by looking for such solutions that show a more regular translation behaviour, namely an equal and constant phase shift in T and S while going up over a distance \mathbf{a}_D :

$$T_2/T_1 = S_2/S_1 = \exp(-j\phi). \quad (5.1.3)$$

This requirement may be written in a different form:

$$S_1/T_1 = S_2/T_2 = \xi \exp(j\phi). \quad (5.1.4)$$

The ratio in amplitude of the two plane waves in the narrow vacuum sections between the layers, is therefore constant for such solutions. The factor $\exp(j\phi)$ is included in eq. (5.1.4) to obtain consistency with the value of ξ used later.

Whether such solutions exist can be determined by substituting eqs (5.1.3) and (5.1.4) in eq. (5.1.2), leading to

$$\exp\{j(-\phi + \mathbf{k}_i \cdot \mathbf{a}_D)\} = 1 + jq_0 + jq\xi$$

and

$$\exp\{j(\phi + \mathbf{k}_i \cdot \mathbf{a}_D)\} = 1 + jq_0 + jq/\xi. \quad (5.1.5)$$

For a given direction of \mathbf{k}_i the equations can be solved for ξ and $\exp(j\phi)$. Apparently there exist solutions that show the simple translation behaviour expressed in eqs (5.1.3) and (5.1.4). These solutions will be referred to as *modes of propagation*. Characteristic for the modes is that apart from a phase shift their behaviour is identical in all unit cells*). If \mathbf{k}_i is given there are two solutions for ξ and $\exp(j\phi)$, but for given ξ there is only one solution for $\exp(j\phi)$.

For moderate values of ξ , i.e. $q \ll |\xi| \ll 1/q$, the right-hand side of eqs (5.1.5) is close to unity, so that both $\phi - \mathbf{k}_i \cdot \mathbf{a}_D$ and $\phi + \mathbf{k}_i \cdot \mathbf{a}_D$ have to be close to a multiple of 2π :

$$\begin{aligned} -\phi + \mathbf{k}_i \cdot \mathbf{a}_D &= -p2\pi + q_0 + q\xi, \\ \phi + \mathbf{k}_i \cdot \mathbf{a}_D &= (n + p)2\pi + q_0 + q/\xi. \end{aligned} \quad (5.1.6)$$

The term $2\pi n$ is included to make $\mathbf{k}_i \cdot \mathbf{a}_D$ close to $n\pi$, i.e. the Bragg condition for the n th-order reflexion. The factor p is an arbitrary integer.

Darwin applies eqs (5.1.6) to the symmetrical Bragg case only. We shall proceed in a more general way. For one mode of propagation the phase is known (apart from a multiple of 2π) in all planes midway between two adjacent layers. We want to introduce now a vector \mathbf{k} that describes the phase in these planes correctly by the phase factor $\exp(-j\mathbf{k} \cdot \mathbf{r})$. Hence

*) For cut-off modes and for modes in absorbing crystals (see chapter 8) there is a decrease or increase in both T and S while going from cell to cell.

*) $k_i = \frac{\omega}{c}$, hadde schrijver moeten vermelden!

— 19 —

$$\phi = \mathbf{k} \cdot \mathbf{a}_D$$

Bragg $\rightarrow \vec{k}_i - \vec{k} = 2p\vec{b}_D$

$$(5.1.7)$$

and

$$\frac{1}{2} (\mathbf{k}_i + \mathbf{k}_i') \cdot \mathbf{t} = \mathbf{k}_i \cdot \mathbf{t} = (\mathbf{k} - 2p\mathbf{b}_D) \cdot \mathbf{t},$$

where \mathbf{t} is a unit vector parallel to the layers in the plane of incidence. According to the definition of \mathbf{b}_D we have (eq. (5.1.1))

$$\mathbf{b}_D \cdot \mathbf{a}_D = \pi.$$

It may now be verified that \mathbf{k} has to satisfy the conditions

$$(\mathbf{k} - 2p\mathbf{b}_D)^2 = \omega^2/c^2 + V_0 + V_n \xi$$

and

$$(\mathbf{k} - 2p\mathbf{b}_D - 2n\mathbf{b}_D)^2 = \omega^2/c^2 + V_0 + V_n/\xi.$$

With the aid of eq. (4.2.1) q_0 and q are replaced by V_0 and $V_n = V_{nkl}$. The higher-order terms in q and q_0 are neglected. The parameter p is still arbitrary.

stel $c = q_0 + q \xi$, dan:
 is (5.1.6) equiv. met:
 $\vec{k} - \vec{k}_i = (2n + \frac{c}{\pi}) \vec{b}_D$,
 (5.1.8) is afgeleid uit
 de absolute waarde
 (5.1.8) van deze
 vergelijking
 met verwaarlozing van
 termen q_0^2 en q^2 .
 en met (4.21)

5.1.3. Wave vector characterizing the wave field inside the crystal

The vector \mathbf{k} introduced in the previous sub-section is a wave vector but in a restricted sense. The wave vectors of waves in uniform media give the difference in phase between any two points 1 and 2 via $\mathbf{k} \cdot (\mathbf{r}_2 - \mathbf{r}_1)$. In our case the phase is given correctly at points midway between two layers. For other points the phase is not given by $\mathbf{k} \cdot \mathbf{r}$. The immediate consequence of this restriction is that the vector \mathbf{k} cannot be determined from eqs (5.1.8); the integer p is still free. A convention has to be introduced to make \mathbf{k} uniquely determined.

In the *electron-band* theory the convention is that \mathbf{k} shall lie in a coherent region of \mathbf{k} -space (the Brillouin zone), that is chosen beforehand; in our case, for example, the region is where $(\alpha - 1) \mathbf{b}_D^2 < \mathbf{k} \cdot \mathbf{b}_D \leq (\alpha + 1) \mathbf{b}_D^2$ with α arbitrary but fixed *).

In the dynamical theory of X-ray diffraction another convention is used. Before we can say which one, the wave fields inside the crystal have to be examined in more detail. Up till now the variation of T and S within the layer has been left out of consideration, but we need it now. Since these variations are not known in detail we have to rely on qualitative arguments.

In a mode of propagation, where T and S have the same phase difference and amplitude ratio midway between two layers, the variation in T and S will be identical in all unit cells. Hence it is permitted to write for the total amplitude W :

$$W = W_{\mathbf{k}}(\mathbf{r}) \exp(-j\mathbf{k} \cdot \mathbf{r}),$$

where $W_{\mathbf{k}}$ is periodic in \mathbf{r} , with period \mathbf{a}_D :

$$W_{\mathbf{k}}(\mathbf{r}) = W_{\mathbf{k}}(\mathbf{r} + \mathbf{a}_D).$$

The periodic function can be written as a Fourier series:

*) Usually α is set equal to 0.

$$W_{\mathbf{k}}(\mathbf{r}) = \sum_m W_{\mathbf{k},m} \exp(j2m\mathbf{b}_D \cdot \mathbf{r}).$$

The local amplitude W is then, for any value of \mathbf{r} ,

$$W = \sum_m W_{\mathbf{k},m} \exp\{-j(\mathbf{k} - 2m\mathbf{b}_D) \cdot \mathbf{r}\}. \quad (5.1.9)$$

The total wave field consists of an infinite number of plane-wave components, each with a well defined amplitude (if $W_{\mathbf{k}}$ is known) and wave vector. The respective \mathbf{k} -values lie $2\mathbf{b}$ apart. To characterize the translation behaviour of the wave field it is sufficient to give the \mathbf{k} -vector of one plane-wave component. It is immaterial which one, because $\exp j(\mathbf{k} - 2p\mathbf{b}_D) \cdot \mathbf{a}_D = \exp j\mathbf{k} \cdot \mathbf{a}_D$.

An example is shown in fig. 5.2. The circles represent points midway between

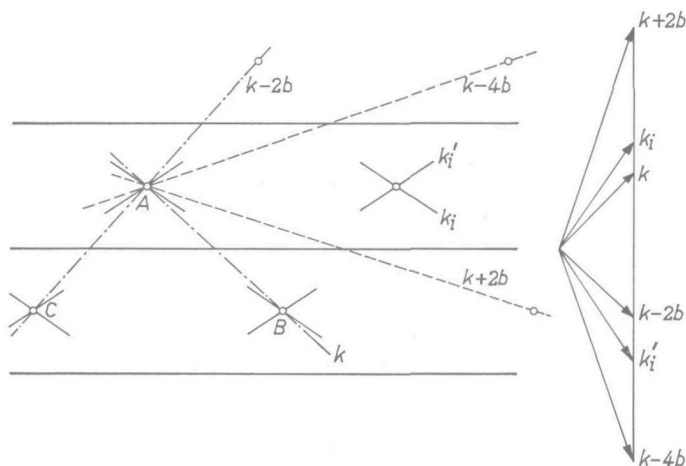


Fig. 5.2. Lines of equal phase in Darwin's model of a crystal. The points A, B and C lie midway between layers of atoms in vacuum. The drawn lines labeled k_i and k_i' are lines of equal phase of the incident and reflected waves, respectively. Inside the atom layers the phase is not known. The total wave field inside the crystal can be decomposed into an infinite number of plane-wave components. There are two predominant ones with wave vectors \mathbf{k} and $\mathbf{k} - 2\mathbf{b}_D$. The lines of equal phase for these two components (known everywhere) are given as dash-dot lines. For the two other components, with small amplitudes, the lines of equal phase are given as dashed lines. All \mathbf{k} -vectors of the plane-wave components lie a multiple of $2\mathbf{b}_D$ apart. Note that the reflexion is of the first order. In the figure the subscript D in \mathbf{b}_D is omitted.

the layers where the phase of T is the same. The lines of equal phase of T are given also (labeled k_i). The lines are perpendicular to the vector k_i given in the right-hand side of the figure. It is important to note that lines of equal phase in A and B do not lie in line, because of the interaction with the layer. The deviation is small as follows from eq. (5.1.2). We shall deal with a mode of propagation, for which eq. (5.1.3) is valid. Accordingly lines of equal phase of S also pass through the circles, although the phase of S and T need not be the same there. They are perpendicular to k_i' and therefore make the same angle

with the layer as the lines of equal phase of T . We see that, when the Bragg condition is nearly satisfied, the lines of equal phase of S make a small angle with the line AC. In the description of the wave field with plane-wave components the lines of equal phase for each component are straight throughout the crystal. A few examples have been drawn. They are labeled with the corresponding \mathbf{k} -vectors on the right-hand side of the figure. In view of the small difference in orientation between \mathbf{k}_i and \mathbf{k} , and between \mathbf{k}_i' and $\mathbf{k} - 2\mathbf{b}_D$, when there is diffraction, we may expect that the plane-wave components \mathbf{k} and $\mathbf{k} - 2\mathbf{b}_D$ have a much larger amplitude than the other components; the ratio is of the order of q ($\approx 10^{-5}$). Accordingly we conclude that in the Fourier-series equation (5.1.9) only two terms are predominant.

In view of this result it is not surprising that in the dynamical theory of X-ray diffraction the wave is characterized by the \mathbf{k} -vector of one of its predominant plane-wave components. The major advantage is that the modulus of the characterizing wave vector is now close to ω/c . To remove the last ambiguity we shall choose that wave vector of the two for which $\mathbf{k} \cdot \mathbf{b}_D$ is positive, as was done in fig. 5.2. According to this convention we may write for eqs (5.1.8):

$$\mathbf{k}^2 = \omega^2/c^2 + V_0 + V_n \xi$$

and

$$(\mathbf{k} - 2n\mathbf{b}_D)^2 = \omega^2/c^2 + V_0 + V_n/\xi. \tag{5.1.10}$$

Far off Bragg angle there are 2 possibilities:

- (1) The line AC is far from perpendicular to \mathbf{k}_i' . The value of S must be small ($\xi \rightarrow 0$), and the only predominant component is \mathbf{k} with

$$\mathbf{k}^2 = \omega^2/c^2 + V_0, \quad \xi \rightarrow 0. \tag{5.1.11}$$

- (2) The line AB is far from perpendicular to \mathbf{k}_i . Now the value of T is very small and the only predominant component is $\mathbf{k} - 2\mathbf{b}$, with

$$(\mathbf{k} - 2n\mathbf{b}_D)^2 = \omega^2/c^2 + V_0, \quad |\xi| \rightarrow \infty. \tag{5.1.12}$$

Although there is only one predominant plane-wave component, we note that in this limiting case $|\mathbf{k}|$ is not close to ω/c and that \mathbf{k} is not the wave vector of this predominant component.

From eq. (5.1.9) one might conclude that the wave field inside the crystal contains only plane-wave components with wave vectors $\mathbf{k} - 2p\mathbf{b}_D$. This is not true. In his treatment Darwin assumed the waves in vacuum between the layers to be plane parallel. In reality this is not the case since there will be a modulation in planes parallel to the layer. This periodicity may be analysed in a Fourier series also, with \mathbf{b} -vectors parallel to the layer and amplitudes of the same order of magnitude as the amplitudes of the components that were neglected above ($\mathbf{k} - 2p\mathbf{b}_D$, with $p \neq 0, n$). In general one must expect that the wave field is given by

$$W = \sum_{hkl} W_{\mathbf{k},hkl}(\mathbf{r}) \exp \{-j(\mathbf{k} - 2\mathbf{b}_{hkl}) \cdot \mathbf{r}\}, \quad (5.1.13)$$

or written in a slightly different way (the Bloch form),

$$W = W_{\mathbf{k}} \exp(-j\mathbf{k} \cdot \mathbf{r}), \quad (5.1.14)$$

where $W_{\mathbf{k}}$ is identical in all primitive unit cells.

5.2. Von Laue's treatment

Von Laue solves the dynamical problem by reducing it to the propagation of electromagnetic waves in a periodic medium. The electric-field strength has to satisfy the differential equation

$$\Delta \mathbf{E} - \nabla(\nabla \cdot \mathbf{E}) = -(1 + \psi) \mathbf{E} \omega^2/c^2. \quad (5.2.1)$$

The susceptibility ψ , discussed in sec. 2.5, is periodic in three dimensions and can be expanded in a triple Fourier series:

$$\psi = \sum_m \psi_m \exp(j2\mathbf{b}_m \cdot \mathbf{r}), \quad (5.2.2)$$

where m is any set of 3 integers.

Von Laue proposes as solution a sum of transverse plane-parallel waves:

$$\mathbf{D} = \epsilon_0(1 + \psi) \mathbf{E} = \sum_p \mathbf{D}_{\mathbf{k}-2\mathbf{b}_p} \exp \{-j(\mathbf{k} - 2\mathbf{b}_p) \cdot \mathbf{r}\}, \quad (5.2.3)$$

where p is again a set of 3 integers. In view of experimental evidence and Darwin's results, he asserts that according to specific circumstances, a small number of plane-wave components are predominant above all other components. Only a limited number of components have to be taken into account, all other amplitudes are zero. To determine \mathbf{k} unambiguously, we shall follow the convention discussed in the previous sub-section.

As is shown in many textbooks on X-ray diffraction the proposed solution satisfies the differential equation for given ω . The following three cases can be distinguished:

- (1) There is only one predominant plane-wave component, with amplitude $D_{\mathbf{k}-2\mathbf{b}_p}$. The only relevant wave vector, $\mathbf{k} - 2\mathbf{b}_p$, is denoted by \mathbf{k} according to the X-ray convention. The relation between \mathbf{k} and ω now reads:

$$\mathbf{k}^2 = \omega^2/c^2 + V_0. \quad (5.2.4)$$

- (2) There are two predominant plane-wave components, because of the interaction with one set of reflecting planes ($hkl) \equiv n$. Now the two relevant wave vectors are denoted by $\mathbf{k} = \mathbf{k} - 2\mathbf{b}_p$ and $\mathbf{k}' = \mathbf{k} - 2\mathbf{b}_{p+n} = \mathbf{k} - 2\mathbf{b}_n$, giving

$$\mathbf{k}^2 = \omega^2/c^2 + V_0 + V_n \xi, \quad (5.2.5)$$

$$(\mathbf{k} - 2\mathbf{b}_n)^2 = \omega^2/c^2 + V_0 + V_n/\xi,$$

with

$$\xi = D_{\mathbf{k}-2\mathbf{b}_n}/D_{\mathbf{k}}. \quad (5.2.6)$$

Here ξ is defined at the location of the reference electron in the calculation of the structure factor.

- (3) There are 3 or more predominant plane-wave components, because of the simultaneous interaction with two or more sets of reflecting planes. This situation is outside the scope of this thesis. We remark only that in such situations Von Laue's treatment allows for a rigorous treatment, whereas Darwin's approach excludes such a possibility in its basic assumption.

5.3. Basic equations of the dynamical theory

The solution obtained along the lines given by Darwin (eq. (5.1.10)) and the solution found by Von Laue (eq. (5.2.5)) are identical. In the further development we shall use the following notation for the basic equations of the dynamical theory:

$$\mathbf{k}^2 = \omega^2/c^2 + V_0 + V_1 \xi, \quad (5.3.1)$$

$$\mathbf{k}'^2 = (\mathbf{k} - 2\mathbf{b})^2 = \omega^2/c^2 + V_0 + V_1/\xi,$$

with

$$\xi = D_{\mathbf{k}-2\mathbf{b}}/D_{\mathbf{k}}. \quad (5.3.2)$$

In the limiting cases far off Bragg angle we have

$$\mathbf{k}^2 = \omega^2/c^2 + V_0, \quad D_{\mathbf{k}-2\mathbf{b}} \rightarrow 0 \quad (5.3.3)$$

or

$$(\mathbf{k} - 2\mathbf{b})^2 = \omega^2/c^2 + V_0, \quad D_{\mathbf{k}} \rightarrow 0. \quad (5.3.4)$$

The angular region in the plane of incidence, for which diffraction takes place (moderate values of ξ) is very narrow because $|V_0|$ and $|V_1|$ are much smaller than ω^2/c^2 . In those terms that are relatively small, we shall often replace \mathbf{k} by \mathbf{k}_0 and \mathbf{k}' by \mathbf{k}_0' , where \mathbf{k}_0 and \mathbf{k}_0' satisfy Bragg's equation exactly.

The basic equations apply also to the case of absorbing crystals, where V_0 and V_1 are complex (sec. 2.6). It now follows immediately that \mathbf{k} and ξ are complex also. Complex values of \mathbf{k} give rise to an exponential increase or decrease of the amplitudes $D_{\mathbf{k}}$ and $D_{\mathbf{k}-2\mathbf{b}}$ via the phase factor $\exp(-j\mathbf{k} \cdot \mathbf{r})$. Their ratio is constant, however. Having allowed for complex ξ -values we see that in non-absorbing crystals the wave vector \mathbf{k} may be complex also. The resulting exponential decrease or increase in amplitude is named *extinction*, and the corresponding wave fields cut-off modes. A detailed discussion of absorption and extinction is given in chapter 8.

6. MODES OF PROPAGATION, GROUP VELOCITY AND ω -SURFACE

6.1. Introduction

In the previous chapter it was shown that in periodic media there exist modes of propagation for electromagnetic waves. In contrast to the kinematical approach where in the case of diffraction the reflected wave is generated from the incident wave, the dynamical theory considers primarily wave fields where incident and reflected wave are in dynamical equilibrium. Their ratio is unchanged, while going from unit cell to unit cell. In this chapter the variation of the amplitude over a unit cell for such a mode of propagation is discussed, together with the direction of energy flow that is associated with it. Finally the relation between the wave vector \mathbf{k} and the frequency is discussed. For given ω all allowed values of \mathbf{k} lie on a surface in \mathbf{k} -space. In the literature this surface is usually called the *dispersion surface*. We prefer the name *ω -surface*, since dispersion is commonly associated with a frequency dependence, whereas here the frequency is constant and the dependence of $|\mathbf{k}|$ on its direction is important (anisotropy).

6.2. Modes of propagation

In the case of interaction with one set of reflecting planes the mode of propagation contains two predominant plane-wave components. The upward-travelling wave with wave vector \mathbf{k} and amplitude $\mathbf{D}_{\mathbf{k}}$ and the downward-travelling wave with wave vector $\mathbf{k} - 2\mathbf{b}$ and amplitude $\mathbf{D}_{\mathbf{k}-2\mathbf{b}} = \xi\mathbf{D}_{\mathbf{k}}$. In the σ -polarization the vectors $\mathbf{D}_{\mathbf{k}}$ and $\mathbf{D}_{\mathbf{k}-2\mathbf{b}}$ are parallel to each other and parallel to the reflecting planes. In the π -polarization $\mathbf{D}_{\mathbf{k}}$ and $\mathbf{D}_{\mathbf{k}-2\mathbf{b}}$ lie in the plane of incidence. Since we shall restrict ourselves to a narrow region around the Bragg angle (including the limits far off Bragg angle), the angle between $\mathbf{D}_{\mathbf{k}}$ and $\mathbf{D}_{\mathbf{k}-2\mathbf{b}}$ may be set equal to 2θ .

The total amplitude \mathbf{D} is according to eq. (5.2.3)

$$\mathbf{D} = \mathbf{D}_{\mathbf{k}} \exp(-j\mathbf{k} \cdot \mathbf{r}) + \mathbf{D}_{\mathbf{k}-2\mathbf{b}} \exp\{-j(\mathbf{k} - 2\mathbf{b}) \cdot \mathbf{r}\}. \quad (6.2.1)$$

The magnitude of \mathbf{D} is easily shown to be

$$D = |\mathbf{D}_{\mathbf{k}}| (1 + \xi^2)^{1/2} \{1 + 2K \xi \cos(2\mathbf{b} \cdot \mathbf{r}) / (1 + \xi^2)\}^{1/2} \quad (6.2.2)$$

for both directions of polarization. The factor before the brackets is the root-mean-square of the amplitudes of the two components. In fig. 6.1 a few examples of the variation of D within the unit cell are given for a first-order reflexion. The polarization assumed was σ with $K=1$. For ξ either 0 or ∞ , D is independent of \mathbf{r} , and there is only one predominant plane-wave component. For $\xi = \pm 1$ the two plane-wave components have equal amplitude and their interference pattern gives rise to nodes of zero amplitude. There is a standing

wave in the direction perpendicular to the reflecting planes. In the π -polarization the amplitude in the modes are finite even for $\xi = \pm 1$. The vectors \mathbf{D}_k and \mathbf{D}_{k-2b} cannot cancel since they are not parallel. For given root-mean-square

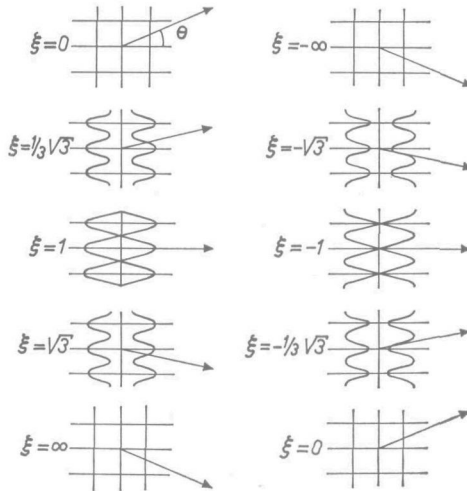


Fig. 6.1. The variation in amplitude of the dielectric displacement over the unit cell for some modes of propagation in the σ -polarization. The horizontal lines indicate the centre of the atom layers. The vectors indicate the direction of power flow.

amplitude the pattern is the same for ξ and $1/\xi$, showing the equivalence of the two plane-wave components. Finally the difference in modes with positive and negative values of ξ has to be noted. If $\xi < 0$ the amplitude is a minimum in the reflecting planes; for $\xi > 0$ it is a maximum *).

It is possible to construct wave fields with the nodes in intermediate positions. The value of ξ , however, has then to be complex, leading to exponentially decreasing or increasing amplitudes, as was pointed out already in sec. 5.3.

6.3. Power flow, group velocity and velocity of energy transport

The time average of the power flow in a wave field is given by the real part of the product $\mathbf{E} \times \mathbf{H}^*/2$, where \mathbf{H}^* is the complex conjugate of \mathbf{H} . In our case we are interested in the power flow averaged over the unit cell in a direction perpendicular to the reflecting planes:

$$\mathbf{P} = \int_z^{z+d} \text{Re} \{ \mathbf{E} \times \mathbf{H}^* \} dz/2d. \quad (6.3.1)$$

Substituting the solution proposed by Von Laue and neglecting all terms which are of the order ψ or smaller, gives for real values of ξ :

*) If $\theta > 45^\circ$ the reverse is true for the π -polarization ($K < 0$).

$$2\omega\epsilon_0\mathbf{P}/c^2 = |\mathbf{D}\mathbf{k}|^2\mathbf{k}_0 + |\mathbf{D}\mathbf{k}-2\mathbf{b}|^2\mathbf{k}_0' \\ = |\mathbf{D}\mathbf{k}|^2(1 + \xi^2)\{\mathbf{k}_0 - \mathbf{b} + \mathbf{b}(1 - \xi^2)/(1 + \xi^2)\}. \quad (6.3.2)$$

The power flow is hence equal to the vector sum of the power flow in the two components. The effect of the interference between the two components is eliminated by taking the average over the unit cell. The component of \mathbf{P} along the reflecting planes (parallel to $\mathbf{k}_0 - \mathbf{b}$) depends only on the root-mean-square amplitude of the wave field. The component perpendicular to the reflecting planes (parallel to \mathbf{b}) is strongly dependent on ξ . For $\xi = 0$, \mathbf{P} is parallel to \mathbf{k}_0 and for $\xi = \infty$, \mathbf{P} is parallel to \mathbf{k}_0' . For $\xi = \pm 1$ the two components have equal amplitude and the power flow must be parallel to $\mathbf{k}_0 + \mathbf{k}_0' = 2(\mathbf{k}_0 - \mathbf{b})$, i.e. parallel to the reflecting planes, in agreement with eq. (6.3.2).

The direction of the energy flow is also found by calculating the group velocity \mathbf{v}_g :

$$\mathbf{v}_g = \nabla_{\mathbf{k}} \omega. \quad \rightarrow \quad \vec{v}_g = \nabla_{\mathbf{k}} \omega \quad (6.3.3)$$

By taking $\nabla_{\mathbf{k}}$ of the basic equations (5.3.1) and eliminating $\nabla_{\mathbf{k}}$ one finds

$$\mathbf{v}_g\omega/c^2 = \mathbf{k}_0 - \mathbf{b} + \mathbf{b}(1 - \xi^2)/(1 + \xi^2). \quad (6.3.4)$$

In absorbing crystals and in the case of cut-off modes complications arise. It may be shown, however, that even in these cases the first of eqs (6.3.2) is still valid. Accordingly we may write in general

$$2\omega\epsilon_0\mathbf{P}/c^2 = |\mathbf{D}\mathbf{k}|^2(1 + |\xi|^2)\{\mathbf{k}_0 - \mathbf{b} + \mathbf{b}(1 - |\xi|^2)/(1 + |\xi|^2)\}. \quad (6.3.5)$$

This Poynting vector allows for the definition of a new velocity \mathbf{v}_e , the velocity of energy transport. It is defined as the ratio of \mathbf{P} to the average energy density per unit volume ($\approx |\mathbf{D}\mathbf{k}|^2/2\epsilon_0$):

$$\mathbf{v}_e\omega/c^2 = \mathbf{k}_0 - \mathbf{b} + \mathbf{b}(1 - |\xi|^2)/(1 + |\xi|^2). \quad (6.3.6)$$

For non-absorbing crystals and real values of ξ , \mathbf{v}_e is identical with \mathbf{v}_g .

6.4. The ω -surface

Before discussing the ω -surface in detail, we consider first the shape of the ω -surface in the electron-band convention (see sub-section 5.1.3) for weak interaction ($V_1 \rightarrow 0$). The general expression for the ω -surface off Bragg angle is (eq. (5.1.8))

$$(\mathbf{k} - 2p\mathbf{b}_D)^2 = \omega^2/c^2 + V_0.$$

The value of the integer p has then to be adjusted in such a way that $(\mathbf{k} - 2p\mathbf{b}_D) \cdot \mathbf{b}_D$ lies between given limits. The vector $\mathbf{k} - 2p\mathbf{b}_D$ for this value

of p is denoted by \mathbf{k} . We shall use as boundaries for the Brillouin zone

$$-\mathbf{b}_D^2/2 \leq \mathbf{k} \cdot \mathbf{b}_D < 1.5 \mathbf{b}_D^2.$$

In the example of fig. 6.2 the intersection of the ω -surface with a plane through \mathbf{b}_D is shown. The circle has a radius $(1 + \frac{1}{2} \psi_0)\omega/c$. The ω -surface consists of branches, in which parts of the circle are easily recognized. In point A the wave field has as predominant component the plane wave with wave vector

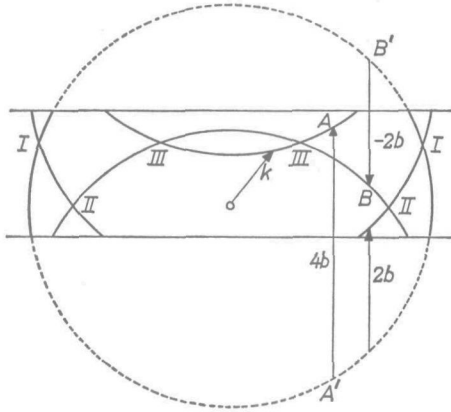


Fig. 6.2. An ω -surface in the electron-band convention. The points I, II and III correspond to the \mathbf{k} -vectors giving the first-, second- and third-order reflexion, respectively ($\mathbf{b} = \mathbf{b}_D$).

corresponding to point A'. In point B the wave with wave vector of point B' is predominant. Interesting points are the intersections, since there the wave field may have two predominant plane-wave components with wave vectors $2n\mathbf{b}_D$ apart. Apparently the Bragg condition is satisfied in these points. It is easily

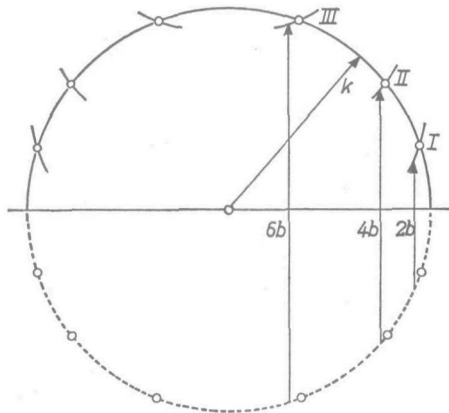


Fig. 6.3. The ω -surface in the X-ray convention for the same frequency as in fig. 6.2. The points I, II and III again correspond to the first-, second- and third-order reflexion ($\mathbf{b} = \mathbf{b}_D$).

verified that in the points labeled I, II and III the reflexions are of the first, second and third order, respectively.

In fig. 6.3 the other convention introduced in sub-section 5.1.3, is shown. Far off Bragg angle the wave field is characterized with the wave vector of its predominant plane-wave component, corresponding to a circle around the origin as ω -surface. Bragg reflexion is expected according to the basic equations (5.1.10), whenever $\vec{k}' = \vec{k} - 2\vec{n}$

$$\mathbf{k}^2 - (\mathbf{k} - 2\mathbf{n}_D)^2 = 4\mathbf{n}_D \cdot (\mathbf{k} - \mathbf{n}_D) = V_n (\xi - 1/\xi) \approx 0.$$

These regions are indicated by the small circles. They are labeled again I, II and III to indicate the order of reflexion n . It was shown, however, that in the limit $\xi \rightarrow \infty$ the ω -surface is given by eq. (5.1.12):

$$(\mathbf{k} - 2\mathbf{n}_D)^2 = \omega^2/c^2 + V_0,$$

a circle with the same radius as the one given in the figure, but now with centre $2\mathbf{n}_D$. The relevant parts of these circles are shown also in the figure.

The circles given in figs 6.2 and 6.3 are limiting values for \mathbf{k} if $V_1 \rightarrow 0$. In the X-ray case the value of V_1 is so small in comparison with ω^2/c^2 that appreciable deviations occur only in the immediate vicinity of the intersections. The scale has to be magnified by approximately a factor of $|\psi|^{-1}$ ($\approx 10^5$) in order to bring out the details. In fig. 6.4 an example is shown. The reciprocal-

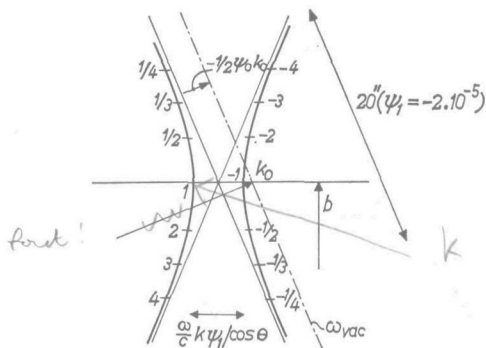


Fig. 6.4. Detail of the ω -surface in the region where Bragg reflexions occur. The value of ξ is given as parameter along the ω -surface.

lattice vector for the reflexion is \mathbf{b} . The ω -surface, given in eqs (5.3.1), is a hyperbola with the circles $\omega^2/c^2 + V_0 = \mathbf{k}^2$ or $(\mathbf{k} - 2\mathbf{b})^2$ as asymptotes. In view of the large scale they may be considered as straight lines. The shortest distance between the branches is $|\psi_1|\omega/c \cos \theta$. In the scale of fig. 6.3 this distance is less than 10^{-4} cm. Since diffraction only occurs if the deviation from the limiting circles is small ($|\xi|$ not too far from unity) the angular region for dif-

fraction in the plane of incidence is very narrow. The intersection with the sphere of radius ω/c is also given in fig. 6.4 (ω_{vac}).

The ω -surfaces for the two directions of polarization are different. The asymptotes are the same, but since K for the π -polarization is smaller than unity, the distance between the branches is in the π -polarization smaller than in the σ -polarization.

In fig. 6.4 the value of ξ is given as a parameter along the branches. On the left-hand branch ξ is positive, on the right-hand branch negative ($V_1 < 0$)*). For the limiting values of ξ , 0 or ∞ , the ω -surface approaches the appropriate circle for \mathbf{k} off Bragg angle. In the plane $\mathbf{b} \cdot (\mathbf{k} - \mathbf{b}) = 0$, $\xi = \pm 1$. The group velocity is normal to the ω -surface, according to eq. (6.3.3). From fig. 6.4 it follows that the direction of \mathbf{v}_g changes appreciably for a minute change in \mathbf{k} . The variation of \mathbf{v}_g with ξ (eq. (6.3.4)) is much less rapid. Therefore we prefer ξ to characterize the mode of propagation instead of \mathbf{k} .

In absorbing crystals and for cut-off modes, ξ is in general complex. Such situations need a closer inspection, which is given in chapter 8.

6.5. Wave fields consisting of two modes

The modes of propagation do not change in amplitude as they travel through the unbounded crystal. This is not merely a result from the assumption that the crystal does not absorb X-ray energy. In fact, we have been looking for such solutions via the equations (5.1.4) and (5.2.3). Solutions with variable amplitude in non-absorbing crystals are obtained by considering wave fields that consist of two (or more) modes of propagation. An important example is the combination of the two modes with $\xi = 1$ and $\xi = -1$. Since these modes have a different phase velocity along the reflecting planes it is possible to find a place A (fig. 6.5) where the upward-moving components are in phase and accordingly



Fig. 6.5. If the total wave field consists of two modes with $\xi = 1$ and $\xi = -1$, the power flow is not parallel to the reflecting planes everywhere. It oscillates between the directions of \mathbf{k}_0 and \mathbf{k}_0' . The distance AC is 2π times the "Pendellösung"-length L .

the downward-moving components in anti-phase. If the two modes have equal amplitudes the last two components cancel. The total wave field in A then consists of two plane waves travelling almost parallel to \mathbf{k}_0 . The Poynting vector accordingly makes an angle θ with the reflecting planes. But this situation cannot exist everywhere, because of the difference in phase velocity of the two modes. If the distance between the two \mathbf{k} -vectors is given by $\Delta\mathbf{k}$, the upward-travelling

*) If $\theta > 45^\circ$, the sign of K is reversed in the π -polarization.

components are in anti-phase a distance $\pi/|\Delta\mathbf{k}|$ further along the reflecting planes (point B). The upward-travelling components cancel and the Poynting vector makes an angle $-\theta$ with the reflecting planes. Still one distance $\pi/|\Delta\mathbf{k}|$ further along the reflecting planes the situation is identical with that in A. So if two modes of equal amplitudes with $\xi = 1$ and -1 , resp., are present in the crystal, the X-ray energy is transported along the reflecting planes over long distances, and at the same time oscillates in a direction perpendicular to the reflecting planes. In fig. 6.5 the “path” of the energy transport is shown. The period AC plays an important part later. It is connected with the “Pendel-lösung”-length L , in the following way:

$$L = 1/|\Delta\mathbf{k}| = \cos(\theta)\omega/c|V_1| = d \sin(2\theta)/\pi|\psi_1|. \quad (6.5.1)$$

From this example it is clear that any combination of two modes of propagation results in a gradually changing wave field. All such solutions, however, will be periodic, with a period equal or longer than $2\pi L$.

The gradual change in the direction of the energy flow is closely connected with the primary extinction discussed in sec. 4.3. In point A we have the situation that is treated in the kinematical theory. All atoms are subject to the field strength of one plane-parallel wave. The generation of the reflected wave causes the rotation of \mathbf{P} from \mathbf{k}_0 towards \mathbf{k}_0' . From the discussion given above it follows that the suggestion, made in sec. 4.3, to account for primary extinction by introducing an “absorption” coefficient is inadequate, because it would never lead to oscillations in the direction of \mathbf{P} .

The “Pendellösung”-length L may be considered as a characteristic length for the diffraction phenomenon. Propagation over distances short compared to L , has only a small effect on the wave fields. A kinematical approach is sufficient to calculate the change. Over distances large compared to L , the kinematical theory is incorrect and the dynamical theory has to be applied. The interaction between the two predominant plane-wave components is manifest only over distances of the order of L or larger.

7. MATCHING AT THE BOUNDARIES

7.1. Definitions

Up till now only wave fields in unbounded crystals have been considered. In this chapter we treat the matching of the wave fields inside and outside the crystal at the boundaries.

For the medium outside the crystal we choose always vacuum. The incident wave is assumed to be plane parallel with wave vector \mathbf{k}_v . Because of diffraction there may appear another plane wave in vacuum, the diffracted wave, with wave vector \mathbf{k}_r . The polarization may be either σ or π . It is the same inside and outside the crystal.

The crystal itself is assumed to be a plane-parallel slab, the boundaries flat and abrupt. The orientation of the surfaces is characterized by the surface normal \mathbf{s} , pointing into the crystal at the front surface, and the parameter γ :

$$\gamma = \mathbf{k}_v \cdot \mathbf{s} / \mathbf{k}_r \cdot \mathbf{s} = \mathbf{k}_0 \cdot \mathbf{s} / (\mathbf{k}_0 - 2\mathbf{b}) \cdot \mathbf{s}. \quad (7.1.1)$$

The small difference between \mathbf{k}_v and \mathbf{k}_0 or between \mathbf{k}_r and $\mathbf{k}_0 - 2\mathbf{b}$ in the region of diffraction has a negligible effect on γ . The value of γ may lie anywhere in between $-\infty$ and ∞ . The extreme cases of $\gamma \approx 0$ (\mathbf{k}_v almost parallel to the surface) and $\gamma \rightarrow \pm \infty$ (\mathbf{k}_r almost parallel to the surface) will not be discussed.

Depending on the sign of γ two situations can be distinguished:

(a) *The Laue case of diffraction*, if $\gamma > 0$. An example is shown in fig. 7.1a.

At the front surface both \mathbf{k}_v and \mathbf{k}_r are pointing into the crystal, and at the

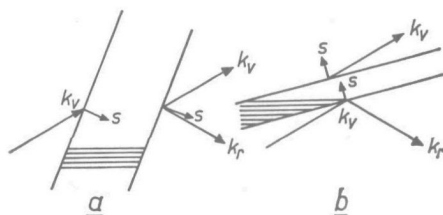


Fig. 7.1. The Laue case (a) and the Bragg case (b) of diffraction. The important difference lies in the direction of \mathbf{k}_r with respect to the surface. In the Laue case \mathbf{k}_r is pointing into the crystal at the front surface, in the Bragg case at the back surface.

back surface both are pointing outwards. Consequently there is in front of the crystal only an incident wave and behind the crystal a transmitted wave (wave vector \mathbf{k}_v) as well as a diffracted wave (wave vector \mathbf{k}_r). In the case $\gamma = 1$, the symmetrical Laue case, the surface is perpendicular to the reflecting planes.

(b) *The Bragg case of diffraction*, if $\gamma < 0$ (fig. 7.1b). Now the orientation of the surface is such, that at the front surface \mathbf{k}_r is pointing into the vacuum. There are an incident and a reflected wave in front of the crystal and only

a transmitted wave (wave vector \mathbf{k}_v) behind the crystal. In the case $\gamma = -1$, the symmetrical Bragg case, the reflecting planes are parallel to the surface.

7.2. Matching of k-vectors *)

The wave fields inside and outside the crystal must have the same periodicity along the surface. Accordingly the wave vector of the modes activated inside the crystal, have to satisfy the relation

$$\mathbf{k} = \mathbf{k}_v + \tau_1 \mathbf{s}, \quad \text{--- } k_v \sin \theta = k \sin \theta' \quad (7.2.1)$$

where τ_1 has to be adjusted in such a way that \mathbf{k} lies on the ω -surface. Since \mathbf{k} is almost equal to \mathbf{k}_v , the value of τ_1 is small compared with ω/c . Substitution of eq. (7.2.1) into the basic equations and eliminating τ_1 leads to (terms in τ_1^2 being neglected)

$$V_1 (\xi - \gamma/\xi) = (\gamma - 1) V_0 + 4\gamma \mathbf{b} \cdot (\mathbf{k}_v - \mathbf{b}). \quad (7.2.2)$$

From this equation follows there are two values of ξ , one for each of the two modes of propagation that are activated inside the crystal. They are closely related to each other:

$$\xi_1 \xi_2 = -\gamma, \quad (7.2.3)$$

a result that we shall use frequently. The magnitude of τ_1 is given by

$$2\tau_1 \mathbf{k}_0 \cdot \mathbf{s} = V_0 + V_1 \xi. \quad (7.2.4)$$

Note that τ_1 is indeed small compared with ω/c in the region of diffraction.

Both modes contain also a predominant plane-wave component $\mathbf{k} - 2\mathbf{b}$ that has to be matched to the reflected wave in vacuum, if such a wave is present (back-surface Laue case and front-surface Bragg case):

$$\mathbf{k} - 2\mathbf{b} = \mathbf{k}_r + \tau_2 \mathbf{s}. \quad \text{--- } k \sin \theta = k' \sin \theta' \quad (7.2.5)$$

In general $\tau_2 \neq \tau_1$, so that \mathbf{k}_r is only approximately equal to $\mathbf{k}_v - 2\mathbf{b}$.

A simple construction for the wave vectors \mathbf{k}_1 and \mathbf{k}_2 of the modes activated inside the crystal, for given \mathbf{k}_v and \mathbf{s} , is shown in fig. 7.2 (fig. 7.2a for the Laue case and fig. 7.2b for the Bragg case). The wave vectors are found as the intersections of the ω -surface with a line parallel to \mathbf{s} through \mathbf{k}_v . In the Laue case of diffraction the two solutions lie on different branches. In view of later discussions it is important to note that the velocity of energy transport is never closely parallel to the surface. Both modes travel into the crystal. At the back surface they decompose into two uncoupled plane waves, one with wave vector \mathbf{k}_v and one with wave vector \mathbf{k}_r . The vector $\mathbf{k}_r + 2\mathbf{b}$ is given in the figure.

*) Although non-absorbing crystals are discussed, all results derived in this and the next section, are valid in absorbing crystals also. Only the appropriate " ω -surface" has to be used.

In the Bragg case of diffraction (fig. 7.2*b*) the two \mathbf{k} -vectors lie on the same branch or there are no intersections at all. If there are two solutions, the energy velocity of one mode (\mathbf{k}_1) is pointing into the crystal and gives an energy flow from the front to the back surface. For the other mode the energy velocity is such that the energy flows from the back surface to the front. Behind the crystal there is only one plane wave parallel to \mathbf{k}_v . In front of the crystal there are two

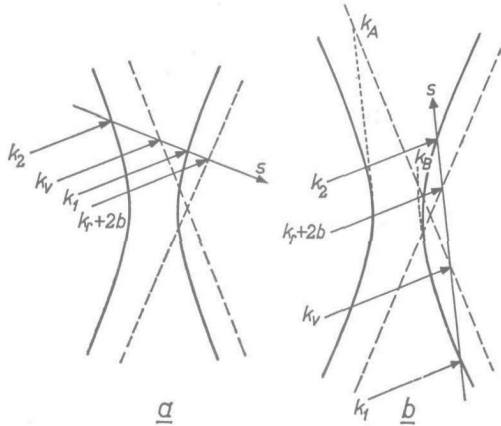


Fig. 7.2. Graphical representation of eq. (7.2.1). The wave vectors \mathbf{k}_1 and \mathbf{k}_2 of the modes excited inside the crystal and the wave vector of the diffracted wave plus the relevant reciprocal-lattice vector ($\mathbf{k}_r + 2\mathbf{b}$) fall on a straight line parallel to the surface normal (\mathbf{s}) passing through the wave vector of the incident wave (\mathbf{k}_v). In the Laue case there are always two solutions for \mathbf{k} , one on each branch (a). In the Bragg case there are either two solutions for \mathbf{k} on the same branch, or no real solutions at all (b).

waves, one parallel to \mathbf{k}_v and the other parallel to \mathbf{k}_r with $\mathbf{k}_r + 2\mathbf{b}$ given in the figure. For \mathbf{k}_v equal to either \mathbf{k}_A or \mathbf{k}_B there are two coincident solutions for \mathbf{k} . The energy velocity of these modes is parallel to the surface. Between \mathbf{k}_A and \mathbf{k}_B there exist no real solutions for \mathbf{k} . However, eq. (7.2.2) may be solved in these situations, but the resulting ξ -values are complex, leading to complex values of \mathbf{k} . We shall deal with these cut-off modes in the next chapter.

7.3. Matching of amplitudes

The second requirement for matching concerns the amplitudes. The tangential components of \mathbf{E} and \mathbf{H} , and the normal components of \mathbf{D} and \mathbf{B} have to be continuous. In view of the small change in the "optical density" some simplifications are possible. In the first place one may neglect the wave reflected from the surface as if it were a mirror (the \mathbf{k} -vector of this wave is the other intersection of the ω -surface in vacuum, with the line parallel to \mathbf{s} through \mathbf{k}_v). Secondly the matching of the total amplitude of \mathbf{B} and \mathbf{D} suffices. Working out this condition shows that it is equivalent to matching the dielectric displacements inside and outside the crystal, of the upward- and downward-travelling waves separately.

Far off Bragg angle the wave penetrates the crystal without change in amplitude. Near Bragg angle distinction must be made between the Laue and the Bragg cases, as well as between the front and back surfaces.

$$\begin{aligned}
 \text{Laue case: front surface: } & D_0 = D_1 + D_2, \\
 & 0 = \xi_1 D_1 + \xi_2 D_2, \\
 \text{back surface: } & D_t = D_1' + D_2', \\
 & D_r = \xi_1 D_1' + \xi_2 D_2';
 \end{aligned} \tag{7.3.1}$$

$$\begin{aligned}
 \text{Bragg case: front surface: } & D_0 = D_1 + D_2, \\
 & D_r = \xi_1 D_1 + \xi_2 D_2, \\
 \text{back surface: } & D_t = D_1' + D_2', \\
 & 0 = \xi_1 D_1' + \xi_2 D_2';
 \end{aligned} \tag{7.3.2}$$

here D_0 , D_r and D_t represent the amplitudes in vacuum of the incident, reflected and transmitted wave, respectively. The two modes activated inside the crystal are characterized by ξ_1 and ξ_2 , respectively, their amplitudes being D_1 and D_2 at the front surface and D_1' and D_2' at the back surface. The relation between the amplitudes with and without prime is determined by the phase behaviour of the mode via the \mathbf{k} -vector.

Note that in the Bragg case the amplitude of the reflected wave in front of the crystal depends on what happens at the back surface.

7.4. Total reflexion

In the discussion of the \mathbf{k} -matching for the Bragg case of diffraction (sec. 7.2) it was pointed out that there is a region of directions of \mathbf{k}_v where the solutions for ξ are not real. According to eq. (7.2.2) this region is given by

$$2V_1(-\gamma)^{1/2} < (\gamma - 1)V_0 + 4\gamma\mathbf{b} \cdot (\mathbf{k}_v - \mathbf{b}) < -2V_1(-\gamma)^{1/2}. \tag{7.4.1}$$

The value of ξ is then

$$\xi = (-\gamma)^{1/2} \exp(j\varphi), \tag{7.4.2}$$

with

$$2(-\gamma)^{1/2} V_1 \cos \varphi = (\gamma - 1)V_0 + 4\gamma\mathbf{b} \cdot (\mathbf{k}_v - \mathbf{b}). \tag{7.4.3}$$

There are two possible solutions for ξ , one giving rise to an exponentially decreasing amplitude for deeper penetrations (via the complex \mathbf{k} -vector) and one giving an exponential increase.

Imagine now (fig. 7.3) a plane wave with a wave vector \mathbf{k}_v satisfying the condition (7.4.1), striking a crystal of such thickness that the exponentially decreasing mode is attenuated to a negligible amplitude before it reaches the back surface. The mode with increasing amplitude is then not excited at the

front surface. From the first pair of eq. (7.3.2) it follows that the reflected wave and the incident wave have an amplitude ratio

$$D_r/D_0 = \xi_1.$$

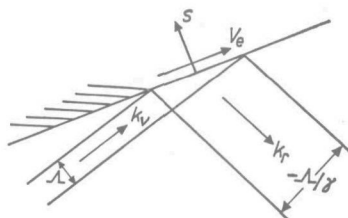


Fig. 7.3. If there are no real solutions for \mathbf{k} in the Bragg case the net power flow inside the crystal is parallel to the surface and the incident wave is totally reflected. The crystal is assumed to be thick and non-absorbing.

With the aid of fig. 7.3 one may deduce that the ratio of the X-ray power impinging on (I_0) and reflected from (I_R) a unit area of the surface is given by

$$I_R/I_0 = -(1/\gamma)|D_r/D_0|^2 = -|\xi_1|^2/\gamma. \quad (7.4.4)$$

Above we found $|\xi|$ to be equal to $(-\gamma)^{1/2}$ (eq. (7.4.2)), so that

$$I_R/I_0 = 1.$$

Apparently the reflexion is total in the region where the solutions for ξ and \mathbf{k} are complex. The incident X-ray energy is not transported into the crystal but reflected completely. This is in agreement with the fact that in these cases the velocity of energy transport is parallel to the surface, as may be verified easily with the aid of eq. (6.3.6) taking into account the definition of γ (eq. (7.1.1)).

If \mathbf{k}_p is oriented outside the region of total reflexion the velocity of energy transport is pointing into the crystal and the reflexion coefficient is smaller than unity.

In absorbing crystals the reflexion coefficient is always smaller than unity. A net influx of power is necessary to maintain the wave field present inside the crystal. If the absorption per "Pendellösung"-length is small, however, the reflectivity is still close to unity over an appreciable region in \mathbf{k}_p (see fig. 9.14).

In the later discussions the region of high reflectivity, occurring in the Bragg case of diffraction only, plays an important part. In this region the familiar concepts of absorption coefficient and X-ray lose their normal meaning.

8. ABSORPTION AND EXTINCTION

8.1. Introduction

In this chapter exponentially damped modes are discussed. Such modes we have already found in non-absorbing crystals in the Bragg case of diffraction and total reflexion (sec. 7.4). The decrease in amplitude is due to a special interference phenomenon: *extinction*. In absorbing crystals such modes must always be present, because part of the X-ray energy in the wave field is transformed into other forms of energy. However, in absorbing crystals extinction may take place also, but it is then always mixed with absorption. A sharp distinction between the two types of attenuation is not possible.

According to sec. 5.3, exponentially damped modes are obtained by making V_0 , V_1 and ξ complex. The following notation will be used:

$$\begin{aligned} V_0 &= \underline{V}_0 + jW_0, \\ V_1 &= \underline{V}_1 + jW_1, \\ \xi &= |\xi| \exp(j\varphi), \quad 0 \leq |\varphi| \leq \pi. \end{aligned} \tag{8.1.1}$$

A bar underneath the symbol denotes the real part. In practical cases both $|W_0|$ and $|W_1|$ are small compared with $|V_0|$ and $|V_1|$. The wave vector \mathbf{k} has to be complex too:

$$\mathbf{k} = \underline{\mathbf{k}} + j\mathbf{K}. \tag{8.1.2}$$

The real part describes the phase behaviour and the imaginary part the amplitude behaviour. The planes in real space perpendicular to \mathbf{K} are planes of equal amplitude and the relative decrease in amplitude per unit length in the direction of \mathbf{K} is given by $|\mathbf{K}|$.

In non-absorbing crystals and no extinction the two basic equations allow for the determination of $|\underline{\mathbf{k}}|$ and ξ if ω and the direction of $\underline{\mathbf{k}}$ are given. In the general case with complex parameters the basic equations represent four relations from which a solution may be obtained if the directions of both $\underline{\mathbf{k}}$ and \mathbf{K} are given. For a given orientation of the surface we know that the component of \mathbf{k} parallel to the surface has to be continuous and that the vector \mathbf{K} must be perpendicular to the surface since the planes of equal amplitude are parallel to the surface. The boundary condition, eq. (7.2.1), still applies, the adjustable parameter τ_1 being complex. Although the problem of diffraction in a plane slab of an absorbing perfect crystal is now completely solvable, a complication arises, in comparison with non-absorbing crystals, since the parameters $|\mathbf{K}|$, $|\xi|$ and φ depend on the orientation of the surface at which the mode was generated. The origin of the complication is that we had to introduce the vector \mathbf{K} to describe the damping. In optics and in the kinematical theory the attenuation is usually accounted for by means of a *scalar* parameter, the ab-

sorption coefficient, giving the relative decrease in power flow per unit length in the direction of the power flow. The question we want to discuss is under what conditions the use of an absorption coefficient is allowed and when it is imperative to use the attenuation vector \mathbf{K} .

Let us compare modes of propagation with the same direction of energy transport, but generated at surfaces with different orientations. These modes have the same value of $|\xi|$ since \mathbf{v}_e is a function of $|\xi|$ only (eq. (6.3.6)). The vector \mathbf{K} has an orientation and magnitude that is sensitive to the direction of the surface normal. The notion absorption coefficient now implies that the relative decrease in amplitude in the direction of \mathbf{v}_e is insensitive to a change in \mathbf{s} . In other words, the definition of an absorption coefficient,

$$\mu = -2\mathbf{K} \cdot \mathbf{v}_e/|\mathbf{v}_e|, \quad (8.1.3)$$

is an adequate one, as long as the value of μ is independent of the orientation of \mathbf{K} in respect to \mathbf{v}_e .

In this chapter it will be shown that an absorption coefficient is an adequate description of the damping if the velocity of energy transport is not closely parallel to the surface. In all other cases where \mathbf{v}_e is almost parallel to the surface, viz. total reflexion and glancing incidence, the orientation of \mathbf{s} with respect to \mathbf{v}_e plays a part in the attenuation in the direction of \mathbf{v}_e . It must be remarked that this limitation in the applicability of μ is also present in optics. In the case of total reflexion the decrease in amplitude of the light wave in the less dense medium is not given correctly by the absorption coefficient.

In view of this result we shall distinguish between two types of modes (excluding the case of glancing incidence):

(1) *Cut-off modes*, where the decrease in amplitude is mainly due to extinction. The transport of energy in these modes is almost parallel to surface. The small component of the power flow into the crystal is only necessary to maintain the wave field inside the crystal. The greater part of the incident X-ray power is reflected. In the mathematical treatment the attenuation has to be described with the vector \mathbf{K} . We shall show that the phase angle φ in ξ may have any value that is not close to either 0 or $\pm \pi$. The magnitude of $\mathbf{K} \cdot \mathbf{v}_e/|\mathbf{v}_e|$ is not constant for given $|\xi|$, but still depends on φ . The real part of the wave vector does not lie close to the ω -surface discussed in sec. 6.4.

(2) *Surface-independent modes*, where the decrease in amplitude is mainly due to absorption. The velocity of energy transport of these modes is not closely parallel to the surface. The relative decrease in power flow may be described with an absorption coefficient. The magnitude of $\mathbf{K} \cdot \mathbf{v}_e/|\mathbf{v}_e|$ is now independent of φ , which is always close to either 0 or $\pm \pi$. The real part of the wave vector always lies very close to the branches of the ω -surface. In the mathematical treatment of such modes the parameters V_0 , V_1 , \mathbf{k} and ξ can be considered as real, provided an absorption coefficient is attributed to the mode characteristics.

If such a treatment gives $\xi^2 = -\gamma$ then the modes have cut-off character and the approximation of real parameters is incorrect.

In non-absorbing crystals the modes activated in the crystal are either surface-independent and then undamped, or cut-off modes. In absorbing crystals the distinction is not sharp. It is possible to activate modes with properties in between, namely in the regions just outside total reflexion in the Bragg case. Since these regions are narrow for low absorption coefficients, we shall not deal with them.

Experimentally it has been found that the relative decrease in amplitude per wavelength is always very small. The higher-order terms in \mathbf{K} in comparison with higher-order terms in \mathbf{k} shall be neglected. This procedure leads to the inconsistent result $|\mathbf{K}| \approx \omega/c$ when either \mathbf{k}_o or \mathbf{k}_r is closely parallel to the surface (glancing incidence or glancing reflexion), situations that are left out of consideration.

Finally it is supposed that \mathbf{s} lies in the plane of incidence. If this is not the case, the calculations below give the component of \mathbf{K} in the plane of incidence and \mathbf{s} represents the unit vector in the plane of incidence parallel to the projection of the surface normal on this plane.

8.2. Mathematical treatment

The equations involved in the mathematical treatment of exponentially damped modes are rather complicated. In this section a number of equations are given. The discussion comes in later sections.

To characterize the material it is convenient to introduce

$$g = W_0/\underline{V}_1, \quad \epsilon = W_1/W_0, \quad r = \underline{V}_0/\underline{V}_1. \quad (8.2.1)$$

Far off Bragg angle the basic equations read

$$\begin{aligned} \underline{\mathbf{k}}^2 &= \omega^2/c^2 + \underline{V}_0 \\ 2\underline{\mathbf{k}} \cdot \mathbf{K} &= W_0. \end{aligned} \quad (8.2.2)$$

The term \mathbf{K}^2 is neglected. The second equation shows that the component of \mathbf{K} in the direction of $\underline{\mathbf{k}}$ is the only relevant one. It is small compared with ω/c .

Near to Bragg angle we obtain

$$\begin{aligned} \underline{\mathbf{k}}^2 &= \omega^2/c^2 + \underline{V}_1 \{r + \cos(\varphi)|\xi| - \epsilon g \sin(\varphi)|\xi|\}, \\ (\underline{\mathbf{k}} - 2\mathbf{b})^2 &= \omega^2/c^2 + \underline{V}_1 \{r + \cos(\varphi)/|\xi| + \epsilon g \sin(\varphi)/|\xi|\}, \\ 2\underline{\mathbf{k}} \cdot \mathbf{K} &= \underline{V}_1 \{g + \sin(\varphi)|\xi| + \epsilon g \cos(\varphi)|\xi|\}, \\ 2(\underline{\mathbf{k}} - 2\mathbf{b}) \cdot \mathbf{K} &= \underline{V}_1 \{g - \sin(\varphi)/|\xi| + \epsilon g \cos(\varphi)/|\xi|\}. \end{aligned} \quad (8.2.3)$$

We shall introduce the dimensionless parameters A , B , C and D , corresponding

to the components of $\underline{\mathbf{k}} - \mathbf{k}_0$ and \mathbf{K} parallel and perpendicular to the reflecting planes in units of the reciprocal "Pendellösung"-length L :

(8.2.4)

$$\begin{aligned} -2L(k_{\parallel} - k_0 \cos \theta) &= r + C = r + \frac{1}{2}(|\xi| + |\xi|^{-1}) \cos \varphi - \frac{1}{2}\epsilon g(|\xi| - |\xi|^{-1}) \sin \varphi, \\ -2L(k_{\perp} - k_0 \sin \theta) \tan \theta &= A = \frac{1}{2}(|\xi| - |\xi|^{-1}) \cos \varphi - \frac{1}{2}\epsilon g(|\xi| + |\xi|^{-1}) \sin \varphi, \\ -2L K_{\parallel} &= g + D = g + \frac{1}{2}(|\xi| - |\xi|^{-1}) \sin \varphi + \frac{1}{2}\epsilon g(|\xi| + |\xi|^{-1}) \cos \varphi, \\ -2L K_{\perp} \tan \theta &= B = \frac{1}{2}(|\xi| + |\xi|^{-1}) \sin \varphi + \frac{1}{2}\epsilon g(|\xi| - |\xi|^{-1}) \cos \varphi. \end{aligned}$$

Since the parameters A , B , C and D are functions of the two variables $|\xi|$ and φ only, there must exist two relations between them:

$$AB - CD = -\epsilon g, \tag{8.2.5}$$

$$A^2 - B^2 - C^2 + D^2 = -1 + \epsilon^2 g^2.$$

For given value of $|\xi|$ and φ both $\underline{\mathbf{k}}$ and \mathbf{K} are single-valued. All values of $\underline{\mathbf{k}}$ fall in a well-defined region of \mathbf{k} -space. It is bounded by the hyperbolae

$$C^2 - A^2 = 1 \tag{8.2.6}$$

and

$$C^2 - A^2 = -\epsilon^2 g^2. \tag{8.2.7}$$

The first one corresponds with the expression for the ω -surface for undamped modes ($g = 0$ and real values of ξ). In fig. 8.1 an example is shown. The scale is the same as in fig. 6.4. The numerical values underlying the figure are

$$g = 0.125, \quad \epsilon = 0.8, \quad \tan \theta = 0.5.$$

For an arbitrary value of φ the values of $\underline{\mathbf{k}}$ fall on the hyperbola

$$C^2 - A^2 = \cos^2 \varphi - \epsilon^2 g^2 \sin^2 \varphi. \tag{8.2.8}$$

The influence of extinction or absorption is hence determined by the value of φ . If φ is close to 0 or $\pm \pi$, the vector $\underline{\mathbf{k}}$ lies close to the ω -surface for no absorption ($g \rightarrow 0$). Only when $\cos^2 \varphi$ is significantly less than unity, are appreciable deviations from the ω -surface present. The values of $\underline{\mathbf{k}}$ for a given value of $|\xi|$ fall on ellipses that touch the 4 hyperbola branches given in eqs (8.2.6) and (8.2.7). Note that for small values of g these ellipses are very eccentric.

The allowed values for \mathbf{K} fall between the hyperbolae

$$D^2 - B^2 = \epsilon^2 g^2, \tag{8.2.9}$$

and

$$D^2 - B^2 = -1. \tag{8.2.10}$$

In fig. 8.2 this region is shown. The scale is the same as in fig. 8.1 so that $|\mathbf{K}| \ll \omega/c$, except when \mathbf{K} is almost parallel to the asymptotes. It is easily verified, however, that there either the incident or the reflected wave is closely

parallel to the surface (\mathbf{K}/s), a possibility deliberately left out of discussion. For a given value of $|\xi|$ the possible values of \mathbf{K} fall on an ellipse that touches the four branches of the hyperbolae given by eqs (8.2.9) and (8.2.10). For small

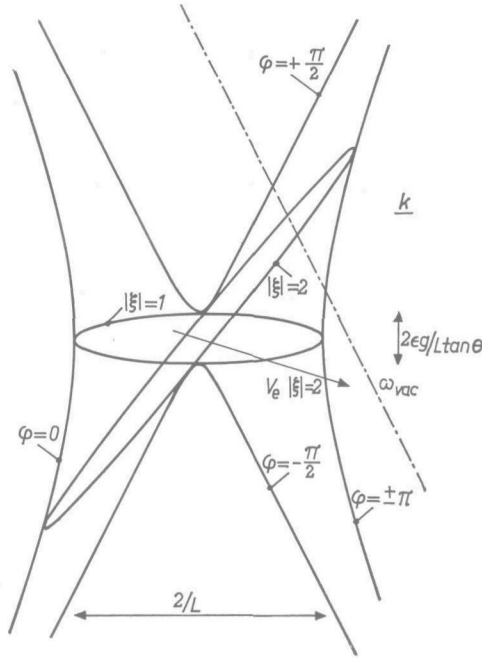


Fig. 8.1. If one allows for complex values of ξ , the real part of the possible wave vectors for given frequency fall within a region bounded by the hyperbolae. The ellipses represent the possible values of \mathbf{k} for given $|\xi|$. The phase angle in ξ is φ .

values of ϵg they are very eccentric. All modes with given $|\xi|$ have the same velocity of energy transport \mathbf{v}_e (eq. (6.3.6)). It can be shown by straightforward calculation that \mathbf{v}_e is parallel to the short axis of the ellipse. For a given value of φ the possible \mathbf{K} -values fall on the hyperbola:

$$D^2 - B^2 = (\epsilon g)^2 \cos^2 \varphi - \sin^2 \varphi. \quad (8.2.11)$$

For a given orientation of the surface an incident plane-parallel wave generates inside the crystal only those modes for which \mathbf{K} is parallel to the surface normal. It may be verified that in the terms now introduced, the condition \mathbf{K}/s leads to

$$g + D = B(\gamma + 1)/(\gamma - 1). \quad (8.2.12)$$

Elimination of B and D from eqs (8.2.5) and (8.2.12) gives a relation between A and C :

$$(A^2 - C^2 + 1 - \epsilon^2 g^2)[(\gamma - 1) A - (\gamma + 1) C]^2 =$$

$$= g^2 [(\gamma - 1)^2 (C + \epsilon)^2 - \{(\gamma - 1) A + (\gamma + 1) \epsilon\}^2]. \quad (8.2.13)$$

Since A and C correspond to the components of \mathbf{k} perpendicular and parallel to the reflecting planes, respectively, eq. (8.2.13) gives the allowed values of \mathbf{k} for given orientation of the surface and given ω . Apparently this “ ω -surface”

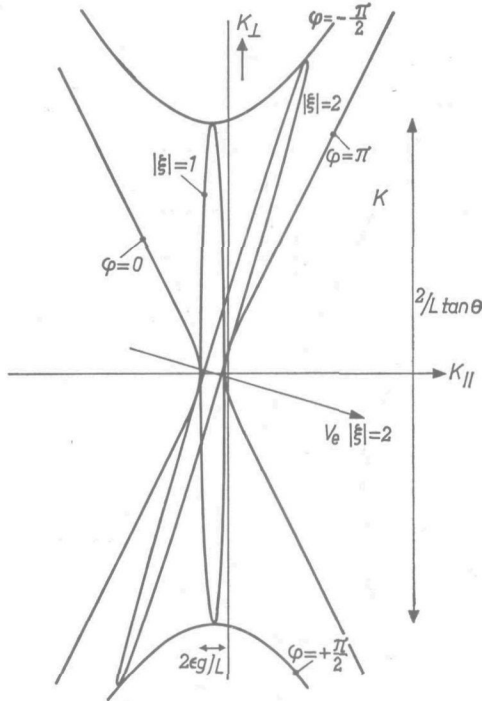


Fig. 8.2. The counterpart of fig. 8.1, giving the imaginary part of the possible wave vectors for given ω . If $|\xi|$ is given the \mathbf{K} -values fall on an ellipse with the short axis parallel to the velocity of energy transport.

does not coincide with the ω -surface found for undamped modes (eq. (8.2.6)). To distinguish between the two types of ω -surfaces we shall refer to the relation between \mathbf{k} and ω for absorbing crystal slabs of given orientation, as “ ω -surface”.

For given A and C the components of \mathbf{K} are easily found from

$$D = g (C + \epsilon)(\gamma - 1) / \{(\gamma + 1) C - (\gamma - 1) A\}$$

(8.2.14)

and

$$B = g \{(\gamma - 1) A + (\gamma + 1) \epsilon\} / \{(\gamma + 1) C - (\gamma - 1) A\}.$$

8.3. The “ ω -surface”

In absorbing crystals the real part of the wave vector of a mode of propagation does not fall on the ω -surface for undamped modes discussed in sec. 6.4.

In this section the new “ ω -surface” is discussed for two simple cases: the symmetrical Laue case and the symmetrical Bragg case. Further we shall show that because the experimentally determined values of ϵg are small, the “ ω -surface” practically coincides with the ω -surface for undamped modes, except for the cut-off modes, which have a velocity of energy transport almost parallel to the surface.

In the *symmetrical Laue case* ($\gamma = 1$) the “ ω -surface” is given by (see eq. (8.2.13))

$$A^2 = (C^2 - 1) (1 + \epsilon^2 g^2 / C^2), \quad (8.3.1)$$

where A and C are related to the components of $\mathbf{k} - \mathbf{k}_0$ perpendicular and parallel to the reflecting planes (eqs (8.2.4)). In fig. 8.3 the “ ω -surface” is drawn

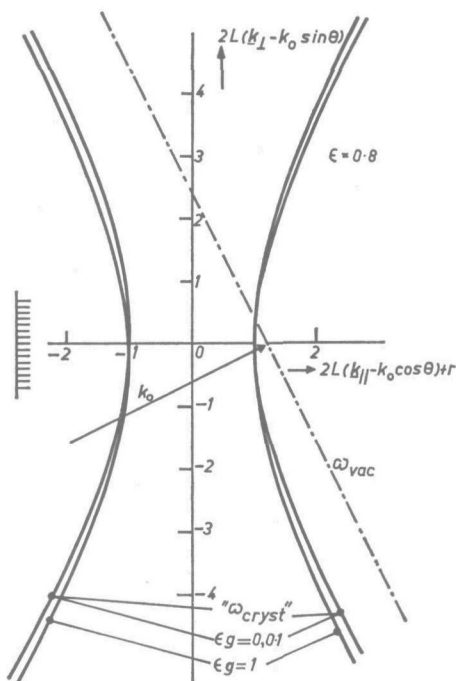


Fig. 8.3. The “ ω -surface” in the symmetrical Laue case for different values of g .

for $\epsilon g = 0, 0.1$ and 1 . The curve for $\epsilon g = 0$ is the ω -surface discussed earlier. For $\epsilon g = 0.1$, the difference with the ω -surface is so small that it cannot be shown in the figure. Only for the extremely large value of $\epsilon g = 1$ is there a significant deviation. Since practical values of ϵg are smaller than 0.1 the deviations are negligible in the symmetrical Laue case. An immediate consequence thereof is that the phase angle φ in ξ remains always close to either 0 (left-hand branch) or $\pm \pi$ (right-hand branch) and all possible modes are surface-independent.

In the *symmetrical Bragg case* ($\gamma = -1$) the “ ω -surface” is given by

$$A^2 = C^2 - 1 + g^2 \{-1 + \epsilon^2 + (C + \epsilon)^2/A^2\}. \quad (8.3.2)$$

In fig. 8.4 it is drawn for the same values of ϵg as used in fig. 8.3. Only one branch is shown, namely that one for which the energy velocity is pointing into the crystal ($|\xi| \leq 1$). The other branch is found by reversing the sign of the vertical axis. For $\epsilon g = 0$ the “ ω -surface” consists of two parts: the ω -surface

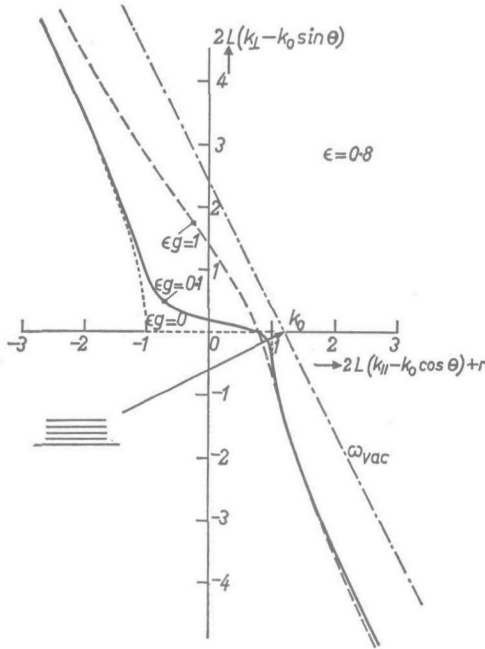


Fig. 8.4. The “ ω -surface” in the symmetrical Bragg case for different values of g .

for undamped, surface-independent modes and a horizontal straight line (dotted curve). Along this straight line $|\xi|$ is unity and accordingly, the velocity of energy transport is parallel to the surface. The matching of such modes of propagation with plane-parallel waves in vacuum requires that in vacuum the power flow is parallel to the surface also, indicating a reflexion of 100% (total reflexion). The phase angle φ is not equal to 0 or $\pm \pi$. Hence the modes must have cut-off character with an exponential decrease ($0 < \varphi < \pi$) or an exponential increase ($-\pi < \varphi < 0$) in amplitude in the direction perpendicular to the surface and energy transport.

For $\epsilon g = 0.1$ the sharp kinks in the “ ω -surface” for $\epsilon g = 0$, are replaced by smooth bends. The deviations in \underline{k} due to absorption and extinction are only appreciable near to and in between these bends. In this region the value of $|\xi|$ is close to unity, indicating strong reflexion and φ is neither close to 0

or $\pm \pi$, showing that the cut-off character is strong. Outside this region of the " ω -surface" the deviations from the ω -surface are small and the value of φ is either close to 0 (left-hand branch) or close to $\pm \pi$ (right-hand branch).

For $\epsilon g = 1$ the deviations are large in the left-hand side and centre of the figure. On the right-hand side the deviations remain small.

From these examples we draw the conclusion that if ϵg is small the relation between \mathbf{k} and ω is not significantly influenced by the finite value of ϵg , except for such situations that the energy velocity of the mode is parallel to the surface (total reflexion). This conclusion may be verified also by considering the general expression for the " ω -surface", eq. (8.2.13). The right-hand side is small for small values of g . In the left-hand side either the first or the second factor has to be small. If the first factor is small one obtains the expression for the ω -surface for undamped modes in a first approximation. If the second factor is small the \mathbf{k} -value must satisfy the condition

$$(\gamma - 1) A = (\gamma + 1) C.$$

In the limit $g \rightarrow 0$ this corresponds to (eq. (8.2.4))

$$|\xi|^2 = -\gamma.$$

It is easily verified that this condition leads to modes of propagation with an energy transport parallel to the surface.

8.4. Absorption coefficient

As pointed out in the introduction to this chapter we want to introduce an absorption coefficient

$$\mu = -2\mathbf{K} \cdot \mathbf{v}_e / |\mathbf{v}_e|$$

to describe the relative decrease in power flow per unit length in the direction of the power flow. To make this definition an adequate one, it must be required that μ is insensitive to the direction of \mathbf{K} . It is not necessary that μ be independent of the direction of \mathbf{v}_e , the direction of energy transport.

From eqs (8.2.4) and the expression (6.3.6) for \mathbf{v}_e it follows immediately:

$$-2L \mathbf{K} \cdot \mathbf{v}_e / c = g \cos(\theta) \{1 + 2\epsilon |\xi| \cos(\varphi) / (1 + |\xi|^2)\}. \quad (8.4.1)$$

The influence of the surface orientation is expressed in the factor $\cos \varphi$. Now we found in the previous section that $\cos^2 \varphi$, the measure for the distance between \mathbf{k} and the ω -surface, is close to unity, if the velocity of energy transport is not closely parallel to the surface. By excluding this possibility, we can write for $\cos \varphi$ either 1 or -1 , dependent on whether \mathbf{k} is close to the left-hand branch or the right-hand branch of the ω -surface. Thus we find

$$\mu = g \{1 + 2\epsilon \xi / (1 + \xi^2)\} \cos(\theta) c / |\mathbf{v}_e| L,$$

where ξ is now a real parameter, either positive or negative. This value of μ is

insensitive to the orientation of the surface at which the mode with given $|\xi|$ was excited. Therefore we refer to these modes as surface-independent modes. The only necessary condition is $\sin^2 \varphi \ll 1$. This result follows also from fig. 8.2, where the possible values of \mathbf{K} are shown. For given $|\xi|$ the vectors \mathbf{K} fall on a very eccentric ellipse. The variable along the ellipse is φ . Since the power flow of all these modes is parallel to the short axis, we see that over a large portion of the ellipse $\mathbf{K} \cdot \mathbf{v}_e$ is constant. Appreciable deviations do occur only near the ends of the long axis, where φ is far from either 0 or $\pm \pi$ and where the vector \mathbf{K} , which is parallel to \mathbf{s} , is almost perpendicular to \mathbf{v}_e .

The value of the absorption coefficient far off Bragg angle, μ_0 , is found by setting ξ equal to either 0 or $\pm \infty$ and $|\mathbf{v}_e| = c$:

$$\mu_0 = g \cos(\theta)/L = -W_0 c/\omega. \tag{8.4.2}$$

The expression for μ now reads

$$\mu = \mu_0 \{1 + 2\epsilon\xi/(1 + \xi^2)\} c/|\mathbf{v}_e|. \tag{8.4.3}$$

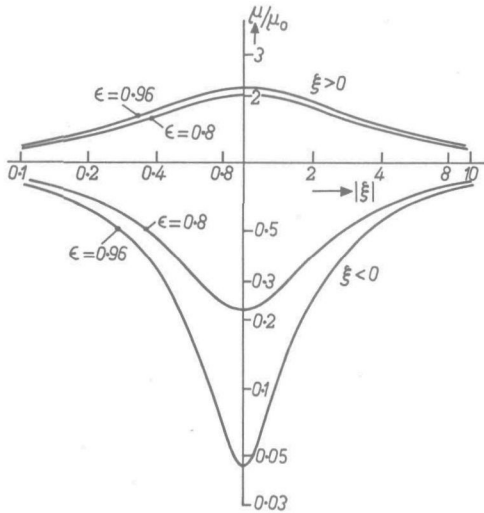


Fig. 8.5. The value of μ/μ_0 , as calculated from eq. (8.4.3), vs $|\xi|$, for two different values of ϵ ($\tan \theta = 0.5$). Note that the absorption is enhanced for $\xi > 0$ and reduced for $\xi < 0$. The minimum value of μ/μ_0 is equal to $(1 - \epsilon)/\cos \theta$.

In fig. 8.5 the values of μ/μ_0 are plotted as a function of $|\xi|$ for two values of ϵ . If ξ is positive (left-hand branch) the absorption is enhanced. If ξ is negative (right-hand branch) the absorption is reduced. The value of μ is minimum for $\xi = -1$. It is equal to $\mu_0 (1 - \epsilon)/\cos \theta$. For the σ -polarization and a location of the absorbing electrons close to the reflecting planes, ϵ is close to unity, leading to a minimum value of μ much smaller than μ_0 . The

explanation is simple. The mode with $\xi = -1$ has its nodes with zero amplitude, in the reflecting planes (see fig. 6.1). Thus the electric field is very small at the location of the absorbing electrons. For $\xi = 1$ the electric field is strong there, thereby leading to enhanced absorption. This very low absorption coefficient for the mode with $\xi = -1$ in the σ -polarization is responsible for the phenomenon of anomalous transmission in perfect crystals.

9. X-RAY BEAMS

9.1. Introduction

In view of the further development of the theory to lightly deformed crystals we want to introduce X-ray beams in the same way as in geometrical optics where light rays are introduced to describe the path of light energy through prisms, lenses and inhomogeneous media. Such rays of light are supposed to have the following properties:

(1) The width, A , of the beam is constant in a uniform medium provided the path length is shorter than A^2/λ , with λ the wavelength. Beyond this path length the beam diverges with apex angle λ/A , because of diffraction.

(2) The electromagnetic energy present in the ray travels in the direction of the path.

(3) The wave field inside the beam is characterized by one wave vector \mathbf{k} . Along the path this value of \mathbf{k} is constant. At a boundary between different media the directions of the paths (parallel to \mathbf{k}) are matched by using Snell's law.

(4) The intensity of the ray is given by

$$I = \int_S \mathbf{P} \cdot \mathbf{u} \, dS, \quad (9.1.1)$$

where \mathbf{P} is the local value of the Poynting vector and S the cross-sectional area of the beam perpendicular to an arbitrary unit vector \mathbf{u} . The relative decrease in intensity of the ray per unit path length is given by an absorption coefficient.

In this chapter we shall discuss the question whether or not it is possible to introduce well-behaved X-ray beams with the same properties. The procedure is to construct a wave packet in a given plane of incidence, centred around one complex value of the wave vector \mathbf{k} , all satisfying the basic equations of the dynamical theory *). We choose the wave packet in such a way that along the surface of a semi-infinite crystal the wave field becomes localized around a certain point O . Having done this, the amplitude distribution inside the crystal may be calculated.

In most cases, excepting the ones mentioned below, a beam in the sense of geometrical optics results. Such well-behaved beams have all the properties mentioned above. Only as far as diffraction is concerned has a modification to be introduced in the condition mentioned under (1). This condition is an immediate consequence of the curvature of the " ω -surface", a circle with radius $2\pi/\lambda$ in the optical case. According to the dynamical theory the " ω -surface" is curved stronger in the diffraction region, the radius of curvature in

*) Use is made of a packet of pairs of plane-wave components. The question whether or not the beams that are used in practice, can be considered as such a packet, is left out of consideration.

\mathbf{k} -space being of the order of L^{-1} , where L is the “Pendellösung”-length. Accordingly we have now to state that the beam starts to diverge after having travelled a distance λ^2/L (see fig. 9.1).

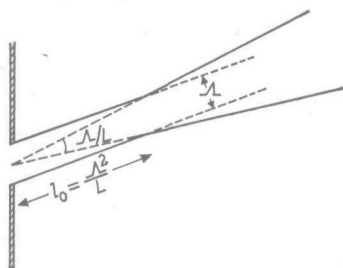


Fig. 9.1. The effect of diffraction (in optical sense) on the width of an X-ray beam in a crystal when the Bragg condition is (nearly) satisfied. The influence is similar to the diffraction of light beams, but the “Pendellösung”-length L plays the important part and not the wavelength.

However, we shall show that in the Bragg case of diffraction in or close to the region of total reflexion (sec. 7.4) the localized wave field inside the crystal does not have any of the properties (2), (3) and (4) mentioned above. In chapter 8 it was shown that in these cases an absorption coefficient is not an adequate description of the relative decrease in intensity. The properties (2) and (3) are absent because of the cut-off character of the modes and the inherent strong dependence of the imaginary part of the wave vector on the precise orientation of the real part. It should be noticed that in optics a strong variation of \mathbf{K} with \mathbf{k} is present also in the case of total reflexion. A beam of light striking the surface of a less dense medium under such an angle that total reflexion takes place, does not give a well-behaved beam in the less dense medium.

9.2. Gaussian wave packet in the linear approximation

9.2.1. Definition

To obtain a space-limited wave field a Gaussian wave packet is used, centred around the wave vector $\mathbf{k}_c + j\mathbf{K}_c$. Furthermore we shall use the linear approximation to evaluate the characteristics of the other modes in the packet. In doing so the curvature of the “ ω -surface” is eliminated and therewith the diffraction as discussed in the previous section. All phenomena found below have nothing to do with diffraction in the optical sense. They are a consequence of the fact that the attenuation vector \mathbf{K} and the parameter ξ are not constant in the wave packet.

$$\begin{aligned} \underline{\mathbf{k}} &= \mathbf{k}_c + h\mathbf{p}, \\ \mathbf{K} &= \mathbf{K}_c + h\mathbf{q}s, \\ \xi &= \xi_c (1 + h d \ln \xi/dh). \end{aligned} \tag{9.2.1}$$

The unit vector \mathbf{p} is tangential to the “ ω -surface” in the point \mathbf{k}_c . The param-

eter q relates the change in the imaginary part to the change in the real part of the wave vector. Its magnitude is discussed below; it may be smaller or larger than unity depending on the location of \mathbf{k}_c on the “ ω -surface”. In fig. 9.2 we show the coordinate system that is used: the z -axis is normal to the surface and the x -axis lies in the surface and in the plane of incidence. The vector \mathbf{p}

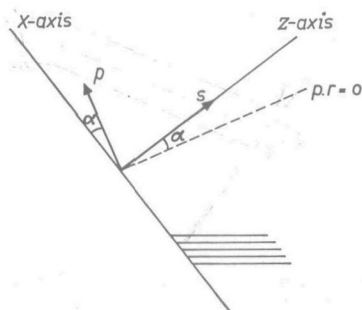


Fig. 9.2. The coordinate system used in this chapter.

makes an angle α with the x -axis. From the discussions in sec. 8.3 it follows that $\alpha = 90^\circ$ in the boundaries of the region of total reflexion, provided there is no absorption. In all other cases $|\alpha|$ is smaller than 90° . It is easily verified that

$$\tan \alpha = dk_z/dk_x \quad (9.2.2)$$

and

$$q/\cos \alpha = dK/dk_x. \quad (9.2.3)$$

The amplitude distribution over the wave packet is taken as Gaussian:

$$dD = A \cos(\alpha) \exp\{-A^2 \cos^2(\alpha) h^2/2\} dh / (2\pi)^{1/2}. \quad (9.2.4)$$

The total amplitude, D_i , of the upward-travelling components is now found to be

$$D_i = \exp\{-j\mathbf{k}_c \cdot \mathbf{r} + \mathbf{K}_c \cdot \mathbf{r} + (q\mathbf{s} \cdot \mathbf{r} - j\mathbf{p} \cdot \mathbf{r})^2/2A^2 \cos^2 \alpha\}, \quad (9.2.5)$$

and the total amplitude, D_r , of the downward-travelling components

$$D_r = \xi_c D_i \{1 + (q\mathbf{s} \cdot \mathbf{r} - j\mathbf{p} \cdot \mathbf{r}) (d \ln \xi/dh)/A^2 \cos^2 \alpha\}. \quad (9.2.6)$$

9.2.2. Upward-travelling wave field

Let us first consider the variation in D_i . Along the surface ($\mathbf{s} \cdot \mathbf{r} = 0$) the magnitude of D_i is given by

$$|D_i| = \exp(-x^2/2A^2); \quad \mathbf{s} \cdot \mathbf{r} = 0. \quad (9.2.7)$$

The amplitude is a maximum for $x = 0$, it has dropped to $\exp(-\frac{1}{2})$ for $x = \pm A$ and may be considered as negligible for much larger values of $|x|$. Inside the crystal along a line parallel to the surface, the amplitude is maximum for $\mathbf{p} \cdot \mathbf{r} = 0$. Apparently the deepest penetration takes place in the direction

perpendicular to \mathbf{p} and parallel to the group velocity of the packet $(\partial\omega/\partial\mathbf{k})_{\mathbf{k}=\mathbf{k}_c}$. Along any line $z = \text{constant}$ the amplitude has dropped to $\exp(-\frac{1}{2})$ at a distance $\pm \Lambda$ from the line $\mathbf{p} \cdot \mathbf{r} = 0$. From this point of view the wave field corresponds to a beam of constant width, penetrating deeply into the crystal (fig. 9.3). It must be remarked, however, that the direction of deepest penetra-

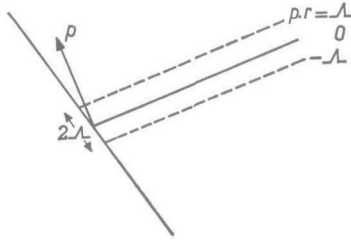


Fig. 9.3. In the upward-travelling wave field that results from a Gaussian wave packet, the amplitude distribution in a plane parallel to the surface is such that it drops to $\exp(-\frac{1}{2})$ of the maximum on the lines $\mathbf{p} \cdot \mathbf{r} = \pm \Lambda$. The maximum itself occurs at $\mathbf{p} \cdot \mathbf{r} = 0$.

tion may deviate appreciably from the direction of energy transport (see sec. 9.2.4). For large values of z the expression (9.2.5) for D_i cannot be correct. The magnitude of D_i along the centre line of the beam is given by

$$|D_i| = \exp[\mathbf{K}_c \cdot \mathbf{r} + q^2 z^2 / 2\Lambda^2 \cos^2 \alpha]; \quad \mathbf{p} \cdot \mathbf{r} = 0. \quad (9.2.8)$$

The value of \mathbf{K}_c is such that inside the crystal $\mathbf{K}_c \cdot \mathbf{r}$ is negative, corresponding to a decreasing amplitude. But we see from eq. (9.2.8) that sufficiently deep into the crystal the amplitude starts to rise again and eventually may reach amplitudes exceeding those in the surface. This unreasonable result is an immediate consequence of the linear approximation. Along the entrance surface the amplitude distribution is given by eq. (9.2.4). Deeper inside the crystal the amplitude distribution is changed, because the different modes suffer a different phase shift and a different attenuation. The difference in phase shift causes the beam to travel perpendicular to \mathbf{p} and is further of minor importance. The difference in attenuation causes a shift in h -value for which the amplitude is a maximum. It is easily verified that at a depth $\mathbf{s} \cdot \mathbf{r} = z$ the maximum in amplitude occurs at

$$h_m = qz / \Lambda^2 \cos^2 \alpha. \quad (9.2.9)$$

The attenuation vector \mathbf{K}_c' of the mode with maximum amplitude is according to the linear approximation

$$\mathbf{K}_c' = \mathbf{K}_c + \mathbf{s}z (q/\Lambda \cos \alpha)^2.$$

Apparently there must come a region where $\mathbf{K}_c' \cdot \mathbf{r}$ is positive, corresponding to an increasing amplitude. Long before that point, however, the linear approximation is incorrect, so that the increasing amplitude does not worry us.

However, this result demonstrates a feature that is of great importance, namely that the central mode of the wave packet is not the same one along the central line. With increasing penetration the central wave vector moves in the direction of weaker attenuation. In the Gaussian wave packet this phenomenon is not perceptible in the amplitude distribution (fig. 9.3) because of the specific character of the wave packet. Had we chosen a square-wave packet (dD constant over a finite region of h) then the effect would have manifested itself. After penetrating deeply into the crystal only the mode with the least attenuation survives and the corresponding wave field must be infinitely wide. Such a behaviour is in contrast to property (3) mentioned in the previous section. Hence a beam in the sense of geometrical optics cannot be obtained unless $q = 0$. We believe, however, that by not looking too deep inside the crystal this phenomenon will not play too important a part. A suitable upper limit in the change of the central \mathbf{k} follows from the condition that it must stay well within the original packet. Thus

$$|h_m| < (\Lambda \cos \alpha)^{-1}. \tag{9.2.10}$$

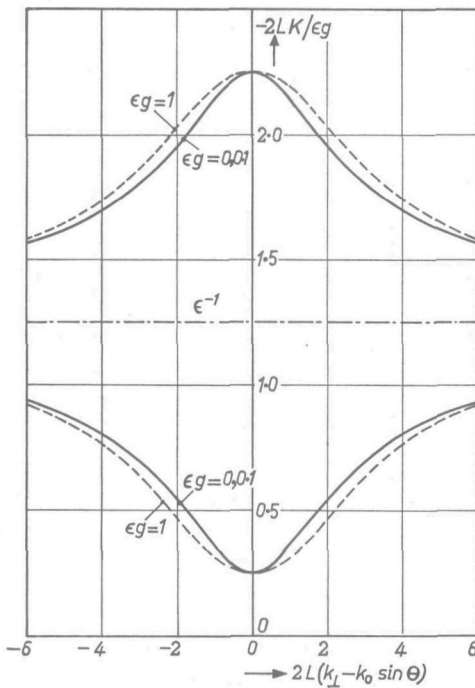


Fig. 9.4. The imaginary part of the wave vector as a function of the component of the wave vector parallel to the surface in the symmetrical Laue case. The curves for $g = 0$ and $g = 0.1$ coincide. The larger negative values correspond to modes on the left-hand branch of the ω -surface, the smaller negative values to modes on the right-hand branch.

The corresponding value for the penetration z_m , beyond which the central mode shifts appreciably is

$$z_m = \Lambda \cos(\alpha)/|q|. \quad (9.2.11)$$

For a well-behaved beam we require that this penetration be much larger than its width Λ , so that well-behaved beams are present only, if

$$|q|/\cos \alpha \ll 1. \quad (9.2.12)$$

To obtain an idea of the magnitude of $|q|/\cos \alpha$, we have to calculate $|\mathbf{K}|$ as a function of k_x . In figs 9.4 and 9.5 $|\mathbf{K}|$ is plotted versus k_x for the symmetrical Laue and Bragg cases, resp. Note the difference in scale along the vertical axes. The slope of the curve is equal to $q/\cos \alpha$ (eq. (9.2.3)) and hence equal to Λ/z_m apart from the sign. In the symmetrical Laue case the slope is always small. For small values of ϵg the maximum value of $|q|/\cos \alpha$ is $0.4 \epsilon g \tan \theta$. Hence the beam is always well-behaved. In the symmetrical Bragg case $|\mathbf{K}|$ rises to

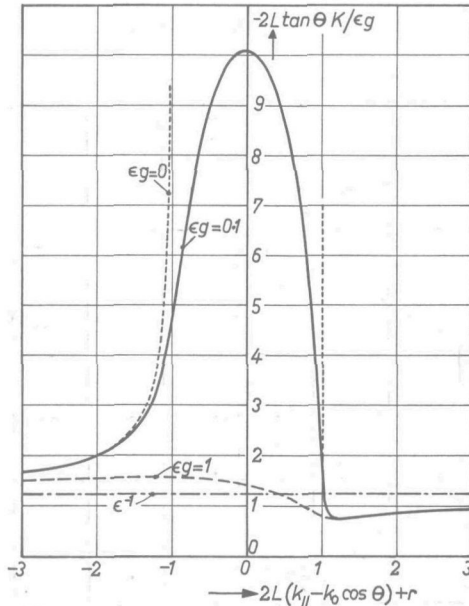


Fig. 9.5. The counterpart of fig. 9.4 for the symmetrical Bragg case. The large negative values of \mathbf{K} are caused by extinction.

high values in the region of total reflexion because of extinction. The slope of the curve is much steeper and the corresponding value of $|q|/\cos \alpha$ much larger. In the case of $\epsilon g = 0.1$ its maximum values are 20 and 70 on the left-hand and right-hand side of the maximum in $|\mathbf{K}|$, respectively. In the entire region where extinction is predominant ^{*}), the beams are not well-behaved.

^{*}) The narrow region near the maximum in $|\mathbf{K}|$ is left out of consideration.

A detailed study of the value of $|q|/\cos \alpha$ in non-symmetrical cases shows that whenever the extinction is strong $|q|/\cos \alpha$ is large and whenever extinction is negligible $|q|/\cos \alpha$ is small. In sec. 8.1 a few characteristics of cut-off modes in contrast to surface-independent modes were given. We can add now that surface-independent modes give well-behaved beams, whereas cut-off modes give beams in which the characteristics of the central mode change appreciably over penetrations less than its width.

9.2.3. Downward-travelling wave field

The variation of D_r over the crystal is not exactly the same as that of D_i , because the mode parameter ξ is not constant over the wave packet. We shall choose the beam so wide that the value of ξ for $|h| = (\Lambda \cos \alpha)^{-1}$ deviates only very little from ξ_c . According to eq. (9.2.1) we must have

$$a_r = (\Lambda \cos \alpha)^{-1} d \ln |\xi|/dh, \quad |a_r| \ll 1$$

and

$$a_i = (\Lambda \cos \alpha)^{-1} d\varphi/dh, \quad |a_i| \ll 1.$$

We shall investigate the behaviour in the region of interest only: $z < z_m$ (eq. (9.2.11)) and within a few times Λ from the centre line of the upward-travelling wave field. Equation (9.2.6) may then be rewritten as

$$D_r = \xi_c D_i [1 + a_r q z / |q| z_m + a_i \{x/\Lambda + \tan(\alpha) z/\Lambda\}], \quad (9.2.14)$$

where the last three terms within the brackets are small compared to unity. Straightforward calculation of the maxima in D_r along a line parallel to the surface shows that these maxima fall on the straight line:

$$x/\Lambda + \tan(\alpha) z/\Lambda = a_i.$$

This line is parallel to the line of deepest penetration, found in the previous sub-section, but displaced over a distance $x_a = a_i \Lambda$. Since we assumed $|a_i|$ to be much smaller than unity the displacement is always small compared with the beam width. The displacement is largest when the phase angle φ changes sharply in the neighbourhood of \mathbf{k}_c . For well-behaved beams φ is close to either 0 or $\pm \pi$ and cannot change appreciably, so that for those beams the displacement is negligible. Everywhere within the well-behaved region we find $D_r/D_i = \xi_c$. For $z > z_m$ the ratio D_r/D_i is constant along a line parallel to the surface but its value is no longer equal to ξ_c .

For beams consisting of modes with strong cut-off character the displacement may be larger. In fig. 9.6 an example is shown. The matching at the surface in this Bragg case requires the presence of two beams in front of the crystal: the incident beam exactly fitting the upward-travelling wave field along the surface

and the reflected beam, fitting the downward-travelling wave field. Apparently the incident beam must penetrate the crystal over a short distance z_d , before it is fully reflected. For non-absorbing crystals it may be shown that the penetration depth is such that for an infinitely wide incident wave the amplitude would have dropped there to $\exp(-\frac{1}{2})$.

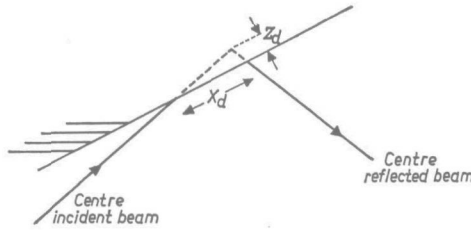


Fig. 9.6. In the region of strong reflexion in the Bragg case of diffraction the centre lines of the incident and diffracted beams do not cross in the surface. The incident beam has to penetrate into the crystal before it is strongly reflected.

9.2.4. Power flow

The expression (6.3.1) for the Poynting vector can be used to calculate the local value of \mathbf{P} within the beam. By neglecting all terms of the order ψ or smaller one obtains

$$2\varepsilon_0\omega \mathbf{P}/c^2 = \text{Re} \{-j(D_i \nabla D_i^* + D_r \nabla D_r^*)\}.$$

The gradient in D_i and D_r consists of two parts. One arises from the change in phase and is of the order $|D|/\lambda$. The other is due to the limitation in space of the wave field. It is of the order $|D|/A$. Since the width of the beam is large compared with the wavelength the latter contribution can be neglected, leading to

$$2\varepsilon_0\omega \mathbf{P}/c^2 = |D_i|^2 \mathbf{k}_0 + |D_r|^2 (\mathbf{k}_0 - 2\mathbf{b}). \quad (9.2.15)$$

In the interesting region the relation between D_i and D_r is given in eq. (9.2.14):

$$2\varepsilon_0\omega \mathbf{P}/c^2 = |D_i|^2 [\mathbf{k}_0 + |\xi_c|^2 (\mathbf{k}_0 - 2\mathbf{b}) \{1 + 2a_r q z / |q| z_m + 2[x/A + \tan(\alpha)z/A] a_i\}].$$

In a first approximation the power flow is parallel to the velocity of energy transport of the central mode \mathbf{k}_c . Small corrections have to be applied because of the terms proportional to a_r and a_i .

Well-behaved beams consist of surface-independent modes as was shown in sub-section 9.2.2. For such modes the phase angle φ remains close to either 0 or $\pm \pi$. A first consequence thereof is that a_i is very small and the correction term with a_i negligible. Secondly, the “ ω -surface” in the region of surface-independent modes practically coincides with the ω -surface defined for un-

damped modes. Accordingly the direction of deepest penetration (parallel to $\mathbf{v}_g = \partial\omega/\partial\mathbf{k}$) is the same as the direction of the velocity of energy transport of the central mode (normal to the ω -surface). For $z < z_m$ the central mode is \mathbf{k}_c so that \mathbf{P} is parallel to the direction of deepest penetration throughout this region. For deeper penetrations the central mode shifts to weaker attenuation as pointed out in sub-section 9.2.2 with a corresponding shift in ξ and the direction of \mathbf{P} . It is easily verified that the correction term proportional to a_r accounts for this phenomenon. An example of such a well-behaved beam in the Bragg case of diffraction outside the region of total reflexion is shown in fig. 9.7a.

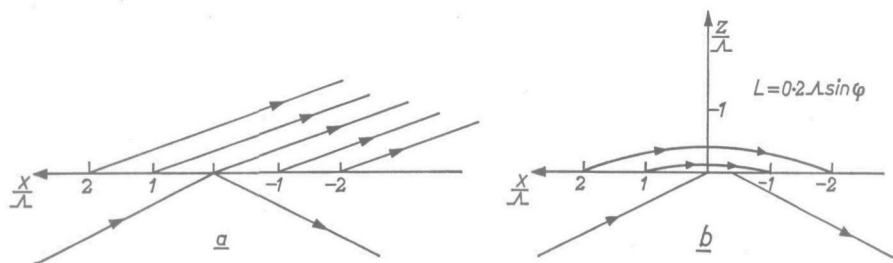


Fig. 9.7. Lines of power flow in X-ray beams nearly satisfying the Bragg condition. In (a) the case of a well-behaved beam. The direction of power flow is the same everywhere and not closely parallel to the surface. In (b) the case of a not well-behaved beam. The lines of power flow are curved and closely parallel to the surface. The penetration is small compared with the beam width.

Beams that are not well-behaved consist of modes with strong cut-off character. The phase angle φ may have any value not close to either 0 or $\pm \pi$. The value of φ changes sharply over the wave packet corresponding to a relatively large value of a_i . Moreover the real part of \mathbf{k} does not lie closely to the branches of the ω -surface. According to the example shown in fig. 8.4, the normal to the “ ω -surface” in this region makes a large angle with the surface and accordingly with the power flow. It can be shown that the direction of \mathbf{v}_g always makes a large angle with \mathbf{v}_e in the region of total reflexion where the activated modes have strong cut-off character. Apparently the beams in this region do not have the property (2) mentioned in sec. 9.1. To shed some light on this strange result we treat in some detail the beam activated in a non-absorbing crystal and the symmetrical Bragg case inside the region of total reflexion. The power flow associated with each mode in the packet is parallel to the surface, the direction of deepest penetration perpendicular to the surface. Since $|\xi| = 1$ for all modes, $a_r = 0$. The value of a_i is easily shown to be $-2L/\lambda \sin \varphi$ (0.4 in fig. 9.7b). According to the previous sub-section the centre lines of the incident beam and the reflected beam do not intersect in the surface. They lie a distance $2L/\sin \varphi$ apart. For positive values of x , $|D_i|$ is slightly larger than $|D_r|$, leading to a power flow into the crystal under a small angle with the surface. For

negative values of x , $|D_i|$ is smaller than $|D_r|$ resulting in a power flow out of the crystal. In fig. 9.7*b* two paths of the X-ray energy inside the crystal are shown, together with the centre lines of the incident and reflected beams. For sufficiently wide beams ($|a_i| \ll 1$) the decrease in amplitude along the line $x = 0$ is almost the same as if the wave field were infinitely wide. Accordingly the centre lines of the incident and reflected beams intersect on the path starting at the point $x = A$, where $|D_i| = \exp(-\frac{1}{2})$. The other path starting at $x = 2A$ penetrates four times deeper.

It is evident that the flow pattern in fig. 9.7*b* does not correspond to a well-behaved beam. The extinction prohibits the power flow from entering the crystal. Nevertheless there is a slight penetration but the field deeper inside the crystal along the line of penetration is determined by the very small power influx far away from the centre of the incident beam. In the case of well-behaved beams (fig. 9.7*a*) the field deep inside the crystal along the line of penetration is determined by the power influx in the immediate neighbourhood of the centre of the incident beam.

The *intensity* of the beam is defined in eq. (9.1.1). For sufficiently wide beams ($|a_r|, |a_i| \ll 1$) and not too deep penetrations ($z < z_m$) the total power flow passing through a plane parallel to the surface is equal to

$$I = (1 + |\xi_c|^2/\gamma) \exp[-2|\mathbf{K}_c|z] \cdot (\pi)^{1/2} \Lambda c^2 \mathbf{k}_0 \cdot \mathbf{s} / 2\epsilon_0 \omega.$$

According to the previous chapter it is permissible for well-behaved beams, where all modes are surface-independent, to replace $-2|\mathbf{K}_c|z$ by $-\mu l$, where l is the distance along the path measured from the surface. Hence

$$I = C(1 + |\xi_c|^2/\gamma) \exp(-\mu l), \quad (9.2.16)$$

where C is directly proportional to the maximum amplitude squared of the upward-travelling wave field in the beam along the surface.

9.3. Well-behaved beams in plane-parallel crystal slabs

In this section the use of beams in plane-parallel crystal slabs is demonstrated. All numerical examples concern the reflexion (220) in germanium with Cu K α radiation. The parameters used in the calculations are

$$\begin{aligned} \theta &= 22.7^\circ, & \psi_0 &= -2.85 \cdot 10^{-5} - 8.62 \cdot 10^{-7} j, \\ \mu_0 &= 352 \text{ cm}^{-1}, & \psi_1 &= -2.14 \cdot 10^{-5} - 8.27 \cdot 10^{-7} j, \\ |\mathbf{b}| &= 3.151 \text{ \AA}^{-1}, & \epsilon &= 0.9592, & g &= 0.0403. \end{aligned} \quad (9.3.1)$$

The values of ψ_0 , ψ_1 and ϵ were obtained by Okkerse^{18,19}. In fig. 9.8 the " ω -surface" for the symmetrical Laue case with this reflexion is shown. Along the straight line, ω_{vac} , the deviation from the exact Bragg angle is given in seconds of arc. In the right-hand part the value of $\mu/\cos \theta$ for the slowly

damped modes in the σ -polarization is given on the same vertical axis as the " ω -surface". Note the strong reduction in comparison with $\mu_0/\cos \theta = 382 \text{ cm}^{-1}$.

In the *Laue case of diffraction* one incident beam generates four well-behaved beams inside the crystal, two in the σ -polarization and two in the π -polarization. The values of ξ follow from eq. (7.2.2) where V_0 and V_1 may be considered as real parameters. In fig. 9.9 the behaviour of the beams in the σ -polarization is shown, together with the " ω -surface" (schematic). The beams labeled I

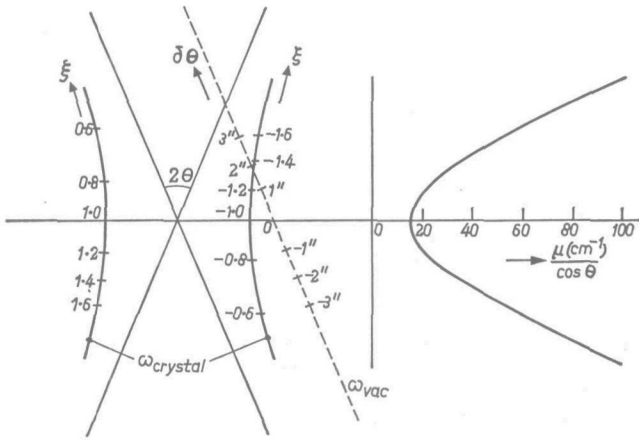


Fig. 9.8. The ω -surface for the (220) reflexion in germanium, using $\text{CuK}\alpha$ radiation. The deviation from the exact Bragg angle, $\delta\theta$, is indicated along ω_{vac} . In the right-hand part $\mu/\cos \theta$ for the slowly damped modes is plotted on the same vertical axis as the left-hand part. The parameters used in drawing this figure are given in eq. (9.3.1).

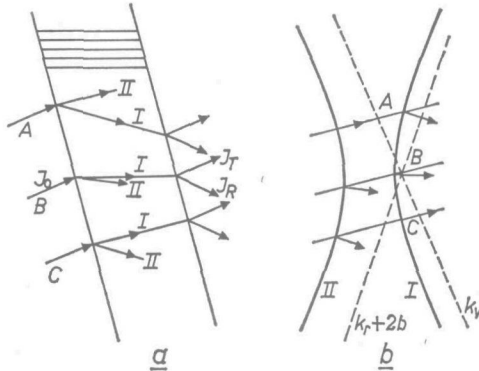


Fig. 9.9. The direction of the two beams generated in a crystal (Laue case) by a monochromatic incident beam depends strongly on the precise direction of this beam. In the figure the resulting beams for three orientations of \mathbf{k}_{v0} are shown. Their direction is parallel to the normal of the ω -surface at the central mode of the beam. The beams labelled I suffer reduced absorption (right-hand branch), the beams labeled II enhanced absorption (left-hand branch).

correspond to \mathbf{k} -vectors on the right-hand branch and are damped slowly. The beams labeled II suffer an enhanced absorption. They travel parallel to the normal of the ω -surface. From the boundary conditions (eqs (7.3.1)) follow the relations between the beam intensities. If the intensity of the incident beam in the proper polarization direction is I_0 , the intensity of the beam characterized with ξ inside the crystal is given by

$$I = I_0 \gamma / (\gamma + \xi^2).$$

During passage through the crystal the intensity is reduced because of absorption (eq. (9.2.16)). At the back surface the beam decomposes into two beams, one parallel to \mathbf{k}_v and one parallel to \mathbf{k}_r , with $\mathbf{k}_r + 2\mathbf{b}$ indicated in the figure. The emerging intensities are

$$I_T = I_0 \gamma^2 \exp(-\mu l) / (\gamma + \xi^2)^2$$

and

$$I_R = I_0 \gamma \xi^2 \exp(-\mu l) / (\gamma + \xi^2)^2.$$

(9.3.2)

In figs 9.10a and b a few numerical examples are given for the slowly damped

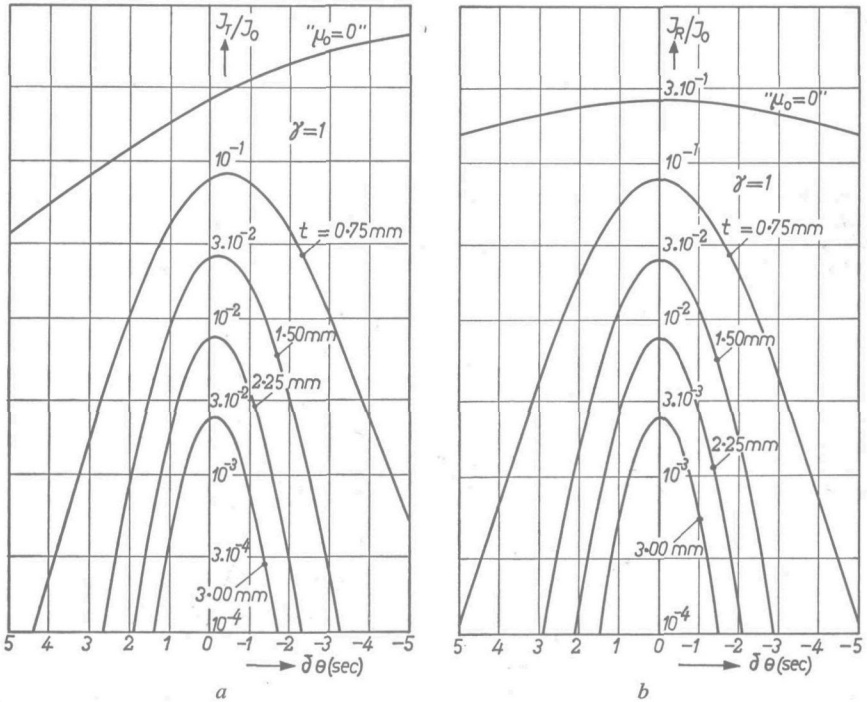


Fig. 9.10. The intensities emerging from Ge-crystal slabs of different thicknesses t in the symmetrical Laue case as a function of angle of incidence. The upper curves give the pre-exponential factors in eqs (9.3.2). The reflexion is (220) with $\text{CuK}\alpha$ radiation; (a) gives the transmitted intensity, travelling parallel to \mathbf{k}_v ; (b) gives the reflected intensity, travelling parallel to \mathbf{k}_r .

modes in the σ -polarization and the symmetrical Laue case ($\gamma = 1$). The transmitted intensity I_T and the reflected intensity I_R are maximum for $\delta\theta \approx 0$, because there μ is minimum. The slight deviation in $\delta\theta$ from 0 for I_T is due to the pre-exponential term, the uppermost curves in fig. 9.10. Appreciable transmission takes place within a few seconds of arc only. Since μ increases with $|\delta\theta|$ the transmission peaks become narrower for thicker crystals. For the smallest thickness used in the figures (0.75 mm) and $\delta\theta = 0$ the intensities ($I_T = I_R$) emerging from the crystal for the four modes are

σ -polarization	reduced absorption:	$I_T/I_0 = 7.8 \cdot 10^{-2}$,
	enhanced absorption:	$I_T/I_0 = 1.1 \cdot 10^{-25}$,
π -polarization	reduced absorption:	$I_T/I_0 = 2.2 \cdot 10^{-5}$,
	enhanced absorption:	$I_T/I_0 = 4.0 \cdot 10^{-22}$.

Except the first, they are all negligible.

In fig. 9.11 the transmission peaks for two non-symmetrical Laue cases are given. Now the maxima do not occur at $\delta\theta = 0$ and there is a larger difference

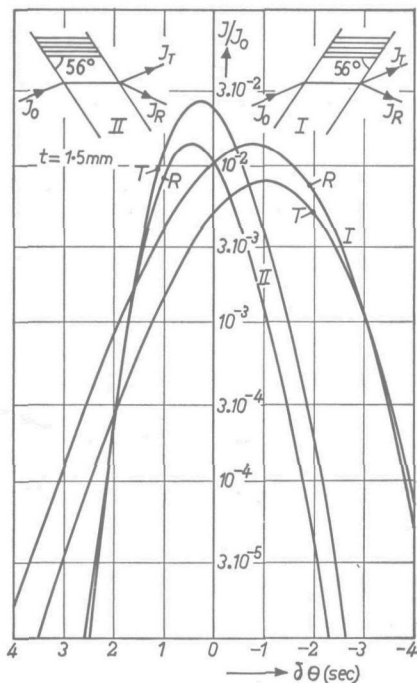


Fig. 9.11. The transmitted and reflected intensities for two non-symmetrical Laue cases as a function of angle of incidence. The reflexion is (220) with $\text{CuK}\alpha$ radiation.

between I_T and I_R in the maxima. Further there is a difference in width of the peaks for the two cases. Note that if case I is a reflexion (220), case II corresponds with the reflexion ($\bar{2}\bar{2}0$). In fig. 9.12 the dependence of the *integrated* intensities T and R on the orientation of the surface is given. The thickness was kept constant, 0.75 mm. The angle between the reflecting planes and the surface normal is β , with $\mathbf{k}_0 \cdot \mathbf{s} = \cos(\theta - \beta) \omega/c$. If $\beta > 0$, similar to case I in fig. 9.11, then R exceeds T . For $\beta < 0$ we find $R < T$. Okkerse¹⁸⁾ gives expressions for the integrated intensities in the symmetrical Laue case as a function of crystal thickness. From his expressions it follows that both T and R are proportional to the structure factor F , in contrast to the kinematical theory where the integrated reflected intensity is proportional to F^2 .

Let us now turn to the *Bragg case of diffraction*. The “ ω -surface” (σ -polarization) is shown in fig. 9.13a. The shape is not drawn accurately. If \mathbf{k}_v lies well

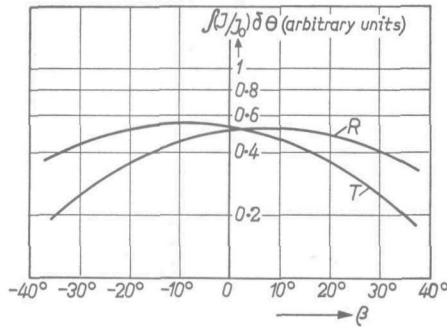


Fig. 9.12. The integrated transmitted (T) and reflected (R) intensities as a function of the angle between the surface normal and the reflecting planes. For case I in fig. 9.11, β is positive.

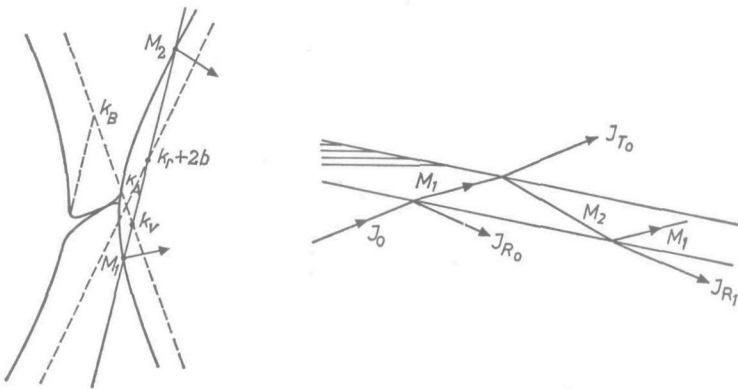


Fig. 9.13. The beams generated in the Bragg case when the incident beam is not totally reflected. The beam M_1 arises from the wave packet centred around mode M_1 and similar for beam M_2 . The incident beam generates beam M_1 and a reflected beam in vacuum. At the back surface beam M_1 generates a transmitted beam and a beam M_2 .

outside the region between \mathbf{k}_A and \mathbf{k}_B , only two well-behaved beams are activated inside the crystal, one in the σ -polarization and one in the π -polarization. In the example of the figure the beam in σ -polarization corresponds to mode M_1 . The other possible mode cannot be activated since it travels from the back surface to the front. The boundary conditions (eq. (7.3.2) with $D_2 = 0$) require the presence of a reflected beam in vacuum; see fig. 9.13b for the paths of the beams. It is easily verified that

$$I_{M_1} = I_0 (1 + \xi_1^2/\gamma)$$

and

$$I_{R_0} = -I_0 \xi_1^2/\gamma.$$

If the crystal is sufficiently thin the beam M_1 reaches the back surface, where it generates a transmitted beam and the other possible beam M_2 :

$$I_{T_0} = I_0 (1 + \xi_1^2/\gamma)^2 \exp(-\mu l)$$

and

$$I_{M_2} = -I_0 \xi_1^2 (1 + \xi_1^2/\gamma) \exp(-\mu l)/\gamma.$$

When beam M_2 strikes the front surface again a second reflected beam is generated together with a beam M_1 in the crystal.

It must be remarked that this approach with beams only makes sense if the thickness is much larger than the beam width, because otherwise the beams overlap and interference takes place.

If \mathbf{k}_v lies near or in between \mathbf{k}_A and \mathbf{k}_B the energy velocity of the activated modes is closely parallel to the surface. The incident beam gives rise to space-limited wave fields, but these do not correspond to well-behaved beams. The values of ξ must now be calculated with eq. (7.2.2) using complex values of V_0 and V_1 . For sufficiently thick crystal slabs (no transmission) the reflexion coefficient is equal to

$$I_R/I_0 = -|\xi|^2/\gamma.$$

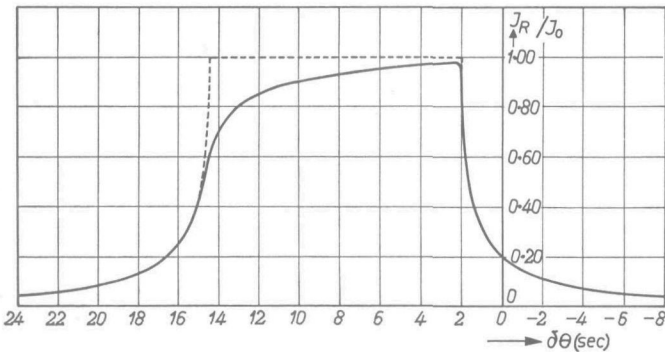


Fig. 9.14. The intensity reflected from a thick Ge crystal in the symmetrical Bragg case vs angle of incidence. The reflexion is (220) with $\text{CuK}\alpha$ radiation. The dotted line gives the reflected intensity in the case of no absorption.

In fig. 9.14 the reflexion coefficient is given as a function of $\delta\theta$ in the symmetrical Bragg case ($\gamma = -1$). It is never equal to unity, because there is always a finite penetration and hence a finite absorption. The reflexion coefficient is maximum on the low-absorption side. The dotted curve gives I_R/I_0 in the limit $g \rightarrow 0$, no absorption. It is unity over the entire range of cut-off modes. For lower values of the reflectivity, where the beams inside the crystal are well-behaved, the curves coincide. An interesting point in fig. 9.14 is further that at $\delta\theta = 0$ the reflectivity is not a maximum. Okkerse²⁰) performed an elegant experiment to verify this result. The width of the reflexion peak is proportional to the distance between the two branches of the ω -surface and hence proportional to the structure factor F . The integrated reflected intensity is accordingly proportional to F and not to F^2 as is found in the kinematical theory.

10. DYNAMICAL THEORY FOR LIGHTLY DEFORMED CRYSTALS

10.1. Introduction

The dynamical theory of X-ray diffraction, discussed in the preceding chapters, is valid for perfect crystals only. The periodicity of the lattice gives in the Fourier expansion of the dielectric constant as relevant parameters one vector and the corresponding amplitude V_1 . In real single crystals the periodicity is disturbed by

- (a) small-angle grain boundaries,
- (b) thermal motion of the atoms,
- (c) elastic strains caused by external forces or temperature gradients,
- (d) isolated dislocations,
- (e) point defects such as vacancies and impurities.

In this section we shall outline how to account for these disturbances.

The *small-angle grain boundaries* have the largest influence on the diffraction phenomenon. Their presence results in a complete breakdown of the dynamical behaviour, as was pointed out by Darwin ⁶⁾ in 1914. He assumed that the small-angle grain boundaries divide the crystal into small perfect blocks with dimensions much smaller than the "Pendellösung"-length L . The orientation of the blocks may differ by angles of up to 1 minute of arc. A plane monochromatic beam impinging upon such a crystal meets on its path through the crystal before it is absorbed, only a few blocks that are oriented properly for diffraction. Because the blocks are small the reflected intensity may be calculated in a kinematical way. The total reflected intensity for one direction of incidence is small compared with the incident intensity. In practice one measures the integrated reflected intensity, either by using a divergent incident beam, or by rocking the crystal through the Bragg angle. Now the mosaic crystal reflects more than the perfect crystal, since all blocks within the absorption length contribute, whereas in the perfect crystal the wave field does not penetrate deeper than the length L , which is much smaller than $\mu_0^{-1} = L/g \cos \theta$. It has been verified that all thick crystals satisfying the kinematical theory contain small-angle grain boundaries, arising from a more or less systematic arrangement of dislocations.

The effect of *thermal motion* has been treated theoretically also ^{10,18)}. The wavelength of most phonons is smaller than L . The crystal without further defects may be considered as ideal, but with "smoothed out" atoms. The chance Wdu , to find the centre of an atom between distances u and $u + du$ from the reflecting plane, will be a peak function, symmetric with respect to $u = 0$ and narrow with respect to the spacing d between the atom planes. It is assumed that the electron distribution around the nucleus is not disturbed by

the motion. The average value of ψ , denoted by ψ' , at a distance x from the atom plane is now given by

$$\psi'(x) = \int_{-\infty}^{\infty} \psi(x-u) W du,$$

where

$$\psi(x-u) = \sum_n \psi_n \cos \{2\pi n(x-u)/d\}.$$

Because of the symmetry in W we may write

$$\psi_n' = \psi_n \int_{-\infty}^{\infty} \cos(2\pi nu/d) W du.$$

For thermal motion the distribution is Gaussian, giving

$$\psi_n'/\psi_n = \exp(-2\pi^2 n^2 \overline{u^2}/d^2),$$

the well-known Debye-Waller factor.

The thermal motion is a special case of *elastic deformation* of the crystal lattice. In the treatment of elastically deformed lattices, distinction must be made between two extreme situations. Firstly, the deformation is such that the lattice parameter changes very much within the "Pendellösung"-length L . Then the X-ray wave field cannot adjust itself to the new situation further along its path. The treatment is then either the kinematical theory if the same orientation is met only once or a few times over the absorption length (examples are given in sub-section 11.4.4), or the dynamical theory with "smoothed out" atoms if the same orientation is met many times over the length L and the reflected intensity is comparable with the incident intensity (an example is the treatment of thermal motion). The second extreme is that the relevant lattice parameter is almost constant over the length L and changes appreciably after many distances L having been traversed. In this case we believe that the X-ray wave field may adjust itself to the slowly varying lattice parameter ²¹). We introduce the basic assumption that if one mode is present at a certain point, the mode may change its character slowly upon travelling forward, but does not generate other modes and hence remains one well-defined mode. This assertion is hard to prove. It is based on experimental evidence in other fields of physics. For example, a beam of light travelling in a non-uniform medium shows a curved path if the change in refractive index is small over one wavelength. In this chapter we shall derive a solution for the behaviour of a narrow beam in slightly deformed crystals. In special cases of deformed lattices an exact solution can be obtained. The result of such a rigorous treatment, given in chapter 11, shows that the solution obtained in this chapter is correct as a first approximation.

The strain fields around *isolated dislocations and point defects* is in between these two extremes. A general solution for these situations is given by Taupin ²²)

(chapter 12). The generation of new modes is taken into account. To obtain the solution for a specified problem, however, a computer is usually necessary.

10.2. Outline of the ray theory

The theory to be presented now, is limited in its applicability to crystals, with a slightly inhomogeneous strain. In such crystals one expects that the wave field in a small volume around an arbitrary point P can be described in dynamical terms as if the crystal was perfect. Then the wave vector \mathbf{k} , the mode parameter ξ and the group velocity are all well defined. It is clear, however, that this sets an upper limit to the admissible inhomogeneity in the strain (sec. 10.3). In P we construct a beam and we shall try to follow it through the crystal. For a number of reasons this beam has to be well-behaved:

- (1) Only well-behaved beams have constant parameters for the central mode.
- (2) We want to have beams that travel independently, each beside the other, which is impossible for not well-behaved beams over distances much larger than L .
- (3) We want to be independent of the orientation of the surface.

The beam in P travels forward in the direction of the power flow and arrives in Q , where the periodicity of the crystal is changed significantly. The ω -surface does not coincide with the ω -surface in P . The possible changes are discussed in sec. 10.4.

To match the wave fields in P and Q an important assertion has to be made. If the transition in orientation and spacing is sharp (small-angle grain boundary) the matching has to be carried out in the normal way. Each mode in P would generate four modes in Q , two on the same branch and two on the other branch. For a continuous change, however, we expect that one mode remains one mode. Therefore a new ad hoc matching condition is introduced (sec. 10.5) to account for such a behaviour. The beam in P now gives rise to one beam in Q . Although its width and direction may change, the intensity drops only because of absorption. The amplitude matching requires only the use of the appropriate absorption coefficient in the intensity.

In this way it is possible to follow the beam, step by step, through the crystal, giving a complete description of its behaviour (sec. 10.6). A few examples are treated in some detail in sec. 10.7. Numerical examples of beam transmission through deformed crystal slabs are given in refs 21 and 23.

10.3. Reciprocal-lattice vector and structure factor in deformed crystals

The elastic deformation of a crystal is described conveniently by the displacement vector $\mathbf{v}(\mathbf{R})$, giving the displacement of the atom located at \mathbf{R} before the deformation. The new position is

$$\mathbf{r} = \mathbf{R} + \mathbf{v}(\mathbf{R}),$$

or by neglecting higher-order terms in \mathbf{v} :

$$\mathbf{r} = \mathbf{R} + \mathbf{v}(\mathbf{r}). \quad (10.3.1)$$

In the undeformed crystal the reflecting planes are given by

$$2\mathbf{b}' \cdot \mathbf{R} = 2\pi m,$$

where m is an integer and $2\mathbf{b}'$ the relevant reciprocal-lattice vector. In the deformed crystal the reflecting planes are deformed also:

$$2\mathbf{b}' \cdot (\mathbf{r} - \mathbf{v}) = 2\pi m. \quad (10.3.2)$$

They are neither flat nor parallel. One can construct a local vector \mathbf{b} , perpendicular to the reflecting plane and of magnitude π over the distance between two neighbouring reflecting planes:

$$\mathbf{b} = \mathbf{b}' - \nabla_{\mathbf{r}} (\mathbf{b}' \cdot \mathbf{v}). \quad (10.3.3)$$

It must be emphasized, however, that the vector $2\mathbf{b}$ is not a reciprocal-lattice vector as used in the dynamical theory. There it describes the periodicity of the lattice and is constant by definition. Here it is essentially variable, because we want to investigate the influence of deformation. A reconciliation is obtained by remembering that in the dynamical theory \mathbf{b} need not be a constant throughout the *entire* crystal. According to chapter 9 it is possible to introduce well-behaved beams. The properties of the lattice outside the beam cannot have an influence on its behaviour. In view of the fact that the minimum beam width of a well-behaved beam is of the order of the "Pendellösung"-length L , it may be expected that the dynamical theory, as developed in the previous chapters can be applied locally to deformed crystals if the reciprocal-lattice vector does not change appreciably inside a sphere with radius L . A reasonable upper limit for the admissible change in \mathbf{b} is the distance between the branches of the ω -surface. The admissible inhomogeneity in the strain is now easily found to be such that the relative change in \mathbf{b} over a distance d in any direction must be smaller than ψ_1^2 . In most cases of elastic deformation with external means this condition is satisfied. The radius of curvature by bending for example must exceed 10 cm. The internal strains due to isolated dislocations and point defects do not satisfy this condition.

The important parameters V_0 and V_1 require further consideration in deformed crystals. The electron cloud around each nucleus deforms when the interatomic distances change. For example a hydrostatic pressure gives a higher electron density and hence larger values of $|V_0|$ and $|V_1|$. All relative changes, however, are small (of the order of the strain) and so they will be neglected. Hence V_0 and V_1 can be treated as constant. Furthermore, since we shall consider only well-behaved beams, they are considered as real. The absorption is fully accounted for, by introducing an absorption coefficient.

10.4. Effects of the deformation on the ω -surface

Let us consider a point P, located at \mathbf{r} and define there an ω -surface corresponding to the local value of \mathbf{b} and introduce a well-behaved beam, characterized by an arbitrary \mathbf{k} -vector lying on the ω -surface. The beam travels forward in the direction of the group velocity a distance dL , where it arrives in Q, located at $\mathbf{r} + d\mathbf{r}$, with

$$d\mathbf{r} = a dL \nabla_{\mathbf{k}} \omega; \quad a = |\mathbf{v}_g|^{-1}. \quad (10.4.1)$$

In Q the reciprocal-lattice vector has changed by an amount $d\mathbf{b}$:

$$d\mathbf{b} = (d\mathbf{r} \cdot \nabla_{\mathbf{r}}) \mathbf{b}. \quad (10.4.2)$$

Apparently another ω -surface has to be used in Q. In fig. 10.1 the ω -surfaces in P and Q have been drawn for an arbitrary change in \mathbf{b} . In fig. 10.1a the region around \mathbf{k}_0 is reproduced. Since V_0 and V_1 are independent of the strain, the hyperbolae corresponding to the ω -surfaces have the same shape and have the asymptote parallel to ω_{vac} in common. Only a shift in the direction perpendicular to \mathbf{k}_0 is hence allowed. This follows also from the basic equations. We have to calculate the change Δ_1 in \mathbf{k} due to $d\mathbf{b}$ for constant ξ . This gives immediately *)

$$\begin{aligned} \Delta_1 \cdot \mathbf{k}_0 &= 0, \\ \Delta_1 \cdot \mathbf{k}_0' &= 2\mathbf{k}_0' \cdot d\mathbf{b}. \end{aligned} \quad (10.4.3)$$

It is important to note that Δ_1 is zero if $d\mathbf{b}$ is perpendicular to $\mathbf{k}_0 - 2\mathbf{b}'$. In other words: the ω -surface in the region around \mathbf{k}_0 remains unchanged if the component of \mathbf{b} in the direction \mathbf{k}_0' remains constant.

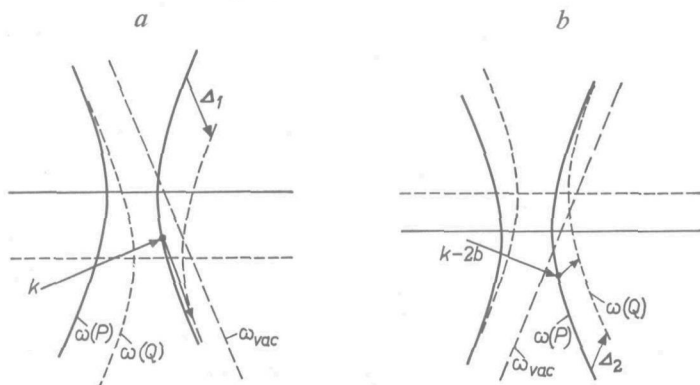


Fig. 10.1. The relative position of the ω -surfaces in two neighbouring points P and Q on the path of one X-ray beam through a deformed crystal. In (a) the area of \mathbf{k} -space around \mathbf{k}_0 is reproduced, in (b) the area around $\mathbf{k}_0' = \mathbf{k}_0 - 2\mathbf{b}$.

*) The magnitudes of Δ_1 and $d\mathbf{b}$ are so small that \mathbf{k} and $\mathbf{k} - 2\mathbf{b}$ may be replaced by \mathbf{k}_0 and $\mathbf{k}_0 - 2\mathbf{b}'$, respectively, vectors defined for the undeformed crystal.

In fig. 10.1*b* the ω -surfaces in P and Q in the region around \mathbf{k}_0' are shown. Now the line ω_{vac} is parallel to the other asymptote and the shift Δ_2 must be perpendicular to $\mathbf{k}_0 - 2\mathbf{b}'$. From the basic equations follows

$$\begin{aligned}\Delta_2 \cdot \mathbf{k}_0 &= 2\mathbf{k}_0 \cdot \mathbf{db}, \\ \Delta_2 \cdot \mathbf{k}_0' &= 0.\end{aligned}\tag{10.4.4}$$

The ω -surface in this part of the \mathbf{k} -space remains stationary if the component of \mathbf{b} in the direction \mathbf{k}_0 is constant.

From fig. 10.1 it is evident that we cannot determine which mode(s) will prevail in Q for given \mathbf{k} in P, without further specification of the problem. A change in \mathbf{k} has to take place since \mathbf{k} in P does not lie on the ω -surface in Q. If the change in \mathbf{b} were abrupt along a certain plane (normal \mathbf{n}) then the procedure would be known. The vector \mathbf{k} in Q would lie on the line through \mathbf{k} in P parallel to \mathbf{n} , giving two possible modes. A similar procedure in the region around $\mathbf{k}_0 - 2\mathbf{b}'$ would give two other possible modes. In total four modes would be activated in Q. Nevertheless we expect, as mentioned before, that for a continuous change in \mathbf{b} only one mode is present in Q. The procedure to find this \mathbf{k} -vector is discussed in the next section.

10.5. Wave-field matching along the path

Before giving a solution for the matching, we inspect first the somewhat analogous, but much simpler case of a beam of light travelling through a medium with variable index of refraction n . There we know that if n varies slowly the path of the beam remains well defined. At any place along the path one value of \mathbf{k} suffices to describe its behaviour. However, the path is curved in general, indicating that \mathbf{k} varies along the path, not only in magnitude because of the change in n , but also in direction. It is well known that $\delta\mathbf{k}$ in this case is parallel to $\nabla_{\mathbf{r}}n$. The component of \mathbf{k} in the plane of equal n remains unchanged. In other words, one must look for that plane in space through the point of observation in which n is constant. Note that the orientation of this plane is independent of \mathbf{k} . The direction of the necessary change in \mathbf{k} is perpendicular to this plane. The magnitude of the change is found from the requirement that the new value of \mathbf{k} must lie on the new ω -surface. This magnitude depends on the direction of \mathbf{k} .

In the X-ray case we shall follow a similar procedure. We have to look for those planes through the point P where the X-ray wave field regards the deformed crystal as uniform. In other words we have to find planes in which the ω -surface remains in the same position in spite of the deformation. In the preceding section it was shown that the two parts of the ω -surface shift over different distances (fig. 10.1). For a finite \mathbf{db} it is in general impossible to find a plane through P in which both parts remain in the same position. It is possible,

however, to find a plane in which the upper part does not shift and another plane in which the lower part is fixed. Therefore we shall use different planes for the two parts of the ω -surface and show later that the new \mathbf{k} in the neighbourhood of \mathbf{k}_0 and the new \mathbf{k}' in the neighbourhood of \mathbf{k}_0' correspond to one and the same mode.

First consider the upper part of the ω -surface. There Δ_1 is equal to zero if the component of \mathbf{b} in the direction \mathbf{k}_0' remains constant (eqs (10.4.3)). Whatever the strain may be, there is always one plane through P in which as a first approximation $\mathbf{k}_0' \cdot \mathbf{b}$ is constant. The assertion *) is now that the change in \mathbf{k} necessary to match the solutions in P and Q is parallel to the normal of this plane:

$$d\mathbf{k} = \tau \nabla_{\mathbf{r}} (\mathbf{b} \cdot \mathbf{k}_0'). \quad (10.5.1)$$

The proportionality factor τ follows from the requirement that $\mathbf{k} + d\mathbf{k}$ must lie on the ω -surface in Q. From the basic equations follows:

$$\begin{aligned} 2\mathbf{k}_0 \cdot d\mathbf{k} &= V_1 d\xi, \\ 2\xi^2(\mathbf{k}_0 - 2\mathbf{b}') \cdot (d\mathbf{k} - 2d\mathbf{b}) &= -V_1 d\xi. \end{aligned}$$

Elimination of $d\xi$ and substituting eqs (10.5.1) and (10.4.2) for $d\mathbf{k}$ and $d\mathbf{b}$, respectively, yields

$$\tau(\mathbf{k}_0 + \xi^2\mathbf{k}_0') \cdot \nabla_{\mathbf{r}}(\mathbf{k}_0' \cdot \mathbf{b}) = 2\xi^2(d\mathbf{r} \cdot \nabla_{\mathbf{r}})(\mathbf{k}_0' \cdot \mathbf{b}).$$

Remembering that $\mathbf{k}_0 + \xi^2\mathbf{k}_0'$ is parallel to \mathbf{v}_g and introducing the expression (10.4.1) for $d\mathbf{r}$, gives

$$\tau = (c^2/\omega) [2\xi^2/(1 + \xi^2)] a dl.$$

With the aid of eq. (10.3.3) to eliminate \mathbf{b} one obtains for the change in \mathbf{k} :

$$d\mathbf{k} = -(c^2/\omega) [2\xi^2/(1 + \xi^2)] a dl \nabla_{\mathbf{r}} (\mathbf{k}_0' \cdot \nabla_{\mathbf{r}}) (\mathbf{v} \cdot \mathbf{b}'). \quad (10.5.2)$$

The change in ξ is equal to

$$d\xi = -4 (c^2/\omega) [\xi^2/(1 + \xi^2)] (a dl/V_1) (\mathbf{k}_0 \cdot \nabla_{\mathbf{r}}) (\mathbf{k}_0' \cdot \nabla_{\mathbf{r}}) (\mathbf{v} \cdot \mathbf{b}'). \quad (10.5.3)$$

Now we turn to the lower part of the ω -surface in the neighbourhood of \mathbf{k}_0' . There the ω -surface remains in the same position if $\mathbf{k}_0 \cdot \mathbf{b}$ is constant (eqs (10.4.4)). Using the same idea that the change in \mathbf{k} necessary for matching is normal to the plane of constant $\mathbf{k}_0 \cdot \mathbf{b}$, leads to

$$d\mathbf{k}' = \tau' \nabla_{\mathbf{r}} (\mathbf{k}_0 \cdot \mathbf{b}).$$

In the same way as above one calculates:

*) For a derivation of this assertion from Maxwell's equations, see ref. 30.

$$d\mathbf{k}' = (c^2/\omega) [2/(1 + \xi^2)] a dl \nabla_{\mathbf{r}} (\mathbf{k}_0 \cdot \nabla_{\mathbf{r}}) (\mathbf{v} \cdot \mathbf{b}') \quad (10.5.4)$$

and

$$d\xi = -4 (c^2/\omega) [\xi^2/(1 + \xi^2)] (a dl/V_1) (\mathbf{k}_0' \cdot \nabla_{\mathbf{r}}) (\mathbf{k}_0 \cdot \nabla_{\mathbf{r}}) (\mathbf{v} \cdot \mathbf{b}'). \quad (10.5.5)$$

Now the question arises whether the solution obtained in the upper part is identical with the solution obtained in the lower part. Since any point on the ω -surface corresponds to one value of ξ only, and we started with one mode, we must require that the expressions (10.5.3) and (10.5.5) for $d\xi$ are identical. If this were not the case the results would be internally inconsistent, since we started with the assumption that one mode remains one mode. The difference in (10.5.3) and (10.5.5) is the order in which \mathbf{k}_0 and \mathbf{k}_0' occur. However, the interchange is admissible so that they are indeed identical.

10.6. Discussion

In the previous sections it was shown that the assertion that a well-behaved beam remains well-behaved, leads to a consistent picture of the beam behaviour inside the deformed crystal. The beam has the opportunity to adapt itself to the gradually changing lattice, because the changes are small over the "Pendelösung"-length. The problem of beam transmission through a deformed crystal is now solved completely. The tangent to the path is given in eq. (10.4.1). It depends on the local value of ξ . The change of ξ along the path is given in eq. (10.5.3). Integrating them simultaneously gives the mathematical expression for the path, together with the ξ -values along the path. The loss in intensity because of absorption is given by the absorption coefficient

$$(dI)/I = -\mu dl, \quad (10.6.1)$$

where μ is a function of ξ and hence variable along the path.

We shall use ξ as the variable mode parameter instead of \mathbf{k} . The major advantage is then that the shift in ω -surface is no longer relevant. Henceforth we shall keep the ω -surface fixed and investigate only the movement of the \mathbf{k} -vector along the ω -surface.

10.7. Examples of beam transmission through deformed crystals

10.7.1. Deformations that do not influence the beam behaviour

Some types of deformation do not influence the behaviour of the beam inside the crystal. A necessary and sufficient condition is that the mode parameter ξ remains constant. A number of possibilities are trivial:

- (a) The displacement vector \mathbf{v} is a linear function of \mathbf{r} , corresponding with a uniform strain. Although the crystal is deformed, it remains perfectly periodic.
- (b) $\xi = 0$ or $\pm \infty$. Now \mathbf{k} is so far off Bragg angle that there is no interaction

with the periodicity of the lattice and it ought to be irrelevant whether there is strain or not.

- (c) The displacement vector \mathbf{v} is perpendicular to \mathbf{b}' . All atoms are displaced parallel to the reflecting planes. Since the distribution of atoms in the reflecting planes plays no part in the diffraction phenomenon, no effect is expected.

One non-trivial possibility is found. The differential operator $(\mathbf{k}_0 \cdot \nabla_{\mathbf{r}})(\mathbf{k}_0' \cdot \nabla_{\mathbf{r}})$ may be rewritten in the form $\cos^2(\theta) \partial^2/\partial z^2 - \sin^2(\theta) \partial^2/\partial x^2$, where z and x are coordinates along and perpendicular to the reflecting planes, respectively. The relevant component of \mathbf{v} ($\parallel \mathbf{b}$) is denoted by u . All deformations, for which

$$\cos^2(\theta) \partial^2 u / \partial z^2 - \sin^2(\theta) \partial^2 u / \partial x^2 = 0,$$

correspond to deformations that leave the path of the X-ray beam unchanged. A simple example is

$$u = xz/l.$$

It may be verified with the aid of eq. (10.3.2) that in this case the reflecting planes remain flat for $x, z \ll l$. However, they are not parallel, but they fan out from a line far outside the crystal ($x = 0, z = -l$). A schematic drawing is given in fig. 10.2. It is at first sight astonishing that in this case the X-ray

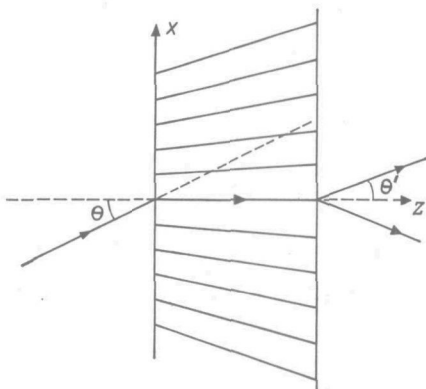


Fig. 10.2. A schematic drawing for the deformation discussed in sub-section 10.7.1. The reflecting planes remain flat but all pass through the line $x = 0, z = -l$. The X-ray transmission is the same as in the undeformed crystal, except for a small change in Bragg angle.

beam behaves as if the crystal was perfect: the beam remains straight, the value of ξ does not change. However, the actual value of \mathbf{k} cannot be constant, since \mathbf{b} changes. Careful measurements carried out by Cole and Brock²⁵⁾ show that the transmitted beam is not exactly parallel to the incident beam. The difference in angle could be explained by assuming that both the incident and the transmitted beam satisfy exactly the Bragg equation. A simple explanation of this effect may be given in more physical terms. In the theory use is made of plane-

parallel waves. The nodal planes in the modes turn out to be flat and equidistant with eventually all atoms lying in them. Making use, however, of cylindrical waves, which obey Maxwell's laws also, the nodal planes all go through the cylinder axis, just as the reflecting planes in the case under discussion now. Hence we expect the cylinder wave to pass through this crystal undisturbed.

10.7.2. Reflecting planes curved, but parallel and equidistant

A simple example of a deformed crystal where the behaviour of the X-ray beam is influenced by the distortion, is a cylindrically curved lattice. In fig. 10.3

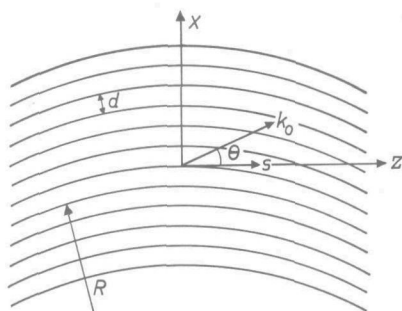


Fig. 10.3. A schematic drawing for the deformation in sub-section 10.7.2. The spacing between the reflecting planes is constant, but there is a curvature of the lattice.

the situation is drawn schematically. The coordinate system that will be used is indicated. The deformation is exaggerated, since it is assumed that the radius of curvature R is many orders of magnitude larger than the spacing d between the reflecting planes.

From the figure it follows immediately that

$$\mathbf{b} = \mathbf{b}' - \nabla_{\mathbf{r}}(\mathbf{v} \cdot \mathbf{b}') = \mathbf{b}' + \alpha z \mathbf{s}. \quad (10.7.1)$$

The proportionality factor α is related to the radius of curvature:

$$\alpha = \sin(\theta) \omega / cR. \quad (10.7.2)$$

Substitution of eq. (10.7.1) into eq. (10.5.3) gives for the variation in ξ :

$$\frac{1}{2} d(\xi - 1/\xi) = 2\omega a dl \cos^2(\theta) \alpha / V_1.$$

The component of \mathbf{v}_g parallel to the reflecting planes is always equal to $c \cos \theta$. Thus

$$ac \cos(\theta) dl = dz$$

and

$$\frac{1}{2} (d/dz) (\xi - 1/\xi) = 2(\omega/c) [\cos(\theta)/V_1] \alpha = \beta. \quad (10.7.3)$$

We choose the origin in such a way that $\xi = \pm 1$ for $z = 0$:

$$\xi - 1/\xi = 2\beta z. \quad (10.7.4)$$

The path of the beam follows from the direction of the group velocity (eq. (6.3.4)):

$$dx/dz = \tan(\theta) (1 - \xi^2)/(1 + \xi^2),$$

leading to

$$\beta(x - C) = \pm \tan(\theta) (1 + \beta^2 z^2)^{1/2}.$$

The upper sign corresponds to weakly damped modes ($\xi < 0$) and the lower sign to strongly damped modes ($\xi > 0$). The arbitrary constant C appears in the solution because the deformation is independent of x . Setting C equal to zero the expression for the path may be rewritten as

$$x^2 - \tan^2(\theta) z^2 = \tan^2(\theta)/\beta^2. \tag{10.7.5}$$

Apparently the path is a hyperbola. In fig. 10.4a an example is given for $a > 0$ and hence $\beta < 0$. The asymptotes are parallel to the directions of the incident and reflected plane-wave components. The branch curved in the same sense as the reflecting planes (the lower one in fig. 10.4a) corresponds to the

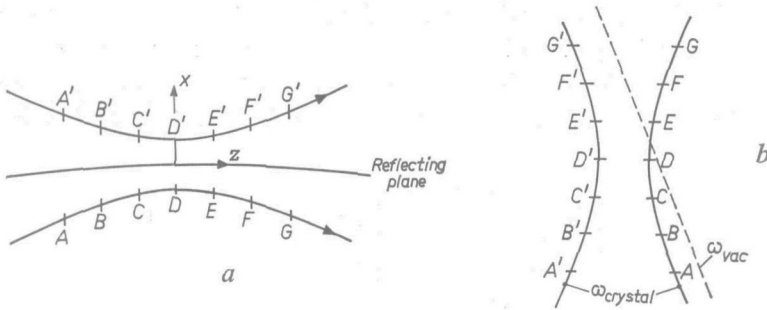


Fig. 10.4. The path of an X-ray beam (a) in a crystal deformed as in fig. 10.3. The wave vector of the mode present at a certain point is given in (b) with the same letter. The ω -surface was kept fixed.

weakly damped modes, the branch curved in the opposite sense to the strongly damped modes. For stronger curvatures of the lattice the path lies closer to the asymptotes. It can be verified that the minimum radius of curvature of the path (points D and D') is directly proportional to the radius of curvature of the reflecting planes:

$$R_{\min} = |\psi_1| R/2 \sin^2 \theta. \tag{10.7.6}$$

The ratio is of the order of 10^{-5} . Because of this small value the reflecting planes may be considered as flat in comparison with the path, and the z -axis as parallel to \mathbf{s} , as was done in deriving eq. (10.7.1).

In fig. 10.4b the ω -surface is shown. The \mathbf{k} -value of the mode prevailing at a certain point is indicated with letters corresponding with fig. 10.4a. Since in the \mathbf{k} -space the distance between a point on the ω -surface and the line DD' is proportional to $-\xi + \xi^{-1}$, and eq. (10.7.4) states that this parameter is

proportional to z , the local \mathbf{k} -vector moves with constant vertical speed along the ω -surface.

The two rays are absorbed in a different way. The absorption is extreme in D and D' , where the path is parallel to the reflecting planes. For the upper ray it is maximum: $(1 + \epsilon) \mu_0 / \cos \theta$, and for the lower ray minimum: $(1 - \epsilon) \mu_0 / \cos \theta$. The general expression for the fractional decrease in intensity (eq. (10.6.1)) may be written in this case as

$$(1/I) (dI/dz) = -\{1 + \epsilon 2\xi / (1 + \xi^2)\} \mu_0 / \cos \theta.$$

The local values of ξ follow from eq. (10.7.4). Integration leads to

$$\ln (I_2/I_1) = -\{1 + (\epsilon/\beta t) \ln (\xi_2/\xi_1)\} \mu_0 t / \cos \theta \quad (10.7.7)$$

for both rays. The parameters ξ_1 and ξ_2 , having the same sign, correspond to the ξ -values at the beginning and the end of the path over the distance t parallel to z . Note that the first term gives the normal absorption as if the beam were travelling straight on. The second term accounts for the anomalous behaviour. It is positive for the weakly damped modes ($|\xi_2| > |\xi_1|$ if $\beta < 0$) and negative for the strongly damped modes ($|\xi_2| < |\xi_1|$ if $\beta < 0$). In fig. 10.5 the logarithms of the beam intensities are given as a function of z . The scale along the vertical axis has to be adjusted in such a way that the straight line III gives the decrease

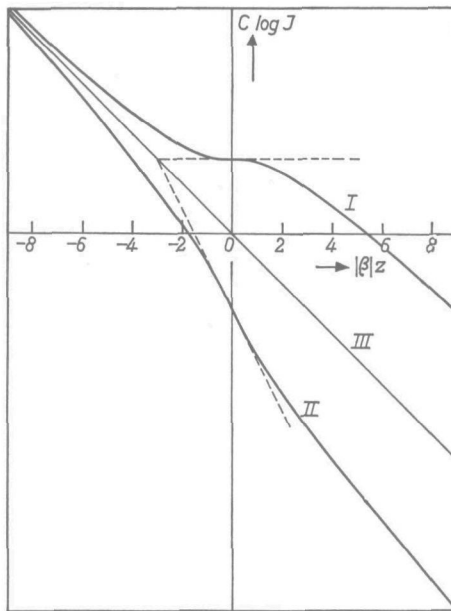


Fig. 10.5. The variation in intensity along the path of the beam in the crystal. Curve I corresponds to the weakly damped beam, curve II to the strongly damped beam and curve III to the decrease in the case where there is no diffraction. The parameter ϵ was set equal to 1.

in intensity due to normal absorption. The curves I and II then give the relative decrease in intensity for the weakly and strongly damped modes, respectively. The parameter ϵ was taken 1, so that the minimum slope is 0, and the maximum slope twice the slope of III.

The beam behaviour can be discussed also without so much mathematics. The crystal, with its cylindrically curved reflecting planes, is from X-ray point of view uniform in any plane through the cylinder axis. We asserted that the necessary change in \mathbf{k} is normal to these planes, i.e. parallel to the z -axis. Note that in this case the directions of $\delta\mathbf{k}$ are the same in the upper and lower part of the ω -surface. If a beam present in A is characterized by \mathbf{k}_A (fig. 10.6) this

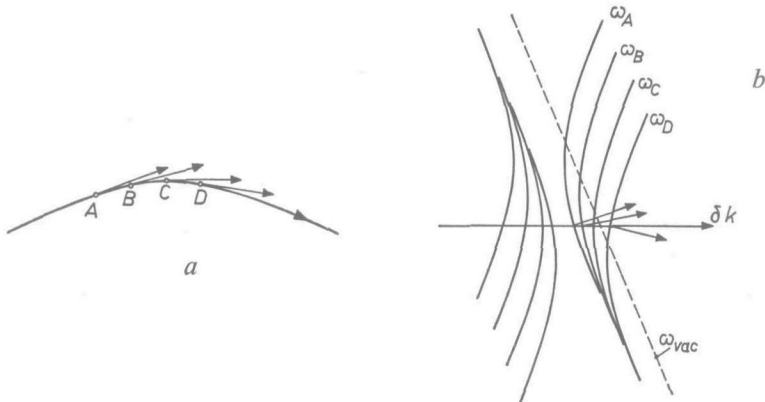


Fig. 10.6. Similar to fig. 10.4. In (a) the curved path of the weakly damped beam is shown; in (b) the ω -surfaces, taking into account the change in \mathbf{b} along the path.

vector must lie on the ω -surface ω_A , determined by the local value of \mathbf{b} in A. The group velocity is pointing upward and the beam travelling further in this direction comes into a region where \mathbf{b} has rotated clockwise over a minute amount (point B). Accordingly the ω -surface moved downward and \mathbf{k}_B is found as the intersection of $\delta\mathbf{k}$ with ω_B on the same branch. The group velocity has turned clockwise also. Proceeding further in this way one arrives at C where \mathbf{v}_g is parallel to the reflecting plane and still further at D with the group velocity pointing more and more downward. The result obtained above that $-\xi + \xi^{-1}$ is proportional to z follows immediately since the shift in ω -surface is proportional to the change in z .

10.7.3. Reflecting planes flat and parallel, but not equidistant

Another example of a simple deformation that influences the beam behaviour is shown in fig. 10.7. The reflecting planes are flat and parallel but their distance increases linearly with increasing z . In the figures the increase per reflecting plane has been exaggerated grossly. The distortion is assumed to be so small that \mathbf{b} may be considered as a smooth function of z :

$$\mathbf{b} = \mathbf{b}' - \nabla_{\mathbf{r}} (\mathbf{v} \cdot \mathbf{b}') = \mathbf{b}' + \alpha z \mathbf{s}, \quad (10.7.8)$$

with $|\alpha z| \ll |\mathbf{b}'|$ everywhere inside the crystal. Note that α is negative in fig. 10.7.

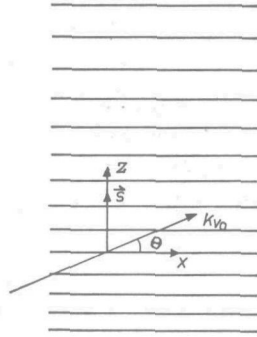


Fig. 10.7. A schematic drawing for the deformation discussed in sub-section 10.7.3. The reflecting planes remain flat but their spacing increases linearly with z .

Proceeding as in the previous case and choosing the plane $x = 0$ in such a way that there $\xi = \pm 1$, leads to

$$\xi - 1/\xi = -4\alpha x \sin(\theta) \tan(\theta) \omega/cV_1 = 2\beta \tan(\theta)x. \quad (10.7.9)$$

The path, determined from the group velocity, is given by the equation

$$z^2 - \tan^2(\theta) x^2 = \beta^2.$$

We note that all results found now, can be deduced from the results in the previous sub-section by replacing x and z there by $z \tan \theta$ and $x \tan \theta$, respectively. For example, the relative decrease in intensity is also given in fig. 10.5, provided the ordinate $|\beta|z$ is replaced by $|\beta| x \tan \theta$.

It is striking that these two types of deformation, being entirely different in nature, have the same influence on the overall beam behaviour. Closer inspection, however, shows that there are marked differences. Let us first compare the paths of different beams that are parallel in the region far off Bragg angle (fig. 10.8). In the case of curved reflecting planes (fig. 10.8a) the paths are shifted



Fig. 10.8. Neighbouring paths in case of curved reflecting planes with constant spacing (a) and in case of flat but not evenly spaced reflecting planes (b).

in a direction perpendicular to the reflecting planes, because in this direction the crystal is uniform. The different paths never cross. In the case of variable spacing

the paths are translated in a direction parallel to the reflecting planes (fig. 10.8*b*). Now the different paths cross over. For neighbouring paths the cross-over lies in the region of $|\xi| \approx 1$. This behaviour indicates that difficulties will arise in this region. More details are obtained by considering the change in \mathbf{k} during passage through the crystal taking the shift in ω -surface into account. In point A (fig. 10.9) the beam is travelling upward. It enters a region of larger spacing between the reflecting planes and hence smaller values of \mathbf{b} . The ω -surface shifts downward and is given by ω_B in B. Since the crystal is uniform in planes that are parallel to the reflecting planes $\delta\mathbf{k}$ must be parallel to \mathbf{b} . In B the group velocity has turned clockwise with respect to \mathbf{v}_g in A. This behaviour continues until the beam arrives in C where \mathbf{v}_g is parallel to the reflecting planes and $\delta\mathbf{k}$ is tangent to ω_C . One would expect that nothing further would happen. Propagation along the reflecting planes would not give any change in lattice parameter and hence could proceed over large distances. According to our results, however, the group velocity continues to rotate clockwise. The beam turns downward thus re-entering the region with larger values of \mathbf{b} . Eventually it arrives in point D on the same reflecting plane as point B. Here the ω -surface

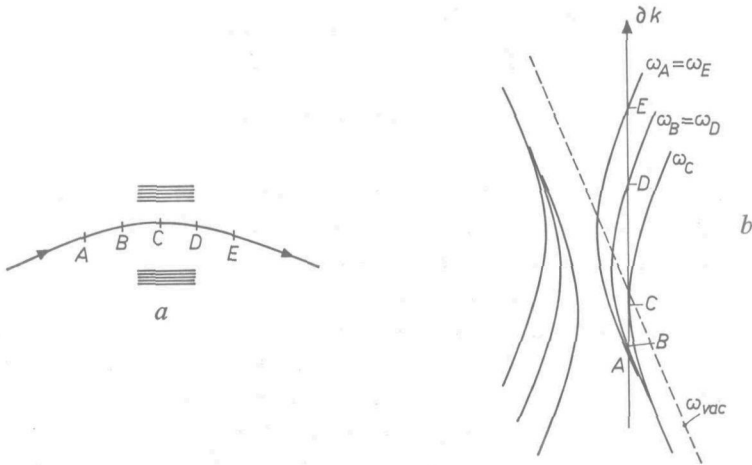


Fig. 10.9. The curved path of the X-ray beam passing through a crystal with variable spacing (a). The local wave vector along the path is given in (b).

is the same as in B, but a different \mathbf{k} -vector is obtained namely at the other intersection of $\delta\mathbf{k}$ with ω_B . Why there is such a behaviour in point C, is not easily understood, although it is similar to the well-known phenomenon in optics, the “fata morgana”, caused by a vertical gradient in the refractive index of air. It may be remarked that the case discussed in the previous sub-section has no analogy in optics.

10.8. Comparison with electron-band theory

It is interesting to compare these results with the electron-band theory. Imagine a single electron moving in a perfect crystal. The wave vector \mathbf{k} and the energy E are chosen in such a way that we have to consider the interaction with one set of lattice planes only. The z -axis is perpendicular to these planes (see fig. 10.10a). The E - k_z curve in such a situation is given schematically in

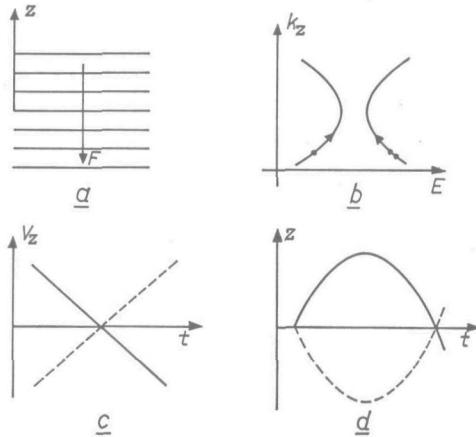


Fig. 10.10. Explanation, see text.

fig. 10.10b. The component of the electron velocity in the z -direction, v_z , is given by $\partial E/\partial k_z$. Imagine now that an electric field is present in the $-z$ -direction. According to wave mechanics k_z increases linearly with time. If the form of the E - k_z curve is known, one can calculate v_z and z as a function of time. In figs 10.10c and 10.10d they are given under the assumption that $E(k_z)$ is a parabola. The drawn lines represent the behaviour of an electron in the band with lower energies, the dashed curves for an electron in the band with higher energies. The interesting part is that the paths are curved also. The phenomenon is essentially the same as in the X-ray case. Here we have a constant lattice spacing but a variable wavelength. In the X-ray case we have a variable spacing and constant wavelength. In the electron case it is known that for sufficiently strong electric fields there is a chance that the electron may "tunnel" from the lower to the higher energy band. In the next chapter it will be shown that in the X-ray case a similar effect may be present if the spacing varies strongly with z .

11. DIFFRACTION IN CRYSTALS WHERE THE STRAIN IS A LINEAR FUNCTION OF ONE SPACE COORDINATE

11.1. Introduction

The ray theory, discussed in the previous chapter, is based upon the assumption that for slowly varying strain, one mode remains one mode. The adjustment of the wave field to the gradually changing lattice requires only a gradual change in wave vector and amplitude. The generation of modes with an appreciably different wave vector should not be necessary. An upper limit for the permissible change in reciprocal-lattice vector per unit distance was derived from the condition that locally the dynamical theory for undeformed crystals should be valid (sec. 10.3). It is not certain that the basic assumption is valid up to this limit. We have been looking for types of strain that allow for an exact solution without making use of this assumption. Such a solution should indicate: (1) the upper limit of applicability of the ray theory and (2) in what respects the ray theory fails for a stronger inhomogeneity in strain.

Fortunately we found such cases, namely crystals where the reciprocal-lattice vector is a linear function of one space coordinate (sz) only:

$$\mathbf{b} = \mathbf{b}' + \alpha z \mathbf{s}. \quad (11.1.1)$$

The two examples discussed in the previous chapter (sub-sections 10.7.2 and 10.7.3) belong to this group.

The orientation of the unit vector \mathbf{s} with respect to \mathbf{b}' is arbitrary. The curved reflecting planes (sub-section 10.7.2) are obtained if \mathbf{s} is perpendicular to \mathbf{b}' ; the flat but not equally spaced reflecting planes (sub-section 10.7.3) by taking \mathbf{s} parallel to \mathbf{b}' . The solutions obtained in this chapter are valid for any value of α , provided \mathbf{b}' may be considered as a smooth function of z .

It must be remarked that in this entire group the direction of strongest inhomogeneity is the same for the upward- and downward-travelling plane-wave components. A check on the correctness of the general matching procedure (sec. 10.5) is not obtained.

In the next section we shall derive the differential equations for the upward- and downward-travelling plane-wave components. They are satisfied by the parabolic cylinder functions. The relevant properties of these functions are given in the appendix. Although the solutions apply to an arbitrary orientation of \mathbf{s} with respect to \mathbf{b}' , we shall treat only the cases discussed in detail in chapter 10. First the results are given (sec. 11.3), thereafter the derivation.

It is shown that the basic assumption "one mode remains one mode" is valid up to the limit given in sec. 10.3. For a stronger inhomogeneity in strain part of the X-ray energy passes on, unaffected by the strain gradient.

11.2. Derivation of differential equations

In the crystals under discussion now, the strain is a linear function of z in the direction of \mathbf{s} . To determine the orientation of \mathbf{s} we shall again use the parameter γ (eq. (7.1.1)), although the crystal is considered to be unbounded.

By slicing the crystal into thin slabs perpendicular to \mathbf{s} , we obtain crystals that may be considered as uniform. The boundary conditions require that the tangential components of \mathbf{k} are the same in all slabs:

$$\mathbf{k} = \mathbf{k}_v + \tau(z) \mathbf{s}. \quad (11.2.1)$$

The vector \mathbf{k}_v is chosen on the ω -surface in vacuum and satisfies Bragg's equation somewhere inside the crystal. The proportionality factor τ has to be adjusted in such a way that \mathbf{k} lies on the " ω -surface" of the slab at z . By neglecting terms with α^2 , $\alpha\tau$ and τ^2 , we obtain from the basic equations:

$$\tau(z) = (V_0 + V_1\xi)/2\mathbf{k}_0 \cdot \mathbf{s} \quad (11.2.2)$$

and

$$V_1(\xi - \gamma/\xi) = (\gamma - 1)V_0 + \gamma 4\mathbf{b}' \cdot (\mathbf{k}_v - \mathbf{b}') + 4\alpha z \mathbf{k}_0 \cdot \mathbf{s}. \quad (11.2.3)$$

In terms with V_0 and V_1 , \mathbf{k}_v is replaced by \mathbf{k}_0 , since the precise orientation of \mathbf{k}_v is not of importance there. Equation (11.2.3) gives two solutions for ξ , indicating that only two modes can be present in any slab. This low number is an immediate consequence of the fact that the directions of inhomogeneity are the same for the upward- and downward-travelling waves.

The amplitude matching at the boundaries requires that the total amplitude D_i of the upward-travelling waves and the total amplitude D_r of the downward-travelling waves are both continuous at the boundary.

Inside an arbitrary slab the total amplitudes vary in the following way:

$$D_i = M \exp(-j\mathbf{k} \cdot \mathbf{r}) + M' \exp(-j\mathbf{k}' \cdot \mathbf{r}) \quad (11.2.4)$$

and

$$D_r = \{\xi M \exp(-j\mathbf{k} \cdot \mathbf{r}) + \xi' M' \exp(-j\mathbf{k}' \cdot \mathbf{r})\} \exp(2j\mathbf{b} \cdot \mathbf{r}). \quad (11.2.5)$$

The parameters characterizing the second mode (M is amplitude of upward-travelling component) are indicated with a prime. To eliminate the rapid change in phase within one unit cell and to make the problem a one-dimensional one, we multiply both amplitudes by $\exp(j\mathbf{k}_v \cdot \mathbf{r})$. Furthermore we shall consider only those points where $\exp(2j\mathbf{b} \cdot \mathbf{r})$ is equal to unity (identical points in the unit cell). We obtain then

$$A_i = M \exp(-j\tau z) + M' \exp(-j\tau' z)$$

and

$$A_r = \xi M \exp(-j\tau z) + \xi' M' \exp(-j\tau' z).$$

With the aid of these equations and the boundary conditions the differential equations for A_i and A_r are now easily found to be

$$2\mathbf{k}_0 \cdot \mathbf{s} \, dA_i/dz = -jV_0A_i - jV_1A_r \quad (11.2.6)$$

and

$$2\mathbf{k}_0 \cdot \mathbf{s} \, dA_r/dz = -j\gamma V_1A_i - j\{\gamma V_0 + 4\gamma \mathbf{b}' \cdot (\mathbf{k}_v - \mathbf{b}') + 4az\mathbf{k}_0 \cdot \mathbf{s}\} A_r. \quad (11.2.7)$$

By suitable substitutions (sec. 11.4) these equations may be reduced to the recurrence formulae for the parabolic cylinder functions, that satisfy Weber's equation.

11.3. Results and discussion

Before giving the derivation, we shall discuss the results of applying the parabolic cylinder functions to our problem. The results are illustrated for the two examples treated in the sub-sections 10.7.2 and 10.7.3.

First the situation of curved, but parallel and equally spaced reflecting planes (fig. 10.3). The regions of large values of $|z|$ are of special interest since the parabolic cylinder functions are known there in closed form. In fig. 11.1 the

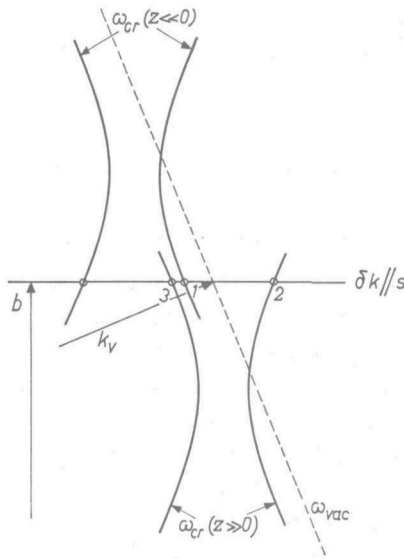


Fig. 11.1. The location of the ω -surfaces at $|z| \gg 0$ for the situation shown in fig. 10.3. The reflecting planes are curved but parallel and equidistant. The figure can be compared with fig. 10.6b. The exact treatment gives mode 1 for $z \ll 0$ and modes 2 and 3 for $z \gg 0$.

ω -surfaces are shown for $z \ll 0$ and $z \gg 0$. The sign of α is positive so that the ω -surface moves downward with increasing z . According to eq. (11.2.1) the wave vectors must lie on a line parallel to \mathbf{s} through \mathbf{k}_v . If one starts with one mode at $z \ll 0$ (mode 1), then there are two possible modes at $z \gg 0$, the points 2 and 3. According to the ray theory we expect only point 2, lying on the same branch as point 1. The exact solution, however, gives a finite amplitude

for both modes 2 and 3. By constructing a Gaussian wave packet centered around \mathbf{k}_v , beams are obtained and the centre line of these beams may be followed in the regions $|z| \gg 0$. They are shown as drawn lines in fig. 11.2.

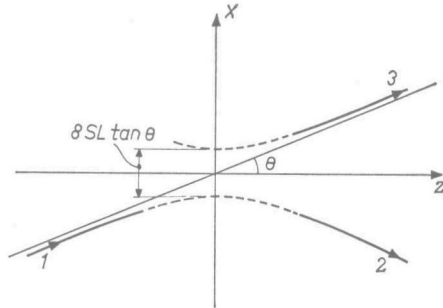


Fig. 11.2. The exact treatment of the wave-field behaviour gives in the case of curved reflecting planes the drawn lines as paths of the beams. The parts 1 and 2 coincide with the path found in the ray theory (see fig. 10.6a). Beam 3 is unexpected.

The mathematical expression of the path is identical with eq. (10.7.5) found with the ray theory. All three paths are part of a hyperbola. Apparently mode 3 corresponds to a beam that passes straight on through the region of strong interaction with the lattice.

It is convenient to introduce the parameter S , to describe the change in strain, instead of α :

$$S = |(\gamma/2\alpha) (V_1/2\mathbf{k}_0 \cdot \mathbf{s})^2|. \quad (11.3.1)$$

The significance of S is illustrated by the fact that the shortest distance between the branches of the extrapolated paths (fig. 11.2) is equal to $8 SL \tan \theta$. For large values of S the branches do not come closely together. For S of the order 1 or smaller the distance between the branches is of the order of the "Pendellösung"-length L , or smaller. The rate of change in strain is then large.

The beam intensities may be calculated also from the parabolic cylinder functions. For $S \gg 1$ (slowly varying strain) the ratio in intensity of beam 2 (I_2) and beam 1 (I_1) is given exactly by eq. (10.7.7) derived with the ray theory. The intensity of the "transmitted" beam 3 (I_3) is then exceedingly small. Apart from normal absorption, based on a straight path, it is given by *)

$$I_3/I_1 = \exp(-2\pi S). \quad (11.3.2)$$

The anomalous behaviour in absorption does not play a part there, because what is gained by reduced absorption in the first part of the path, is lost by enhanced absorption in the second part.

*) It may be expected that for $S \gg 1$ the small intensity of the "transmitted" beam is very sensitive to seemingly unimportant parameters, such as the change in V_1 because of the (variable) strain. Only in the case V_1 constant and a linear dependence of \mathbf{b} on z is the pre-exponential factor equal to unity.

For $S \approx 1$ or smaller the “transmitted” intensity is of the same order as the incident intensity, and the ray theory apparently is no longer valid. It can be shown, by introducing L instead of V_1 in the expression (10.3.1) for S , that the condition $S > 1$ is identical with the condition mentioned in sec. 10.3 necessary to define a local ω -surface.

For $S \ll 1$ we find in non-absorbing crystals as intensity ratios:

$$I_2/I_1 = 2\pi S \quad (11.3.3)$$

and

$$I_3/I_1 = 1 - 2\pi S. \quad (11.3.4)$$

The generation of the “transmitted” beam can be explained qualitatively in the following way. For large negative values of z the wave field is rather far off Bragg angle. The interaction with the lattice is so weak, that in spite of the rapid change in orientation of the lattice, the beam may adjust itself gradually. Near to the top of the path, however, the downward-travelling component of the wave field has to increase so rapidly, in order to obtain the necessary curvature of the path, that the number of reflecting planes is insufficient to generate it. Consequently, part of the X-ray energy has to pass on without being reflected. Such a situation is ideally suited for a kinematical approach. It is shown in sec. 11.4.4 that a kinematical treatment indeed gives eq. (11.3.3). The parabolic cylinder functions apparently span the entire gap between the dynamical and kinematical treatments.

We did not succeed in calculating the path of the beam in the region of smaller values of z , where the top is expected. By using infinitely wide wave fields, however, one can calculate the ratio X in amplitudes of the downward- and upward-travelling components in the region $z \leq 0$. It is shown that for $S \gg 1$ this ratio X is equal to $\xi(z)$, so that indeed one mode remains one mode up to the apex of the path.

The other interesting example that has been investigated in more detail is the case of flat and parallel reflecting planes with linearly increasing mutual distance. The situation is shown in fig. 10.7 and discussed in sub-section 10.7.3. The location of the ω -surfaces for large values of $|z|$ is given in fig. 11.3. For given \mathbf{k}_v there are two possible modes for both $z \gg 0$ and $z \ll 0$. In the exact treatment we find that if the modes 1 and 2 are present for $z \ll 0$, there is a mode 3 for $z \gg 0$. The ray theory gives the modes 1 and 2 on one branch only. Constructing beams we find as centre lines the drawn parts of the hyperbola in fig. 11.4. In agreement with fig. 11.3 the beams 1 and 3 travel upwards and beam 2 downwards. Apparently a “transmitted” beam is present in this case also. In fact all results obtained in the regions of large values of $|z|$ concerning the paths and the intensities are identical with those found in the previous case. A similar agreement with the ray theory ($S \gg 1$) and the kinematical theory ($S \ll 1$) is present.

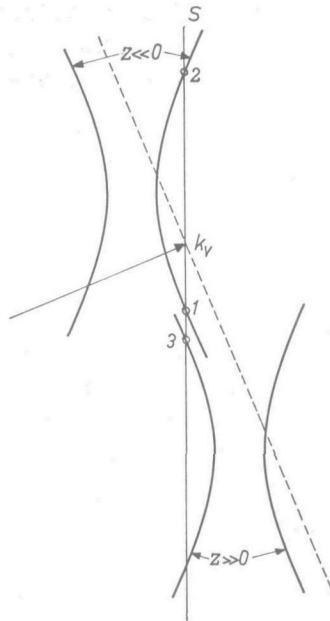


Fig. 11.3. The location of the ω -surfaces at $|z| \gg 0$ for the situation shown in fig. 10.7. The reflecting planes are flat and parallel but not evenly spaced. The exact treatment gives modes 1 and 2 for $z \ll 0$ and mode 3 for $z \gg 0$.

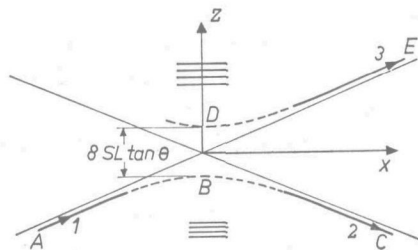


Fig. 11.4. The drawn lines correspond to the paths of the beams following from the exact treatment in the case of not evenly spaced, parallel reflecting planes. Path 1-2 is the same as found in the ray theory (see fig. 10.9a). Beam 3 is unexpected.

In the region of small values of $|z|$ no details of the beam behaviour have been found. We confine ourselves to giving a qualitative argument for the presence of the “transmitted” beam. The tops of the hyperbolic path coincide with the boundary between the regions where normal modes are present and the region where the modes have cut-off character. The upper flank of the beam above B (fig. 11.4) extends into the region of cut-off modes. The decrease in amplitude there is no longer governed by the beam width but by the extinction (see the discussion of fig. 9.6). Although the extinction is strong, it does not

reduce the amplitudes to zero. A small amplitude is still present in the region where ξ is real again (above D). The wave field present there must finally emerge as a "transmitted" beam. It is difficult to make this argument quantitative, even in the case of no absorption. Assuming that only those cut-off modes are activated that give a decreasing amplitude with increasing z , allows us to calculate the amplitude relations in B and D. The major difficulty is the relation in amplitudes in the points A and B on one side and in the points D and E on the other. Although we know that in non-absorbing crystals the intensity remains unchanged along the path, the amplitude ratio cannot be determined without further consideration, because of the singularity in the beam width in the points B and D. It tends to zero there, according to fig. 10.8*b*. By assuming that $|D_D|^2/I_E = |D_B|^2/I_A$ one obtains eq. (11.3.2).

To conclude the discussion we calculate the lowest value of S used in Okkerse's experiments¹⁹⁾ to verify the ray theory. The curvature of the lattice planes is brought about by a temperature gradient of up to 20 °C/cm. The minimum radius of curvature of the reflecting planes is then 83 m and that of the X-ray path 0.6 cm (considering the (220) reflexion and CuK α radiation). The value of S turns out to be slightly less than 600, well above the lower limit of applicability of the ray theory.

11.4. Derivation of results

11.4.1. General solution

The differential equations (11.2.6) and (11.2.7) for A_i and A_r may be transformed into the recurrence relations (A2) and (A3) (see appendix) in two different ways. Either A_i is proportional to D_ν and A_r proportional to $D_{\nu-1}$ or the other way round:

$$\begin{aligned} \text{case I:} \quad & A_i = pD_\nu(u) \exp [\dots], \\ & A_r = pCD_{\nu-1}(u) \exp [\dots], \end{aligned} \tag{11.4.1}$$

$$\begin{aligned} \text{case II:} \quad & A_i = pCD_{\nu-1}(u) \exp [\dots], \\ & A_r = pD_\nu(u) \exp [\dots], \end{aligned}$$

where

$$[\dots] = [\frac{1}{4}u^2 - juV_0/\zeta 2\mathbf{k}_0 \cdot \mathbf{s}], \tag{11.4.2}$$

$$u = \zeta (z + z_r + jz_i), \tag{11.4.3}$$

and p arbitrary. The other parameters have a meaning as given in table I. For a given strain, determining γ and α , there are four possible solutions since the choice between the cases I and II, and the choice between the two roots of ζ^2 are still free.

The special cases discussed in the sub-sections 10.7.2 and 10.7.3 are obtained by considering case I and giving the other parameters values as stated in table II.

TABLE I

Relations between the different parameters introduced

	case I	case II
ζ^2	$-j2\alpha$	$j2\alpha$
ν	$j(\gamma/2\alpha)(V_1/2\mathbf{k}_0 \cdot \mathbf{s})^2$	$-j(\gamma/2\alpha)(V_1/2\mathbf{k}_0 \cdot \mathbf{s})^2$
C	$j(\gamma/\zeta)V_1/2\mathbf{k}_0 \cdot \mathbf{s}$	$j(\gamma/\zeta)V_1/2\mathbf{k}_0 \cdot \mathbf{s}$
$\xi - \gamma/\xi$	$Cu/\nu = -\gamma u/C$	$-\gamma C u/\nu = u/C$
$z_r + jz_i$	$[(\gamma - 1)/2\alpha](V_0/2\mathbf{k}_0 \cdot \mathbf{s}) + (\gamma/\alpha)\mathbf{b}' \cdot (\mathbf{k}_\nu - \mathbf{b}')/\mathbf{k}_0 \cdot \mathbf{s}$	

TABLE II

Parameter values leading to the examples discussed in sub-sections 10.7.2 and 10.7.3

	sub-section 10.7.2	sub-section 10.7.3
γ	1	-1
α	> 0	< 0
$\arg \zeta$	$\frac{3}{4}\pi$	$\frac{1}{4}\pi$
$\arg u; z < 0$	$-\frac{1}{4}\pi$	$-\frac{3}{4}\pi + \Delta$
$\arg u; z > 0$	$\frac{3}{4}\pi$	$\frac{1}{4}\pi + \Delta$
z_r	$(1/\alpha)\mathbf{b}' \cdot (\mathbf{k}_\nu - \mathbf{b}')/\mathbf{k}_0 \cdot \mathbf{s}$	$-(1/\alpha)\mathbf{b}' \cdot (\mathbf{k}_\nu - \mathbf{b}')/\mathbf{k}_0 \cdot \mathbf{s} +$ $-(1/\alpha)V_0/2\mathbf{k}_0 \cdot \mathbf{s}$
z_i	0	$\mu_0/2\alpha \sin \theta$
β	$\alpha 2\mathbf{k}_0 \cdot \mathbf{s}/V_1$	$-\alpha 2\mathbf{k}_0 \cdot \mathbf{s}/V_1$

The parameter Δ is the phase angle of $z + z_r + jz_i$:

$$\tan \Delta = z_i/(z + z_r); \quad |\Delta| < \pi/2. \quad (11.4.4)$$

In the regions $|z| \gg 0$, the value of $|\Delta|$ is small. The imaginary part of V_0 is replaced by μ_0 (eq. (8.4.2)). To give the imaginary part of V_1 we use the parameter δ :

$$V_1 = \underline{V}_1 (1 + j\delta); \quad 0 < \delta \ll 1. \quad (11.4.5)$$

The value of ν in both examples is now given by

$$\nu = jS - 2\delta S,$$

with S defined in eq. (11.3.1).

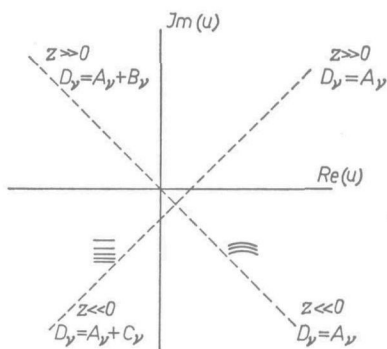


Fig. 11.5. The relation between the complex variable u in the parabolic cylinder functions and the space coordinate z , for the two cases discussed in this chapter.

In fig. 11.5 the relation between u and z for both cases is shown. As pointed out in the appendix the asymptotic values of D_ν for $|u| \gg 0$ depend on the argument of u . In the figure is also indicated which asymptotic value has to be used. The values of $|z|$ are assumed to be so large that R_ν and S_ν (eq. (A8)) may be set equal to unity. In the regions where D_ν contains only one term the resulting values for D_i and D_r will be given the index 1. In the regions where D_ν contains two terms, these parts will be treated separately. The values of D_i and D_r resulting from B_ν or C_ν are given the index 2 and those resulting from A_ν the index 3. Substitution of the expressions for D_ν given in eq. (A7) into eqs (11.4.1) (case I) and adding a factor $\exp(-j\mathbf{k}_\nu \cdot \mathbf{r})$ to obtain D_i and D_r , leads to ($\gamma = \pm 1$)

$$D_{i1} = pu^\nu \exp \{-j\mathbf{k}_\nu \cdot \mathbf{r} - juV_0/\zeta 2\mathbf{k}_0 \cdot \mathbf{s}\}, \quad (11.4.6)$$

$$D_{r1} = D_{i1}C/u = -\gamma D_{i1}/(\xi - \gamma/\xi);$$

$$D_{i2} = -p (2\pi)^{1/2} u^{-\nu-1} \exp \{-j\mathbf{k}_\nu \cdot \mathbf{r} + \frac{1}{2} u^2 + j\gamma\pi\nu - juV_0/\zeta 2\mathbf{k}_0 \cdot \mathbf{s}\}/\Gamma(-\nu),$$

$$D_{r2} = D_{i2}Cu/\nu = (\xi - \gamma/\xi) D_{i2}; \quad (11.4.7)$$

$$\begin{aligned}
 D_{i3} &= pu^v \exp \{-j\mathbf{k}_v \cdot \mathbf{r} - juV_0/\zeta 2\mathbf{k}_0 \cdot \mathbf{s}\}, \\
 D_{r3} &= D_{i3}C/u = -\gamma D_{i3}/(\xi - \gamma/\xi).
 \end{aligned}
 \tag{11.4.8}$$

11.4.2. Reflecting planes curved, but parallel and equidistant

First consider the region where $z \ll 0$. There the argument of u is $-\pi/4$ and the amplitudes are given in eq. (11.4.6). The ratio in amplitude of the downward- and upward-travelling components is

$$X = D_{r1}/D_{i1} = -(\xi - 1/\xi)^{-1}.$$

According to eq. (11.2.3) the value of $\xi - 1/\xi$ is almost real, large and positive. Hence $|D_{r1}|$ is much smaller than $|D_{i1}|$. Apparently the two components form one mode together with a small negative value of ξ as long as $|\xi|$ is much smaller than $1/|\xi|$. This mode corresponds to point 1 in fig. 11.1.

For $z \gg 0$, the total upward- and downward-travelling wave fields are both split into two parts, given in eqs (11.4.7) and (11.4.8). The argument of u is now $3\pi/4$, and $\xi - 1/\xi$ almost real, large and negative. A similar argument as given above shows that D_{i2} and D_{r2} form a mode with ξ large and negative (point 2 in fig. 11.1) and that D_{i3} and D_{r3} form a mode with ξ small and positive (point 3).

To obtain space-limited wave fields we construct a wave packet centered around the wave vector \mathbf{k}_{v0} :

$$\mathbf{k}_v = \mathbf{k}_{v0} + h\mathbf{t},$$

where \mathbf{t} is a unit vector perpendicular to \mathbf{k}_{v0} , tangent to ω_{vac} . The amplitude distribution is chosen as

$$dp = A \exp \{-A^2 h^2/2 + jhV_0 \mathbf{b}' \cdot \mathbf{t}/2a (\mathbf{k}_0 \cdot \mathbf{s})^2\} dh/(2\pi)^{1/2}.$$

The plane $z = 0$ (defining \mathbf{b}') is chosen in such a way, that

$$\mathbf{b}' \cdot (\mathbf{k}_{v0} - \mathbf{b}') = 0,$$

leading to $z_r = 0$ and

$$u = \zeta \{z + h\mathbf{b}' \cdot \mathbf{t}/a\mathbf{k}_0 \cdot \mathbf{s}\} = \zeta \{z + h \sin(\theta)/a\}.$$

For sufficiently large values of $|z|$ it is permissible to write

$$u = \zeta z \exp [h \sin(\theta)/az].$$

The centre line of the beam is found by integrating over the wave packet and determining the maximum in amplitude for given z . Such a procedure leads to

$$z \ll 0 \text{ (mode 1): } x \cos \theta - z \sin \theta = S \sin(\theta)/az,$$

$$z \gg 0 \text{ (mode 2): } x \cos \theta + z \sin \theta = -S \sin(\theta)/az,$$

$$z \gg 0 \text{ (mode 3): } x \cos \theta - z \sin \theta = S \sin(\theta)/az.$$

In a first approximation all 3 paths are part of the hyperbola

$$x^2 - z^2 \tan^2 \theta = \tan^2(\theta) 2S/\alpha.$$

It is easily verified that this equation is identical with eq. (10.7.5) giving the path according to the ray theory. The width of the three beams is the same and independent of z .

The intensity of the beams in these regions is proportional to the magnitude squared of the predominant plane-wave component, the proportionality factors being the same. Denoting the intensity at $z = z_1 \ll 0$ by I_1 , at $z = z_2 \gg 0$ for the "reflected" beam by I_2 and at $z = z_3 \gg 0$ for the "transmitted" beam by I_3 , we find after substituting the proper values of the parameters, as given in table II, into the expressions (11.4.6)-(11.4.8):

$$I_2/I_1 = (-2az_1z_2)^{4\delta S} \exp \{-\mu_0(z_2 - z_1)/\cos \theta\}$$

(11.4.9)

and

$$I_3/I_1 = (-z_1/z_3)^{4\delta S} \exp \{-2\pi S - \mu_0(z_3 - z_1)/\cos \theta\}.$$

According to eq. (11.2.3) the values of ξ for mode 1 (small and negative) and mode 2 (large and negative) are equal to

$$\xi_1 = -(2az_1^2/S)^{-1/2}$$

and

$$\xi_2 = -(2az_2^2/S)^{1/2}.$$

From the definitions of δ , S and β follows:

$$-4\delta S = \epsilon\mu_0/\beta \cos \theta.$$

Substitution of these results in the expression for I_2/I_1 (eq. (11.4.9)) yields immediately eq. (10.7.7) obtained in the ray theory. This identity does not mean, however, that the ray theory is correct for any value of S . In calculating the amplitude D_{r2} the value of $T(-\nu)$ was approximated by using Stirling's series, neglecting all terms with S^{-1} or smaller. Recalculation with more terms shows that a factor

$$\exp \left[-\frac{1}{6}\delta (S^{-1} + 0.1 S^{-3} \dots) \right]$$

(11.4.10)

has to be added. For large values of z , the dependence on z is correct, but an extra loss in energy is taking place in the region of small values of $|z|$. The origin of this loss is expected to be the "tunnelling", i.e. the generation of the "transmitted" beam. For non-absorbing crystals no approximation is necessary (eq. (A20)), leading to

$$I_2/I_1 = 1 - \exp(-2\pi S)$$

(11.4.11)

and

$$I_3/I_1 = \exp(-2\pi S).$$

The fact that for $S \gg 1$ the correction term (11.4.10) is much larger than the

correction term $-\exp(-2\pi S)$ in (11.4.11), indicates that the “chance of tunnelling” is increased by absorption.

Now we turn to the region of small negative values of z . Here we expect for $S \gg 1$, D_{t1} and D_{r1} to be related in such a way that their ratio X is everywhere equal to the local ξ -value that lies in between 0 and -1 , so that they form one mode together. To verify this we calculate X taking into account the factor R_ν (eq. (A8)) that has to be added for smaller values of u :

$$X = CR_{\nu-1}/uR_\nu = -(\xi - 1/\xi)^{-1} R_{\nu-1}/R_\nu. \quad (11.4.12)$$

In the appendix $R_{\nu-1}/R_\nu$ is calculated (eq. (A16)). The important parameter is

$$v = (1 - 4\nu/u^2)^{-1/2}; \quad |\arg v| < \pi/2.$$

According to table I

$$(\xi - 1/\xi)^2 = u^2/\nu.$$

We shall choose the real part of ξ in between 0 and -1 , giving for v :

$$v = (1 - \xi^2)/(1 + \xi^2).$$

Substituting this value in eq. (A16) gives for eq. (11.4.12):

$$X = \xi \{ 1 + (1/\nu) \xi^2/(1 + \xi^2)^2 + (1/\nu^2) \xi^4(3 - 2\xi^2)/(1 + \xi^2)^5 + \\ + (5/\nu^3) \xi^6(1 - 2\xi^2)(3 - \xi^2)/(1 + \xi^2)^8 \dots \}. \quad (11.4.13)$$

For large values of S all terms except the first one are small, showing that up to $z = 0$, where $\xi = -1$, the two plane-wave components form one mode of propagation. A check is obtained by calculating X in the point $z = 0$ ($u = 0$), where the value of the parabolic cylinder function is known also (eq. (A9)):

$$X(0) = 2^{-1/2} C T(\frac{1}{2} - \frac{1}{2}\nu)/T(1 - \frac{1}{2}\nu) = -[C(2\pi)^{1/2}/\nu] \{ 2^{\nu+1} T(-\nu)/[T(-\frac{1}{2}\nu)]^2 \}.$$

Approximating the gamma functions by the Stirling series gives

$$X(0) = -(1 + 1/4\nu + 1/32\nu^2 - 5/128\nu^3 \dots),$$

in agreement with eq. (11.4.13).

11.4.3. Reflecting planes flat and parallel, but not equidistant

In the region of large values of $|z|$ the treatment of this case is very similar to the one given in the previous sub-section. A straightforward analysis along analogous lines does not offer fundamental difficulties. Although it has been carried out, it will not be reproduced here.

In the region of smaller values of $|z|$ complications arise. It is likely that a similar procedure as given in the previous case, now applied to the region $z > 0$, will show that for sufficiently large values of S , one mode remains one

mode. Since the ray theory does not give a beam here, such a procedure is not very worth while. In the region $z < 0$, where the ray theory gives two beams the total amplitudes have to be separated into two parts, one corresponding to the upward-travelling beam and the other to the downward-travelling beam. For $z \ll 0$ this separation is given in the two parts of the parabolic cylinder functions, but it is not certain that for values of z closer to zero such a separation is still correct. We did not succeed in finding details of the wave-field behaviour in this region.

TABLE III

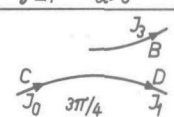
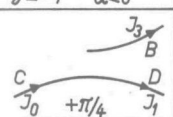
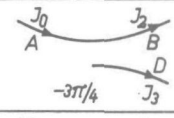
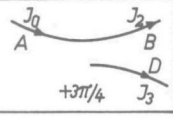
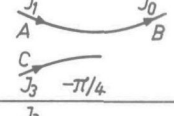
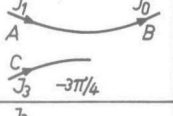
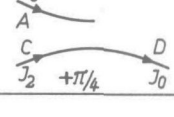
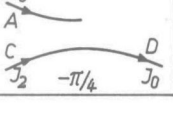
All possible solutions following from the parabolic cylinder functions for the

cases $\gamma = 1, \alpha > 0$ and $\gamma = -1, \alpha < 0$

A: $\xi \rightarrow \infty$ C: $\xi \rightarrow -0$

B: $\xi \rightarrow 0$ D: $\xi \rightarrow -\infty$

$$I_1 = I_0 |2at^2/S|^{4\delta S}; \quad I_2 = I_0 |2at^2/S|^{-4\delta S}; \quad I_3 = I_0 \exp(-2\pi S)$$

	$\gamma=1 \quad \alpha>0$	$\gamma=-1 \quad \alpha<0$
I		
II		
I		
II		

Finally we give in table III a compilation of the four solutions that can be obtained by applying the parabolic cylinder functions to the two types of strain treated above. The solutions discussed in detail are found in the upper row. The paths of the beams are indicated. In the upper 2 rows there is 1 incident beam and 2 emerging beams. In the lower 2 rows there are 2 incident beams with only 1 beam emerging. The parameters characterizing the beam are given in points located symmetrically on the path. The distance between these points

measured along the reflecting planes is either t or 0. In the intensity relations a factor $\exp(-\mu_0 t / \cos \theta)$ has to be added to account for normal absorption. Note that a change in type of mode from C to D or from D to C corresponds to a reduced absorption ($\xi < 0$) in agreement with the drop in intensity either from I_0 to I_1 or from I_2 to I_0 . It must be remarked that in the cases of two incident beams amplitude and phase relations exist between the two, making these solutions impractical. Furthermore, they represent certain combinations of the solutions in the two upper rows and hence provide no new information.

11.4.4. Kinematical approach

In the kinematical theory the reflected intensity is calculated by summing the amplitudes of the wavelets scattered by all unit cells, under the assumption that the amplitude of the incident wave (E_i) is constant. The amplitude U of the wavelet scattered by one unit cell follows from the structure factor and eqs (2.3.2) and (2.5.5) (the phase factor is accounted for later):

$$U = E_i V_1 / 4\pi N, \quad (11.4.14)$$

where N is the number of unit cells per unit volume of the crystal. The reflexion is assumed to take place at a well-defined point within the unit cell. These points for different unit cells lie in the reflecting planes. The distribution of these points over the reflecting planes is irrelevant, since we exclude multiple reflexion. There are Nd reflecting points per unit area in the reflecting plane, if d is the spacing between the reflecting planes.

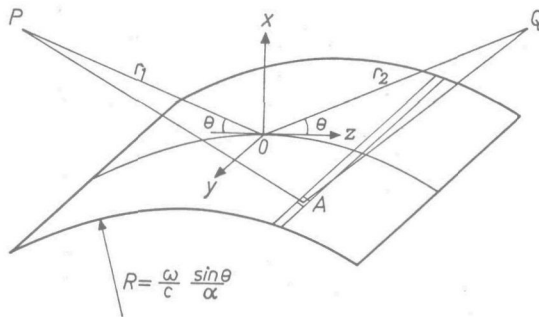


Fig. 11.6. The orientation of the coordinate system used in sub-section 11.4.4. One curved reflecting plane is shown.

In fig. 11.6 is shown one of the curved reflecting planes in the region where the Bragg condition is nearly satisfied. The phase and amplitude of the wavelet arriving in Q via a small area $dydz$ around A is

$$UNd \, dydz \exp [-i2\pi (PA + AQ)/\lambda] / r_2,$$

where

$$PA + AQ = r_1 + r_2 + z^2 \sin(\theta)/R + \frac{1}{2}(1/r_1 + 1/r_2)(y^2 + z^2 \sin \theta).$$

The terms in y and z of order higher than 2 have been neglected. Integration with respect to y and z from $-\infty$ to ∞ gives the total contribution of one reflecting plane:

$$\delta E_r = -j(UNd\lambda/r_2 \sin \theta) [(1/r_1 + 1/r_2)(1/r_1 + 1/r_2 + 2/R \sin \theta)]^{-1/2} \times \\ \times \exp \{-j2\pi(r_1 + r_2)/\lambda\}. \quad (11.4.15)$$

The total amplitude is found by summing the contributions of all reflecting planes. The m th plane gives an additional phase change φ_m with respect to the plane 0 discussed above:

$$\varphi_m \lambda / 2\pi = -2md \sin \theta + \frac{1}{2}(1/r_1 + 1/r_2) m^2 d^2 \cos^2 \theta.$$

The contribution of the first term can be omitted since the relation of Bragg is satisfied. The second term makes only a small jump if m is increased by 1. Hence it is allowed to replace the sum over all reflecting planes by an integration with respect to dx/d , with $-\infty < x < \infty$ and $x = md$. Carrying out this integration and going over to the limits $r_1 \gg r_2 \gg R$ gives for the power reflectivity:

$$I_R/I_0 = |E_r/E_i|^2 = |UN\lambda/E_i \cos \theta|^2 \lambda R/2 \sin \theta.$$

By introducing V_1 with eq. (11.4.14) and replacing R by S via α (eqs (10.7.2) and (11.3.1)) one finds after some manipulation:

$$I_R/I_0 = 2\pi S,$$

in agreement with (11.3.3).

The second case of not equally spaced reflecting planes is somewhat simpler. The contribution of one reflecting plane follows from the derivation given above (eq. 11.4.15)) by setting $R = \infty$ and immediately going over to the limit $r_1 \gg r_2 \rightarrow \infty$:

$$\delta E_r = -jNU\lambda d \exp [-j2\pi(r_1 + r_2)/\lambda] / \sin \theta,$$

identical with eq. (4.2.1). The next step is to calculate the additional phase shift in the contribution of the m th plane, φ_m . According to the definition of α , the z -component of the displacement vector is equal to

$$w = -\alpha d_0 z^2 / 2\pi n,$$

where d_0 is the spacing that satisfies the Bragg equation and n the order of reflexion. Since w gives the relevant part in φ_m we find

$$\varphi_m = 4\pi w \sin(\theta)/\lambda = -\alpha z^2.$$

Replacing again the sum over all reflecting planes by an integral with respect to dz/d_0 , yields for the power reflectivity

$$I_R/I_0 = (NU\lambda/E_i \sin \theta)^2 \pi(-a),$$

which result may be transformed again into eq. (11.3.3).

12. COMPARISON WITH OTHER THEORIES

12.1. Classification

Several authors have given theories for the diffraction of X-rays in deformed crystals. Regarding the approach of the problem these theories can be divided into two classes. In the first place we have the "wave theories". Starting point is the Maxwell equation for \mathbf{E} , (eq. (5.2.1)). The susceptibility ψ is now a complicated function of the space coordinates and no longer periodic. It is assumed, however, that it still may be written in the form

$$\psi = \sum \psi_m \exp(-j\mathbf{b}_m \cdot \mathbf{r}),$$

with \mathbf{b}_m varying slowly with \mathbf{r} and ψ_m constant. For interaction with one set of reflecting planes only, the Maxwell equations contain a large number of terms. By sorting out the terms that give the largest contribution, one obtains two simultaneous differential equations with variable coefficients in D_0 and D_H , the amplitudes of the upward- and downward-travelling plane-wave components, respectively. The actual wave vector \mathbf{k} does not play an important part. The first to publish such an approach were Howie and Whelan²⁶⁾ in the "columnar theory", especially useful in electron diffraction, where the Bragg angle is small. The most elaborate treatment of the X-ray case is given by Taupin²²⁾. His results will be discussed in the next section. Takagi's treatment²⁷⁾ is of earlier date, but in less detail. Since it is in full agreement with Taupin's results, we shall not discuss it. Kato²⁸⁾ shows from the "wave theory" that for sufficiently slowly varying \mathbf{b} a local ω -surface may be defined and the path of a beam satisfies the variational principle:

$$\delta \int_A^B \mathbf{k} \cdot d\mathbf{r} = 0,$$

where A and B represent two fixed points on the path. It is analogous to Fermat's principle in geometrical optics.

In the second place there are "ray theories". Besides our own treatment there is Bonse's treatment²⁹⁾. The basic idea in both is the same: the X-ray energy travels in the direction of the energy transport, determined by the local " ω -surface" and local value of \mathbf{k} . The only relevant question is how to match the \mathbf{k} -vectors in two neighbouring points along the path. Bonse's treatment differs from ours in the \mathbf{k} -matching. He takes into account the imaginary part of the \mathbf{k} -vector, whereas we consider \mathbf{k} to be real.

12.2. Taupin's theory

12.2.1. Results in general terms

In this sub-section the results of Taupin's theory are reproduced. The notation is adapted to the convention used in the previous chapters. For the ampli-

tude of the upward-travelling component Taupin uses the expression

$$\mathbf{D}_i = \mathbf{D}_0(\mathbf{r}) \exp(-j\phi_0). \quad (12.2.1)$$

The function ϕ_0 must be chosen in such a way that the incident wave field in vacuum satisfies this expression also, but with \mathbf{D}_0 a constant. Note that the incident wave need not be plane parallel. The influence of the crystal on the wave field is incorporated entirely in $\mathbf{D}_0(\mathbf{r})$. The downward-travelling wave is given by

$$\mathbf{D}_r = \mathbf{D}_H(\mathbf{r}) \exp(-j\phi_H), \quad (12.2.2)$$

with

$$\nabla\phi_H = \nabla\phi_0 - 2\mathbf{b}(\mathbf{r}). \quad (12.2.3)$$

The vector \mathbf{b} is normal to the reflecting planes and of magnitude $n\pi/d(\mathbf{r})$, where n is the order of the reflexion from the set of reflecting planes of mutual distance $d(\mathbf{r})$. The vector \mathbf{b} is well defined as long as the relative change in strain per distance d is small compared with unity. Note that in our treatment the relative change in strain had to be small per "Pendellösung"-length L , in order to define an ω -surface. Taupin shows that substitution of these proposed solutions in Maxwell's equation and retaining only terms of the first order leads to

$$2j(\mathbf{k}_0 \cdot \nabla) D_0 = V_0 D_0 + V_1 D_H - jD_0(\nabla \cdot \nabla) \phi_0 \quad (12.2.4)$$

and

$$2j(\mathbf{k}_0' \cdot \nabla) D_H = V_0 D_H + V_1 D_0 - (\omega^2/c^2) \alpha_H D_H - jD_H(\nabla \cdot \nabla) \phi_H, \quad (12.2.5)$$

where

$$-(\omega^2/c^2) \alpha_H = 4\mathbf{b} \cdot (\nabla\phi_0 - \mathbf{b}). \quad (12.2.6)$$

Since the vector \mathbf{b} is given by

$$\mathbf{b} = \mathbf{b}' - \nabla(\mathbf{v} \cdot \mathbf{b}'), \quad (12.2.7)$$

the expression for α_H may be approximated to

$$-(\omega^2/c^2) \alpha_H = 4\mathbf{b}' \cdot (\nabla\phi_0 - \mathbf{b}') - 4(\mathbf{k}_0' \cdot \nabla)(\mathbf{v} \cdot \mathbf{b}'). \quad (12.2.8)$$

The function ϕ_0 is arbitrary, apart from the fact that $\exp(-j\phi_0)$ must satisfy the wave equation in vacuum. The choice will depend on the problem that has to be solved. In our discussion we shall use as the incident wave field a plane-parallel wave with wave vector \mathbf{k}_v so that $\nabla\phi_0 = \mathbf{k}_v$. It will be shown later that in practical cases $\nabla \cdot \nabla\phi_H (= 2\nabla \cdot \nabla(\mathbf{v} \cdot \mathbf{b}'))$ is very small compared to the other terms in eq. (12.2.5).

12.2.2. Application to perfect crystals

To demonstrate the significance of Taupin's equations we consider first the case of a perfect crystal ($\mathbf{v} = 0$). According to the dynamical theory a possible solution must read:

$$D_H = \xi D_0 = A \exp j(-\mathbf{k} + \mathbf{k}_v) \cdot \mathbf{r}.$$

Substitution of this solution in Taupin's equations gives

$$2\mathbf{k}_0 \cdot (\mathbf{k} - \mathbf{k}_v) = V_0 + V_1 \xi$$

and

$$2\mathbf{k}_0' \cdot (\mathbf{k} - \mathbf{k}_v) = V_0 + V_1/\xi + 4\mathbf{b}' \cdot (\mathbf{k}_v - \mathbf{b}').$$

Since

$$\mathbf{k}^2 = (\mathbf{k} - \mathbf{k}_v + \mathbf{k}_v)^2 \approx \omega^2/c^2 + 2\mathbf{k}_0 \cdot (\mathbf{k} - \mathbf{k}_v),$$

$$(\mathbf{k} - 2\mathbf{b}')^2 = (\mathbf{k} - \mathbf{k}_v + \mathbf{k}_v - 2\mathbf{b}')^2 \approx \omega^2/c^2 - 4\mathbf{b}' \cdot (\mathbf{k}_v - \mathbf{b}') + 2\mathbf{k}_0' \cdot (\mathbf{k} - \mathbf{k}_v),$$

the basic equations for the dynamical theory (eqs (5.3.1)) follow immediately.

If a plane-parallel wave field strikes the flat boundary (surface normal \mathbf{s}) of a semi-infinite crystal two modes of propagation are activated inside the crystal. The ratio is no longer equal to ξ . It will be denoted by X :

$$X = D_H/D_0. \quad (12.2.9)$$

Since the amplitudes are a function of z in the direction of \mathbf{s} only, one may write

$$2j\mathbf{k}_0 \cdot \mathbf{s} (d/dz) \ln D_0 = V_0 + V_1 X,$$

$$2j\mathbf{k}_0' \cdot \mathbf{s} (d/dz) \ln D_H = V_0 + V_1/X + 4\mathbf{b}' \cdot (\mathbf{k}_v - \mathbf{b}'),$$

or by introducing γ (eq. (7.1.1)) to determine the orientation of \mathbf{s} with respect to \mathbf{k}_0 and \mathbf{k}_0' :

$$2j\mathbf{k}_0 \cdot \mathbf{s} (d/dz) \ln X = (\gamma - 1) V_0 - V_1 (X - \gamma/X) + 4\gamma\mathbf{b}' \cdot (\mathbf{k}_v - \mathbf{b}'). \quad (12.2.10)$$

This equation is satisfied by

$$(1 - X/\xi_1)/(1 - X/\xi_2) = \exp [jV_1 (\xi_1 - \xi_2) z/2\mathbf{k}_0 \cdot \mathbf{s}], \quad (12.2.11)$$

with ξ_1 and ξ_2 the two roots of the equation

$$V_1 (\xi - \gamma/\xi) = (\gamma - 1) V_0 + 4\gamma\mathbf{b}' \cdot (\mathbf{k}_v - \mathbf{b}'). \quad (12.2.12)$$

According to eq. (7.2.2), which is identical with eq. (12.2.12), ξ_1 and ξ_2 are the mode parameters of the two modes activated inside the crystal. Equation (12.2.11) represents the variation in X because of the z -dependent phase difference between the two modes. In sec. 6.5 an example thereof was discussed, the case $\mathbf{b}' \cdot (\mathbf{k}_v - \mathbf{b}') = 0$ in the symmetrical Laue case ($\gamma = 1$). It is easily verified that in that case $\xi_1 = -1$ and $\xi_2 = 1$,

$$X = -j \tan (V_1 z/2\mathbf{k}_0 \cdot \mathbf{s}). \quad (12.2.13)$$

In non-absorbing crystals $|X|$ is periodic in z . The period $2\pi\mathbf{k}_0 \cdot \mathbf{s}/|V_1|$ is equal to 2π times the "Pendellösung"-length L , in agreement with eq. (6.5.1). Taupin's equations apply also to absorbing crystals. In this special case we

find by adding a small imaginary part jW_1 ($W_1 < 0$) to V_1 in eq. (12.2.13) that X tends to -1 for large values of z , in agreement with the fact that the mode with $\xi = -1$ suffers the least absorption.

The important conclusion is that eq. (12.2.10) for X gives correct results in undeformed crystals even in the case that two modes of propagation are present. This is an immediate consequence of the fact that eqs (12.2.4) and (12.2.5) are homogeneous in D_0 and D_H , showing that any combination of D_0 and D_H is a possible solution also. In perfect crystals this may not seem important, but it leads to the expectation that in deformed crystals the generation of new modes inside the crystal is included in Taupin's treatment.

12.2.3. Deformation a function of one space coordinate

Next consider the case of deformed crystals where the deformation is a function of z in the direction of \mathbf{s} only. We assume that the surface on which the incident wave field strikes, is normal to \mathbf{s} . The amplitude and the phase of both D_0 and D_H are again a function of z only. Such situations were discussed in chapter 11 and a direct comparison of Taupin's equations with the rigorous treatment is possible. Introducing eq. (11.1.1) for the deformation gives for the equations (12.2.4) and (12.2.5):

$$2j\mathbf{k}_0 \cdot \mathbf{s} \, dD_0/dz = V_0 D_0 + V_1 D_H, \quad (12.2.14)$$

$$2j\mathbf{k}_0 \cdot \mathbf{s} \, dD_H/dz = \gamma V_1 D_0 + \{\gamma V_0 + 4\gamma \mathbf{b}' \cdot (\mathbf{k}_v - \mathbf{b}') + 4\mathbf{k}_0 \cdot \mathbf{s} a z\} D_H. \quad (12.2.15)$$

The term with $\nabla \cdot \nabla \phi_H$ was omitted. In the special cases we are discussing now it would give a term of the order of αD_H and has to be compared with $V_0 D_H$. According to the definition of α , $|\alpha|$ is equal to $|V_0|$ when the relative change in \mathbf{b} over a distance L is equal to unity, or when S (the parameter used in the previous chapter) has the exceedingly small value of $|\psi_1|$. In any practical case $|\alpha|$ will be much smaller than $|V_0|$ so that $\nabla \cdot \nabla \phi_H$ may be neglected (for $\nabla \cdot \nabla \phi_0 = 0$) in comparison with V_0 .

The equations (12.2.14) and (12.2.15) are identical with eqs (11.2.6) and (11.2.7). Since we could derive from these equations that there is a generation of new modes in strongly deformed crystals, it must be concluded that this phenomenon is included also in Taupin's treatment, in contrast to our ray theory.

The differential equation for X reads in this case

$$2j\mathbf{k}_0 \cdot \mathbf{s} \, (d/dz) \ln X = -V_1 (X - \gamma/X) + (\gamma - 1) V_0 + 4\gamma \mathbf{b}' \cdot (\mathbf{k}_v - \mathbf{b}') + 4\mathbf{k}_0 \cdot \mathbf{s} a z. \quad (12.2.16)$$

The solution of the ray theory is obtained by neglecting the left-hand side of the equation. The two possible values of X then are equal to the two possible values of ξ that follow from the given orientations of \mathbf{k}_v and \mathbf{s} and the local

ω -surface. As we have seen in the rigorous treatment such a procedure is allowed if the change in X is small over a "Pendellösung"-length L . This condition may be derived also from eq. (12.2.16). The contribution of the left-hand term is negligible if the change in X per length L is small, since L is of the order of $|\mathbf{k}_0 \cdot \mathbf{s}/V_1|$. According to the previous sub-section this change is zero in perfect crystals, if only one mode is present. In lightly deformed crystals the parameter of the one mode present changes very little over a distance L .

12.2.4. General deformation

Turning now to the general case we shall show that our ray theory follows from Taupin's equations by a procedure similar to the one used at the end of the previous sub-section. The equation for X may be derived in the general case by multiplying eq. (12.2.4) with the operator $(\mathbf{k}_0' \cdot \nabla) D_0^{-1}$, eq. (12.2.5) with $(\mathbf{k}_0 \cdot \nabla) D_H^{-1}$ and subtracting:

$$\begin{aligned} 2j(\mathbf{k}_0 \cdot \nabla)(\mathbf{k}_0' \cdot \nabla) \ln X = \\ = -(V_1/X^2) \{ \mathbf{k}_0 + X^2 \mathbf{k}_0' \} \cdot \nabla X - 4(\mathbf{k}_0 \cdot \nabla)(\mathbf{k}_0' \cdot \nabla)(\mathbf{v} \cdot \mathbf{b}'). \end{aligned} \quad (12.2.17)$$

If in any direction the strain varies only a little over the distance L , a local ω -surface may be defined. At the surface two modes are activated, each with a well-defined value of ξ , although ξ may vary along the surface. Considering only one type of mode we expect according to the foregoing discussions that the value of ξ of one type of activated mode will vary only a little over the distance L , whereas X corresponding to a pair of modes shows the beat of the two modes. Hence we may neglect the left-hand term if we substitute ξ instead of X :

$$V_1(\mathbf{k}_0 + \xi^2 \mathbf{k}_0') \cdot \nabla \xi = -4\xi^2(\mathbf{k}_0 \cdot \nabla)(\mathbf{k}_0' \cdot \nabla)(\mathbf{v} \cdot \mathbf{b}'). \quad (12.2.18)$$

This equation states that for real (or nearly real) values of ξ and V_1 , we can determine the change in ξ in the direction of the vector $\mathbf{k}_0 + \xi^2 \mathbf{k}_0' = (\omega/c^2)(1 + \xi^2) \mathbf{v}_g$ only. The change $d\xi$ per distance d in the direction of the group velocity is now identical with eq. (10.5.3) following from our treatment. Apparently both treatments are in full agreement with each other, provided the strain varies sufficiently slowly and the phase angles in V_1 and ξ are small.

In the ray theory it is essential that the change in ξ is determined in the direction of the velocity of energy transport. The value of ξ is free in a direction perpendicular to this velocity and the different beams travelling in adjoining regions are independent of each other. Introducing a large phase angle in ξ in eq. (12.2.18) leads to two equations, one for the real parts and one for the imaginary parts. The equations no longer allow for the calculation of the complex ξ along a line if ξ is given on one point on that line, as in the case of real ξ . It is necessary to give the complex value of ξ along the entire entrance surface. Only with this knowledge can ξ be calculated throughout the plane

of incidence. Or, in other words, for larger values of the phase angle in ξ , there are no trajectories in the plane of incidence, along which the ξ variation is insensitive to the variation of ξ along the surface in the plane of incidence.

12.3. Bonse's theory

12.3.1. Summary of results

Bonse investigated experimentally the diffraction in slightly deformed crystals in the Bragg situation. To explain his results a theory is needed which describes the behaviour of wave fields with complex values of ξ . Our theory is of no use, since it is clearly limited to wave fields with almost real ξ -values. Bonse claims to have developed a ray theory which is not limited by this restriction. Although he considers also such slowly varying strains that a local relation between ω and \mathbf{k} may be defined, his theory must be based on more assertions than ours, because in his case the imaginary part of the \mathbf{k} -vector must be matched in adjoining sites also.

Bonse states that for appropriate matching the complex \mathbf{k} -vector must satisfy the following three conditions:

- (1) The basic equations of the dynamic theory have to be satisfied in any arbitrary point and its immediate vicinity.
- (2) The wave vector must correspond to planes of equal phase and planes of equal amplitude. Accordingly

$$\nabla \times \mathbf{k} = 0.$$

- (3) According to (1), \mathbf{k} is not constant in the immediate vicinity of any arbitrary point. It might be expected, however, that the variation is such that the wave field remains as uniform as possible. Bonse therefore introduces the condition *)

$$\nabla (\mathbf{k} - \mathbf{b}) \cdot \nabla (\mathbf{k}^* - \mathbf{b}) = \text{minimum.}$$

The vector $\mathbf{k} - \mathbf{b}$ is introduced instead of \mathbf{k} or $\mathbf{k} - 2\mathbf{b}$, for symmetry reasons.

From these three assumptions the dyad $\nabla (\mathbf{k} - \mathbf{b})$ may be determined as a function of $\nabla \mathbf{b}$. However, Bonse is not interested in the dyad itself, but only in the change of the complex \mathbf{k} -value in the direction of energy flow. The calculation of the change in ξ in the direction of \mathbf{v}_e is now straightforward. The amplitude matching is obtained in a similar way as in our theory, by means of intensities and an "absorption coefficient", as given in eq. (8.4.1), still containing φ .

The results obtained in Bonse's treatment will not be reproduced here. They are rather complicated. Two important conclusions given by the author are: in the first place, for real values of ξ (either positive or negative) the two ray

*) The asterisk indicates the complex conjugate.

theories give identical results; in the second place, in the case of tapering reflecting planes in an absorbing crystal the change in ξ is not zero according to Bonse. This last result is not only in contrast with our theory (see sec. 10.7.1), but also in disagreement with Taupin's result, where even in the case of strong tapering the wave fields travel undisturbed.

12.3.2. Discussion

It is not necessary to discuss the result of Bonse's treatment in the cases that modes are excited with almost real values of ξ . Bonse states in his paper that then the two ray theories are in full agreement. The differences appear in such cases where modes with a strong cut-off character are excited. Therefore only such situations are discussed. Although Bonse refers to the wave fields as "Röntgenwellenfeldstrahlen", the essential point to make it a ray theory is missing, namely that the wave fields under consideration have such a character that a ray may be constructed. In chapter 9 we discussed in detail the necessary conditions. A beam is well-behaved if the central mode has an almost real ξ -value. In perfect crystals the properties of a well-behaved beam remain unchanged along the path. They are fixed entirely by the magnitude of the incident beam in the immediate neighbourhood of the place where the beam is leaving the surface. For modes with complex values of ξ , such that $|\cos \varphi|$ is significantly less than unity the beam is not well-behaved. The properties such as \mathbf{k} and ξ of the central mode, change appreciably for penetrations larger than the width, even in undeformed crystals. At such penetrations the wave field is determined by the power input far away from the centre of the incident beam in the surface. In fact, we feel that this is the reason why in Taupin's results for slightly deformed crystals the complex value of ξ had to be known all along the entrance surface in the plane of incidence, in order to be able to calculate ξ deeper inside the crystal.

Turning now to Bonse's treatment again we note that already in assumption (1) the ray approach is abandoned. The requirement that the wave field satisfies the basic equations in the entire region around an arbitrary point is in sharp contrast with the ray theory where one needs only the requirement that the basic equations are satisfied in the direction of propagation. Assumption (1) brings Bonse's theory nearer to the wave theories.

It will be appreciated that Bonse's third assumption, although reasonable for want of a better, is ad hoc. We shall show that it imposes too stringent a condition on ξ . It must be noted that in his treatment Bonse does not use the full information that is deduced from his assumptions. Of the determined dyad $\nabla(\mathbf{k} - \mathbf{b})$ only the component in the direction of the energy flow is used and from that component the change in ξ is found. The known value of $\nabla(\mathbf{k} - \mathbf{b})$ allows, however, for the determination of $\nabla\xi$. Hence not only the change of ξ in the direction of the energy flow is determined, but also in any direction.

It is sufficient to give ξ on one point of the entrance surface to determine ξ throughout the entire crystal including the surface. The \mathbf{k} -matching in vacuum and crystal requires that eq. (7.2.2) has to be satisfied. Since ξ is known in modulus and argument, both $\mathbf{b} \cdot (\mathbf{k}_v - \mathbf{b})$ and γ may be calculated along the surface. Apparently the third assumption imposes also conditions on the type of wave field that strikes the entrance surface and on the orientation of the surface normal with respect to the reflecting planes. In practical cases these conditions will not be satisfied in general, showing that the solution given by Bonse is overdetermined.

Taupin's treatment shows that for sufficiently slowly varying lattice parameters the complex value of ξ must obey the differential equation (eq. (12.2.18))

$$V_1 (\mathbf{k}_0 + \xi^2 \mathbf{k}_0') \cdot \nabla \xi = -4\xi^2 (\mathbf{k}_0 \cdot \nabla) (\mathbf{k}_0' \cdot \nabla) (\mathbf{v} \cdot \mathbf{b}').$$

If one calculates this component of the vector $\nabla \xi$ following from Bonse's treatment, then exactly the same equation results. Hence it could quite well be that by taking into account the necessary shape of the entrance surface and type of incident wave field Bonse's treatment gives correct results. But as pointed out above, it is unlikely that such a situation is met in practice.

APPENDIX

The parabolic cylinder functions satisfy Weber's equation

$$d^2D_\nu/du^2 = (-\nu - \frac{1}{2} + \frac{1}{4}u^2) D_\nu. \quad (\text{A.1})$$

From Whittaker and Watson's book³¹⁾ we quote the following properties. The solutions with different values of the parameter ν are related to each other by the recurrence formulae:

$$dD_\nu/du = -\frac{1}{2}u D_\nu + \nu D_{\nu-1} \quad (\text{A.2})$$

and

$$dD_{\nu-1}/du = \frac{1}{2}u D_{\nu-1} - D_\nu. \quad (\text{A.3})$$

The asymptotic value of D_ν for large values of u depends on the argument χ of u :

$$-\frac{3}{4}\pi < \chi < \frac{3}{4}\pi: \quad D_\nu = A_\nu(u)R_\nu(u), \quad (\text{A.4})$$

$$\frac{1}{4}\pi < \chi < \frac{5}{4}\pi: \quad D_\nu = A_\nu(u)R_\nu(u) + B_\nu(u)S_\nu(u), \quad (\text{A.5})$$

$$-\frac{5}{4}\pi < \chi < -\frac{1}{4}\pi: \quad D_\nu = A_\nu(u)R_\nu(u) + C_\nu(u)S_\nu(u), \quad (\text{A.6})$$

with

$$\begin{aligned} A_\nu &= u^\nu \exp(-\frac{1}{4}u^2), \\ B_\nu &= -(2\pi)^{1/2} \exp(j\pi\nu)/\Gamma(-\nu)A_{\nu+1}, \end{aligned} \quad (\text{A.7})$$

$$C_\nu = B_\nu \exp(-2j\pi\nu)$$

and

$$R_\nu = 1 - \nu(\nu-1)/2u^2 + \nu(\nu-1)(\nu-2)(\nu-3)/8u^4 - \dots, \quad (\text{A.8})$$

$$S_\nu = 1 + (\nu+1)(\nu+2)/2u^2 + (\nu+1)(\nu+2)(\nu+3)(\nu+4)/8u^4 + \dots$$

The value at $u = 0$ is

$$D_\nu(0) = 2^{\nu/2} \Gamma(\frac{1}{2})/\Gamma(\frac{1}{2} - \frac{1}{2}\nu). \quad (\text{A.9})$$

In the region where $|\arg u| < \frac{3}{4}\pi$ one can calculate the ratio

$$uD_{\nu-1}/D_\nu = R_{\nu-1}/R_\nu = X_\nu. \quad (\text{A.10})$$

Straightforward division of the series $R_{\nu-1}$ by the series R_ν gives

$$X_\nu = 1 + (1 - \nu^{-1})\nu/u^2 + (1 - \nu^{-1})(2 - 3\nu^{-1})(\nu/u^2)^2 + \dots \quad (\text{A.11})$$

The interesting point in this result is that for large values of ν this series is no longer a function of ν/u as in R_ν , but a function of ν/u^2 . This suggests a type of expansion:

$$X_\nu = F_0 + F_1 \nu^{-1} + F_2 \nu^{-2} + \dots, \quad (\text{A.12})$$

where F_0 , F_1 and F_2 are functions of ν/u^2 only. By introducing

$$w = \nu/u^2, \tag{A.13}$$

one can show from the recurrence formulae that

$$2w^2 dX_\nu/dw + wX_\nu = \nu (wX_\nu^2 - X_\nu + 1). \tag{A.14}$$

It turns out by substituting the series (A.12) into (A.14) that an important part is played by

$$v = (1 - 4w)^{-1/2}; \quad |\arg v| < \pi/2. \tag{A.15}$$

Using v as variable instead of w gives for X_ν :

$$X_\nu = \{2\nu/(\nu + 1)\} \{1 - (\nu^2 - 1)/4\nu + (\nu^2 - 1)^2(1 + 5\nu)/32\nu^2 + 5(\nu^2 - 1)^3(1 - 3\nu)(1 + 2\nu)/128\nu^3 \dots\}. \tag{A.16}$$

In the problem we want to discuss it is convenient to introduce

$$\nu = \delta_s S \exp j(\pi/2 + 2\delta), \tag{A.17}$$

where δ_s is either 1 or -1 , and S real and positive. The phase angle δ (the argument of $-V_1$) is small. In the expressions (A.7) for B_ν and C_ν enters $\Gamma(-\nu)$. For $\delta_s = 1$, Stirling's series may be used to approximate its value. Neglecting terms with δ^2 and S^{-1} or smaller, yields

$$\begin{aligned} \ln \{ \Gamma(2\delta S - jS)/(2\pi)^{1/2} \} &= -\frac{1}{2}\pi S - (\frac{1}{2} - 2\delta S) \ln S + \\ &\quad -j[S \ln S - \pi/4 + \delta + \pi\delta S]. \end{aligned} \tag{A.18}$$

For $\delta_s = -1$ one has to use the relation

$$\nu \sin(\pi\nu) \Gamma(\nu) \Gamma(-\nu) = -\pi.$$

If S is sufficiently large one obtains

$$\begin{aligned} \ln \{ \Gamma(jS - 2\delta S)/(2\pi)^{1/2} \} &= -\frac{1}{2}\pi S - (\frac{1}{2} + 2\delta S) \ln S + \\ &\quad +j[S(\ln S - 1) - \pi/4 - \delta - \pi\delta S]. \end{aligned} \tag{A.19}$$

For $\delta = 0$ one can show:

$$\ln \{ |\Gamma(\pm jS)/(2\pi)^{1/2} \} = -\frac{1}{2}\pi S - \frac{1}{2} \ln S. \tag{A.20}$$

The values of A_ν , B_ν and C_ν are now found to be

$$\begin{aligned} \ln A_\nu &= -\frac{1}{4}|u|^2 \cos 2\chi - \delta_s (\chi S + 2\delta S \ln |u|) + \\ &\quad -j[\frac{1}{4}|u|^2 \sin 2\chi + \delta_s S(2\delta\chi - \ln |u|)], \end{aligned} \tag{A.21}$$

$$\begin{aligned} \ln(-B_\nu) &= \frac{1}{4}|u|^2 \cos 2\chi + \frac{1}{2}\pi S - \ln(|u| S^{1/2}) + \delta_s S \{ \chi - \pi + 2\delta \ln(|u|/S) \} + \\ &\quad + j[\frac{1}{4}|u|^2 \sin 2\chi + \pi\delta S + \delta - \chi + \delta_s \{ (\chi - \pi) 2\delta S - \ln(|u|/S) - S - \pi/4 \}], \end{aligned}$$

$$\ln(-C_\nu) = \ln(-B_\nu) + 2\pi\delta_s S + j\delta_s 4\pi\delta S.$$

The values of $A_{\nu-1}$, $B_{\nu-1}$ and $C_{\nu-1}$ follow immediately from the expressions given above, taking into account their definition

$$A_{\nu-1} = A_{\nu}/u; \quad B_{\nu-1} = B_{\nu}u/\nu; \quad C_{\nu-1} = C_{\nu}u/\nu. \quad (\text{A.22})$$

LIST OF FREQUENTLY USED SYMBOLS

a	$= \mathbf{v}_g ^{-1}$, eq. (10.4.1)
\mathbf{a}_D	shortest vector between adjacent atom layers in Darwin's model
$2\mathbf{b}$	reciprocal-lattice vector for the set of reflecting planes under consideration
$2\mathbf{b}_D$	primitive reciprocal-lattice vector in Darwin's model, eq. (5.1.1)
$2\mathbf{b}'$	reference reciprocal-lattice vector in deformed crystals
c	velocity of X-rays in vacuum
c	as index refers to the central mode of the wave packet, eq. (9.2.1)
C	proportionality factor given in table I
d	spacing of reflecting planes in Darwin's model
d_0	reference spacing of reflecting planes in Darwin's model after deformation
$D_\nu(u)$	parabolic cylinder function of the order ν
e	electron charge
g	$= W_0/V_1$, eq. (8.2.1)
h	variable in the description of a wave packet, eq. (9.2.1), sec. 11.4.2
I_0	incident intensity per unit angle of incidence
I_T	transmitted intensity per unit angle of incidence for the beam or the wave travelling parallel to \mathbf{k}_ν
I_R	reflected intensity per unit angle of incidence for the beam or the wave travelling parallel to \mathbf{k}_r
\mathbf{k}	wave vector characterizing the wave field inside the crystal
\mathbf{k}	multi-valued wave vector determining the translation behaviour of the wave field inside the crystal (sub-section 5.1.3)
$\mathbf{k}_i, \mathbf{k}_i'$	wave vectors of the two plane waves present in the vacuum between adjacent atom layers in Darwin's model
$\mathbf{k}_0, \mathbf{k}_0'$	wave vectors, satisfying Bragg's equation, in the incident and diffracted direction, resp.
\mathbf{k}_ν	wave vector of the incident plane wave in vacuum
\mathbf{k}_r	wave vector of the diffracted plane wave in vacuum
$\mathbf{k} + j\mathbf{K}$	complex wave vector inside the crystal, eq. (8.1.2)
\bar{K}	polarization factor, eq. (2.3.1)
L	"Pendellösung"-length, eq. (6.5.1)
m	mass of a free electron
\mathbf{p}	unit vector tangential to the " ω -surface", eq. (9.2.1)
\mathbf{P}	power flow averaged over the unit cell, eq. (6.3.1)
$j\mathbf{q}$	amplitude reflexion coefficient for a single layer of atoms in Darwin's model, eq. (4.2.1)
$j\mathbf{q}_0$	phase change suffered by a plane wave passing through one layer of atoms in Darwin's model, eq. (4.2.1)

q	parameter defined in eqs (9.2.1) and (9.2.3)
r	$= \underline{V}_0/\underline{V}_1$, eq. (8.2.1)
R	integrated reflected intensity; the radius of curvature of a cylindrically curved lattice, figs 10.3 and 11.6
s	normal to the surfaces of a crystal slab, sec. 7.1
S	parameter describing the inhomogeneity in the strain, eq. (11.3.1)
T	integrated transmitted intensity travelling parallel to \mathbf{k}_v
u	variable in the parabolic cylinder functions, eq. (11.4.3) and table I
\mathbf{v}_e	velocity of energy transport inside the crystal, eq. (6.3.6)
\mathbf{v}_g	group velocity of the wave fields inside the crystal, eq. (6.3.4)
V_0	$= \mathbf{k}_0^2 \psi_0$, eq. (2.5.5)
$\overline{V_0 + jW_0}$	complex value of V_0 in absorbing crystals
$\overline{V_1}$	$= K \mathbf{k}_0^2 \psi_1$, eq. (2.5.5)
$\overline{V_1 + jW_1}$	complex value of V_1 in absorbing crystals
$\overline{V_c}$	volume of the unit cell
X	ratio in the total amplitudes of the two plane-wave components, in the case there are two modes of propagation present, both arising from one incident plane wave, sec. 11.3, eqs (11.4.12) and (12.2.9)
α	an angle used in chapter 9 and defined in fig. 9.2; parameter describing the inhomogeneity in the strain, eqs (10.7.2) and (10.7.8)
β	parameter describing the inhomogeneity in the strain, eqs (10.7.3) and (10.7.9)
γ	parameter determining the orientation of the surfaces of the crystal slab with respect to the reflecting planes, eq. (7.1.1)
δ	phase angle in V_1 , eq. (11.4.5)
ϵ	$= W_1/W_0$, eq. (8.2.1)
ϵ	dielectric constant of the crystal on a sub-atomic scale, eq. (2.5.1)
ϵ_0	dielectric constant of vacuum
ζ	proportionality factor, relating the space coordinate z to the variable u in the parabolic cylinder functions, eq. (11.4.3) and table I
θ	Bragg angle
λ	wavelength of the X-rays in vacuum
A	beam width, eq. (9.2.4)
μ	absorption coefficient, eqs (8.1.3) and (8.4.3)
μ_0	absorption coefficient in the case there is no diffraction, eq. (8.4.2)
ν	parameter giving the order of the parabolic cylinder functions, table I
ξ	ratio in the amplitudes of the two predominant plane-wave components in a mode of propagation, eqs (5.1.4) and (5.2.6)
ρ	electron density, eq. (2.2.5)
φ	phase angle in ξ , eq. (8.1.1)
ϕ	phase shift suffered by the wave field after having travelled a distance a_D , in Darwin's treatment, eq. (5.1.3)

- ψ_0 average value of the susceptibility, sec. 2.5
 ψ_1 amplitude of the Fourier component with period \mathbf{b} of the susceptibility,
sec. (2.5)
 ω circular frequency of the X-rays

REFERENCES

- 1) P. P. Ewald, Fifty years of X-ray diffraction, N.V. Oosthoek's Uitgeversmij, Utrecht, 1962.
- 2) M. Laue, W. Friedrich and P. Knipping, Münchener Sitzungsber. **1912**, 363; Ann. Phys. **41**, 971-988, 1913.
- 3) W. L. Bragg, Proc. Camb. phil. Soc. **17**, 43, 1913.
- 4) P. P. Ewald, Ann. Phys. **49**, 1-38, 1916; *ibid.* **49**, 117-143, 1916; *ibid.* **54**, 519-597, 1917.
- 5) G. Borrmann, Phys. Z. **42**, 157-162, 1941.
- 6) C. G. Darwin, Phil. Mag. **27**, 315-333, 1914; *ibid.* **27**, 675-690, 1914.
- 7) M. von Laue, *Ergebn. exact. Naturw.* **10**, 133-158, 1931.
- 8) F. Bloch, Z. Phys. **52**, 555-600, 1928.
- 9) R. de L. Kronig and W. G. Penney, Proc. Roy. Soc. A **130**, 499-513, 1931.
- 10) R. W. James, The optical principles of the diffraction of X-rays, G. Bell and Sons Ltd, London, 1962.
- 11) W. H. Zachariasen, Theory of X-ray diffraction in crystals, J. Wiley and Sons, New-York, 1945.
- 12) M. von Laue, Röntgenstrahlinterferenzen, Akademische Verlagsgesellschaft, Frankfurt a.M., 1960, 3rd ed.
- 13) C. Kittel, Introduction to solid state physics, J. Wiley and Sons, New York, 1959, 2nd ed., p. 1.
- 14) H. Hönl, Z. Phys. **84**, 1-16, 1933; Ann. Phys. **18**, 625-655, 1933.
- 15) J. A. Prins, Z. Phys. **63**, 477-493, 1930.
- 16) R. W. James, Solid State Physics **15**, 55-220, 1963.
- 17) B. W. Batterman and H. Cole, Rev. mod. Phys. **36**, 681-717, 1964.
- 18) B. Okkerse, Philips Res. Repts **17**, 464-478, 1962.
- 19) B. Okkerse and P. Penning, Philips Res. Repts **18**, 82-94, 1963.
- 20) B. Okkerse, Philips Res. Repts **18**, 413-431, 1963.
- 21) P. Penning and D. Polder, Philips Res. Repts **16**, 419-440, 1961.
- 22) D. Taupin, Bull. Soc. franç. Minér. Crist. **87**, 469-511, 1964.
- 23) D. Polder and P. Penning, Acta cryst. **17**, 950-955, 1964.
- 24) J. Berghuis, G. M. Haanappel, M. Potters, B. O. Loopstra, C. H. McGillavry and A. L. Veenendaal, Acta cryst. **8**, 478-483, 1955.
- 25) H. Cole and G. E. Brock, Phys. Rev. **116**, 868-873, 1959.
- 26) A. Howie and M. J. Whelan, Proc. Roy. Soc. A **263**, 217-237, 1961.
- 27) S. Takagi, Acta cryst. **15**, 1311-1312, 1962.
- 28) N. Kato, J. phys. Soc. Japan **18**, 1785-1791, 1963; *ibid.* **19**, 67-77, 1964; *ibid.* **19**, 971-985, 1964.
- 29) U. Bonse, Z. Phys. **177**, 385-423, 1964.
- 30) K. Kambe, Z. Naturforsch. A **20**, 770-786, 1965.
- 31) E. T. Whittaker and G. N. Watson, A course of modern analysis, Cambridge University Press, 1963, 4th ed., pp. 347-351.

Summary

The first part of this thesis deals with the concepts used in the theory of X-ray diffraction. After an historical introduction and motivation of the study, the definition of several important parameters are considered in chapter 2. The geometrical aspects of X-ray diffraction are dealt with in chapter 3. To calculate the intensity of diffracted beams two theories have been developed: the kinematical theory, applicable to mosaic crystals (chapter 4) and the dynamical theory, applicable to perfect crystals (chapters 5 and 6). According to the dynamical theory the simplest form of X-ray-energy transport is a mode of propagation, consisting of a number of plane-wave components. Special attention is paid to the definition of the wave vector characterizing such a mode of propagation and the possible values of the wave vector for given circular frequency: the ω -surface. Other important characteristics such as the composition of the wave field and the associated power flow are also discussed. Since all crystals have finite dimensions, the matching of the wave fields inside and outside the crystal is treated in chapter 7.

Absorption of X-ray energy and extinction of the wave fields by an interference phenomenon present in non-absorbing crystals also, are dealt with in chapter 8. It is shown that under the influence of these phenomena the shape of the ω -surface changes and that the change itself depends on the orientation of the surface with respect to the reflecting planes. In cases where the power flow is not closely parallel to the surface, extinction does not contribute significantly to the damping in amplitude and the change in ω -surface is negligible. The decrease in amplitude is then described adequately with an absorption coefficient. If the power flow is closely parallel to the surface the complex value of the wave vector is very sensitive to the small angle between the power flow and the surface and the extinction plays a greater part than the absorption. The damping must be described with the imaginary part of the wave vector.

Chapter 9 deals with space-limited wave fields inside a crystal. A pencil beam striking a crystal does not always give beam(s) inside the crystal. Only in those cases where the modes of propagation excited have a power flow not closely parallel to the surface does a well-behaved beam result.

An extension of the dynamical theory to lightly deformed perfect crystals is presented in chapter 10. The underlying assumptions are: (1) the dynamical theory may be applied locally to narrow beams, (2) the beam remains well-behaved along its path which need not to be straight, (3) the matching of the wave field along the path is achieved by a postulated procedure analogous to the case of a light beam travelling through an inhomogeneous medium. In principle the theory may be applied to any kind of deformation, provided it is not too inhomogeneous. It leads to expressions for the path of the X-ray beam and the absorption along the path.

To verify the first and second assumption, the examples discussed in chapter 10 are treated again in chapter 11. It is shown that an exact solution is possible by making use of the parabolic cylinder functions. For sufficiently slowly varying strains a good agreement with the ray theory is found, although it was not possible to verify all results of the ray theory. For rapidly varying strains part of the X-ray energy passes on without being affected by the strain. An analogy in the electron-band theory is the phenomenon of "tunnelling". In the case of very rapidly varying strains a kinematical treatment of the examples gives results in agreement with the exact solution. The upper limit of validity of the ray theory, derived on the basis of intuitive arguments, is in accord with the results obtained in this chapter.

In chapter 12 the ray theory is compared with other theories. Taupin's treatment is more general than the one presented here, but for slowly varying strains both theories give the same results. Bonse's theory is an extension of the one presented in chapter 10 to cases where extinction plays an important part. It is argued that his theory in these cases gives correct results only if the incident wave field satisfies certain conditions concerning the amplitude and phase distribution along the surface of the deformed crystal.

Samenvatting

In het eerste deel van dit proefschrift wordt de aandacht gericht op de begrippen, die gebruikt worden in de theorie der diffractie van Röntgenstralen. Na een historische inleiding en een motivering voor deze studie worden verschillende belangrijke parameters besproken in hoofdstuk 2. De geometrische aspecten der Röntgendiffractie komen aan de orde in hoofdstuk 3. Om de intensiteit van de gebroken stralen te berekenen zijn 2 theorieën ontwikkeld: de kinematische theorie, van toepassing op mozaïek-kristallen (hoofdstuk 4) en de dynamische theorie, van toepassing op ideale kristallen (hoofdstukken 5 en 6). Volgens de dynamische theorie is de eenvoudigste vorm van energie-transport door middel van Röntgenstralen een specifieke combinatie van vlakke golven. Speciaal wordt aandacht besteed aan de golfvector, die zulk een combinatie kenmerkt wat haar translatie-gedrag betreft en de verzameling van mogelijke golfvectoren voor een gegeven frequentie ω : het ω -oppervlak. Ook andere belangrijke eigenschappen van zo'n golfveld, zoals de samenstelling als functie van de golfvector en de erbij behorende richting van energiestroom worden besproken. Omdat nu eenmaal alle kristallen eindige afmetingen hebben, wordt de aanpassing van de golfvelden in en buiten het kristal behandeld in hoofdstuk 7.

In hoofdstuk 8 komt aan de orde de vermindering van de amplitude van het golfveld ten gevolge van absorptie en extinctie. Het laatste verschijnsel is een gevolg van interferentie dat ook in niet absorberende kristallen kan optreden. Er wordt aangetoond dat onder invloed van deze verschijnselen de vorm van het ω -oppervlak verandert, en dat de verandering zelf afhangt van de orientatie der reflecterende vlakken ten opzichte van het oppervlak. In die gevallen waar de energiestroom niet nagenoeg evenwijdig aan het oppervlak loopt, zijn de verschillen evenwel te verwaarlozen. De extinctie draagt dan ook maar weinig bij tot de afname in amplitude. Indien de energie vrijwel evenwijdig aan het oppervlak stroomt, dan is de golfvector complex met het imaginaire deel sterk in grootte afhankelijk van de kleine hoek tussen de energiestroom en het oppervlak. De extinctie speelt dan een belangrijker rol dan de absorptie. De afname in amplitude moet dan beschreven worden met het imaginaire stuk van de golfvector.

In hoofdstuk 9 komen ruimtelijk begrensde golfvelden aan de orde. Een nauwe bundel, die vanuit het vacuüm op een kristal valt, geeft niet altijd een straal of stralen in het kristal. Alleen in die gevallen waar de in het kristal opgewekte energiestroom niet nagenoeg evenwijdig aan het oppervlak loopt, ontstaat een zich normaal gedragende straal of stralen in het kristal.

Een uitbreiding van de dynamische theorie, zodat die toepasbaar wordt op vervormde ideale kristallen, wordt gegeven in hoofdstuk 10. De theorie is gebaseerd op de volgende veronderstellingen: (1) de dynamische theorie mag plaatselijk worden toegepast op een smalle bundel, (2) de bundel blijft zich normaal als een bundel gedragen, al behoeft de gevolgde baan niet recht te zijn, (3) de aanpassing van het golfveld langs de baan wordt verkregen met behulp van een postulaat dat veel lijkt op het postulaat in de geometrische optica waarmee de stralengang in inhomogene media kan worden berekend. De theorie kan toegepast worden op welke deformatie-toestand dan ook, behalve in die gevallen, waarbij de deformatie te sterk inhomogeen is. De theorie geeft uitdrukkingen voor de baan die de straal volgen zal en hoe groot de absorptie langs deze baan zal zijn.

Om de juistheid van de eerste 2 veronderstellingen te toetsen, worden in hoofdstuk 11 de voorbeelden uit hoofdstuk 10 nogmaals behandeld. Er wordt aangetoond dat in deze speciale gevallen niet-benaderde oplossingen gegeven kunnen worden door gebruik te maken van de parabolische cylinder-functies. Als de vervorming slechts langzaam verloopt met de plaats, dan is de overeenstemming met de straal-theorie uitstekend, hoewel niet alle resultaten van de straal-theorie gecontroleerd konden worden. Als de vervorming sterk afhangt van de plaats, loopt een gedeelte van de invallende energie recht door, zonder invloed van de snel veranderende deformatie te ondervinden. Een soortgelijk verschijnsel is ook bekend in de theorie der electronen-banden: het "tunnelen" van de ene band in de andere bij voldoende grote veldsterkten. Als de deformatie zeer snel verloopt geeft een kinematische behandeling van de diffractie hetzelfde resultaat als de niet-benaderde oplossing. De bovengrens voor de toepasbaarheid der straal-theorie, die was afgeleid op basis van intuïtieve argumenten, is in goede overeenstemming met de resultaten bereikt in dit hoofdstuk.

Een vergelijking tussen de door ons gegeven straal-theorie en een aantal andere theorieën wordt gegeven in hoofdstuk 12. De theorie ontwikkeld door Taupin is algemener dan de onze, maar voor slechts langzaam veranderende vervormingen geven beide theorieën identieke resultaten. Bonse's theorie is een uitbreiding van de onze tot die gevallen, waarin extinctie niet meer verwaarloosd kan worden. Er wordt aangetoond, dat zijn theorie in die gevallen alleen juiste resultaten geeft, als het opvallende golfveld langs het oppervlak van het vervormde kristal voldoet aan bepaalde voorwaarden wat betreft fase en amplitude.

STELLINGEN

bij het proefschrift van P. Penning

16 februari 1966

I

In de dynamische theorie voor Röntgen-diffractie wordt de grootheid absorptiecoëfficiënt meestal op slordige wijze ingevoerd. Het samenvattend artikel van Batterman en Cole vormt hierop een uitzondering.

B. W. Batterman and H. Cole, *Rev. Mod. Phys.* **36**, 681-717, 1964.

II

De experimentele resultaten van Bonse, beschreven in ¹⁾, geven niet de gezochte bevestiging van zijn theorie ²⁾.

¹⁾ U. Bonse, *Z. Phys.* **177**, 529-542, 1964.

²⁾ U. Bonse, *Z. Phys.* **177**, 385-423, 1964.

III

Het verdient aanbeveling om in de kristal-optica niet de poolfiguur van de phase-snelheid, maar de poolfiguur van de reciproke phase-snelheid te gebruiken.

IV

Het rendement van de ideale energie-transformator, werkend boven 0 °K, die electro-magnetische straling kan omzetten in mechanische, elektrische of chemische energie, is kleiner dan 1.

D. Kahn, *Plant Physiol.* **36**, 539-540, 1961.

L. N. M. Duijsens, *Plant Physiol.* **37**, 407-408, 1962.

V

Omdat Saccocio en Zajac in de mathematische opzet geen volledig gebruik gemaakt hebben van de symmetrie in het geval van simultane diffractie aan 3 gelijkwaardige stelsels (220)-vlakken, misten zij de aansluiting naar minder symmetrische gevallen. Gezien de resultaten van Borrmann en Hartwig verdienen deze wel de aandacht.

E. J. Saccocio and A. Zajac, *Phys. Rev.* **139**, A255-A264, 1965.

G. Borrmann und W. Hartwig, *Z. Kristallogr.* **121**, 401-409, 1965.

VI

De bewering van Oldeman dat in eenzelfde medium de voortplantingssnelheid van de longitudinale golf tenminste 1,7 maal die van de transversale golf zou zijn, is onjuist.

J. Oldeman, *Ned. T. Natuurk.* **31**, 10-15, 1965.

VII

De kwalitatieve verklaring van Brewster's wet vanuit de electronen-theorie, gegeven door Sommerfeld, is voor een goed begrip te simpel.

A. Sommerfeld, *Optics, Lectures on theoretical Physics, Vol. IV*, Academic Press, New York and London, 1964.

VIII

De numerieke factor ($\approx 1/9$) in de relatie tussen de dichtheid der willekeurig over het volume verdeelde dislocaties en de hoekafwijkingen van het rooster, gegeven door Gay e.a., is onjuist berekend.

P. Gay, P. B. Hirsch and A. Kelly, *Acta Met.* **1**, 315-319, 1953.

IX

De formulering van Fermat's principe:

$$\delta \int_A^B \mathbf{k} \cdot d\mathbf{r} = 0$$

is algemener dan de gebruikelijke:

$$\delta \int_A^B n dl = 0.$$

N. Kato, *J. Phys. Soc. Japan* **18**, 1785-1791, 1963.

X

Begaafden hebben de morele plicht hun intellect mede aan te wenden om geestelijk gebrekkigen te helpen zo intensief mogelijk deel te nemen aan de vrije maatschappij.

XI

Een nadere bestudering van de strafprocedure, vigerend binnen een bedrijf, is gewenst.